

OCULAR PHARMACOKINETICS AND EFFICACY OF VARIOUS AMINO
ACID AND DIPEPTIDE PRODRUGS OF GANCICLOVIR

A DISSERTATION IN
Pharmaceutical Sciences
and
Chemistry

Presented to the Faculty of the University
of Missouri - Kansas City in partial fulfillment of
requirements for the degree

DOCTOR OF PHILOSOPHY

by
SRIRAM GUNDA

B.PHARM., Kakatiya University, 2000

Kansas City, Missouri
2012

© 2012
SRIRAM GUNDA
ALL RIGHTS RESERVED

OCULAR PHARMACOKINETICS AND EFFICACY OF VARIOUS AMINO
ACID AND DIPEPTIDE PRODRUGS OF GANCICLOVIR

Sriram Gunda, Candidate for the Doctor of Philosophy Degree

University of Missouri – Kansas City, 2012

ABSTRACT

Herpes simplex virus infections (HSV) in the eye are one of the leading causes of blindness across the world. Current available treatment options to treat HSV infections are solutions of trifluorothymidine (TFT), idoxuridine (IDU), and vidarabine, ganciclovir (GCV) gel and acyclovir (ACV) ointments. Some of the problems associated with thymidine analogues are their ocular and systemic toxicities in long term usage. Even though GCV and ACV have good efficacies against HSV, their limited solubility, poor corneal absorption and diminished ocular bioavailability limits their effectiveness. Ointments and gels are also prescribed to be applied 5-9 times per day, which not only hampers the visibility of patients but also affect their daily life. Often, these antiviral agents are administered along with steroids to reduce the corneal inflammation. Application of ointments and gels restrict the concomitant usage of topical steroids solutions.

To address the above issues, goals were set to prepare high dose topical aqueous solutions and to increase ocular bio-availability of GCV. A series of dipeptide monoester prodrugs and amino acid monoester and diester prodrugs were designed to target the nutrient transporters peptide transporter (hPEPT1) and sodium dependent neutral and cationic transporter ($B^{0,+}$), respectively. The overall objectives of this study are to evaluate cytotoxicity and uptake of prodrugs

in rabbit corneal epithelial cells *in vitro*, and also to estimate corneal absorption, aqueous humor pharmacokinetics and antiviral activity on rabbit models. Pharmacokinetic studies were performed on rabbit models using ocular microdialysis models. Pharmacokinetic parameters were estimated for all the prodrugs and were compared with the parent drug. A prodrug with best pharmacokinetic properties was selected to study for its antiviral activity against HSV-1 in virus inoculated corneal epithelial keratitis rabbit models. In conclusion, L-Tyrosine-L-Valine-GCV among peptide ester prodrugs and L-Valine-GCV among the amino acid ester prodrugs exhibited superior corneal absorption and bioavailability in comparison with GCV. This might be due to the absorption of these drugs *via* both transcellular passive diffusion and hPEPT1 mediated transport across corneal epithelium. L-Tyrosine-L-Valine-GCV was also found to have excellent antiviral activity in comparison with currently available product, TFT.

The undersigned, appointed by the Dean of School of Graduate Studies, have examined a dissertation titled “Ocular Pharmacokinetics and `Efficacy of Various Amino Acid and Dipeptide Prodrugs of Ganciclovir”, presented by Sriram Gunda, candidate for the Doctor of Philosophy degree, and hereby certify that in their opinion it is worthy of acceptance.

Supervisory Committee

Ashim K. Mitra, Ph.D., Committee Chair
Division of Pharmaceutical Sciences

Thomas P. Johnston, Ph.D.
Division of Pharmaceutical Sciences

Kun Cheng, Ph.D.
Division of Pharmaceutical Sciences

Mostafa Badr, Ph.D.
Division of Pharmacology and Toxicology

Zhonghua Peng, Ph.D.
Department of Chemistry

CONTENTS

ABSTRACT	ii
ILLUSTRATIONS	viii
TABLES	xii
ACKNOWLEDGEMENTS	xv
Chapter	
1. INTRODUCTION	1
Overview	1
Statement of problem	1
Objectives	3
2. LITERATURE REVIEW	5
Drug delivery to the eye	5
Anatomy and Physiology of the eye as a barrier to drug delivery	10
Physico-chemical properties effecting ocular drug delivery	15
A prodrug approach to targeted drug delivery	18
Ocular herpes infections, treatments and utility of GCV	25
Effect of pre-corneal events on ocular bio-availability	28
Anterior segment pharmacokinetics following topical administration	32
3. CYTOTOXICITY ASSAYS OF AMINO ACID AND DI-PEPTIDE PRODRUGS OF GCV ON RABBIT PRIMARY CORNEAL EPITHELIAL CELLS (RPCEC)	41
Rationale	41

Methods and materials	41
Results.....	43
Discussion and conclusions	47
4. ANTERIOR CHAMBER PHARMACOKINETICS OF L-ARGININE AND AMINO ACID MONOESTER PRODRUGS OF GCV IN RABBIT EYES AND THEIR INTERACTION WITH B ^{0,+} TRANSPORTER ON THE RABBIT CORNEA AND RABBIT PRIMARY CORNEAL EPITHELIAL CELLS (RPCEC).....	49
Rationale	49
Methods and materials	52
Results.....	64
Discussion and conclusions	75
5. ANTERIOR CHAMBER PHARMACOKINETICS OF DI-PEPTIDE MONOESTER PRODRUGS OF GCV IN RABBIT EYES AND ABSORPTION OF PRODRUGS TARGETING PEPT1 TRANSPORTER ON THE RABBIT CORNEAL EPITHELIUM.....	86
Rationale	86
Methods and materials	89
Results.....	101
Discussion and conclusions	114

6. ORAL ADMINISTRATION AND SYSTEMIC PHARMACOKINETICS OF GCV AND DIPEPTIDE MONOESTER PRODRUG L-TYR-L-VAL-GCV IN JUGULAR VEIN CANNULATED SPRAGUE DAWLEY RATS.....	122
Rationale	122
Methods and materials	126
Results.....	131
Discussion and conclusions	139
7. <i>IN VIVO</i> ANTIVIRAL EFFICACY, SURVIVAL ANALYSIS AND MODELING OF L-TYR-L-VAL-GCV MONOESTER ON HSV-1 INDUCED RABBIT EPITHELIAL KERATITIS MODEL	145
Rationale	145
Methods and materials	147
Results.....	150
Discussion and conclusions	150
8. SUMMARY AND RECOMMENDATIONS.....	155
Summary	155
Recommendations.....	160
LETTERS OF PERMISSIONS	162
REFERENCES	187
VITA	199

ILLUSTRATIONS

Figure	Page
Figure 1. Structure of the Eye.....	6
Figure 2. Picture depicts drugs diffusing across the model ocular barrier by para and trans cellular routes. C- Cell, CN- Cell Nucleus, JP- Junction Proteins, PCD- Paracellular Drug Diffusion, R- Receptor, T- Transporter and TCD- Transcellular Drug Diffusion.....	9
Figure 3. Circumvention of P-gp by prodrug derivitazation.....	19
Figure 4. Transporter targeted prodrug strategy.....	21
Figure 5. Chemical structures of (a) Acyclovir and (b) Ganciclovir.....	27
Figure 6. Flow chart below depicts the effects of precorneal events on the ocular pharmacokinetics.....	33
Figure 7. : Model depicting precorneal and intraocular drug movement following topical dosing.....	36
Figure 8. Above schemes (A to D) are various compartmental models which are frequently used to explain ocular pharmacokinetics.....	37
Figure 9. Cytotoxicity studies performed on rPCEC cells after the incubation of ganciclovir (GCV) and trifluorothymidine (TFT) at 0.2 (blue), 1 (Burgundy) and 5 (Green) mM concentrations for 24h.....	44
Figure 10. Cytotoxicity assays performed on rPCEC cells after the treatment with amino acid monoester and di-ester prodrugs, and di-peptide monoester prodrugs of GCV for 24h. Concentrations of prodrugs used were 0.2 mM (Blue) and 1 mM (Burgundy). Number of experiments performed were, n = 8. Error bars represent mean \pm SD.....	45
Figure 11. Structures of mono and di-ester amino acid prodrugs of GCV.....	54
Figure 12. Corneal infusion well model and microdialysis in rabbit anterior chamber.....	57
Figure 13. Schematic model representation of a single-dose continuous infusion well model to the rabbit eye.....	59
Figure 14. Saturation kinetics of [3 H] L-Arginine uptake in rPCEC cells. Data is represented by mean \pm SD. (n=4).....	66
Figure 15. Interaction studies of [3 H] L-Arginine with B $^{0,+}$ in presence of amino acid monoester and di-esters prodrugs of GCV. Dose dependent inhibition was performed in vitro on rPCEC cells. Data represented are mean \pm SE. (n=4).....	67
Figure 16. Concentration vs Time profile [3 H] L-Arginine (Blue diamonds). Corneal infusion of [3 H] L-Arginine was performed using a well, for 2h on New Zealand albino male rabbits under anesthesia. After 2h, infusion was removed to observe distribution and elimination of the amino acid for 6h. An anterior chamber microdialysis was performed to collect serial samples of aqueous humor dialysate for 8h.....	70

Figure 17. Concentration vs Time profile [³ H] L-Arginine inhibition with 1mM cold L-Arginine (Blue diamonds). Corneal infusion of [³ H] L-Arginine in presence of 1mM cold L-arginine was performed using a well, for 2h, on New Zealand albino male rabbits under anesthesia. Infusion was performed for 2h to observe the absorption phase. After 2h, infusion was removed to observe distribution and elimination of the amino acid for 6h. An anterior chamber microdialysis was performed to collect serial samples of aqueous humor dialysate for 8h.	71
Figure 18. Concentration vs Time profile of [³ H] L-Arginine inhibition with BCH (Blue diamonds). Corneal infusion of [³ H] L-Arginine in presence of 1mM BCH was performed using a well, for 2h, on New Zealand albino male rabbits under anesthesia. Infusion was performed for 2h to observe the absorption phase. After 2h, infusion was removed to observe distribution and elimination of the amino acid for 6h. An anterior chamber microdialysis was performed to collect serial samples of aqueous humor dialysate for 8h.	72
Figure 19. Concentration vs Time profile [³ H] L-Arginine in presence of chloride ion free buffer (Blue diamonds). Corneal infusion of [³ H] L-Arginine in absence of chloride ions was performed using a well, for 2h, on New Zealand albino male rabbits under anesthesia. Infusion was performed for 2h to observe the absorption phase. After 2h, infusion was removed to observe distribution and elimination of the amino acid for 6h. An anterior chamber microdialysis was performed to collect serial samples of aqueous humor dialysate for 8h.	73
Figure 20. Concentration vs Time profile [³ H] L-Arginine in presence of sodium ion free buffer (Blue diamonds). Corneal infusion of [³ H] L-Arginine in absence of sodium ions was performed using a well, for 2h, on New Zealand albino male rabbits under anesthesia. Infusion was performed for 2h to observe the absorption phase. After 2h, infusion was removed to observe distribution and elimination of the amino acid for 6h. An anterior chamber microdialysis was performed to collect serial samples of aqueous humor dialysate for 8h.	74
Figure 21. Corneal absorption and anterior chamber pharmacokinetics γ -L-Glu-GCV. A 2h infusion of γ -L-Glu-GCV administered using well model. Anterior chamber microdialysis was performed to collect aqueous humor dialysate containing bio-reversed GCV. Data points are represented as mean \pm SD. Number of animals used were, n=5.	80
Figure 22. Structures of peptide prodrugs of GCV. L-Valine-GCV, L-Valine- L-Valine-GCV, L-Tyrosine-L-Valine-GCV, and L-Glycine-L-Valine-GCV (from top to bottom in order)	90
Figure 23. Depiction of the experimental and compartmental model. Drug is administered at a constant rate onto the corneal surface (K ₀). Elimination rate from the central compartment is represented by k ₁₀ , and inter-compartmental the distribution rates are described by k _{ap} and k _{pa}	97

Figure 24. Aqueous humor drug Concentration vs Time profiles of regenerated GCV (Blue diamonds) and L-Val-GCV (pink squares) after 2h infusion of L-Tyr-L-Val-GCV (Mean \pm S.D).....	102
Figure 25. Aqueous humor drug Concentration vs Time profiles of regenerated GCV (Blue diamonds) and L-Val-GCV (pink squares) and intact L-Val-L-Val-GCV (Yellow triangles) after 2h infusion of L-Val-L-Val-GCV (Mean \pm S.D).....	103
Figure 26. Aqueous humor drug Concentration vs Time profiles of GCV (Blue diamonds) after 2h infusion of GCV (Mean \pm S.D).	104
Figure 27. Aqueous humor drug Concentration vs Time profiles of regenerated GCV (Blue diamonds) and L-Val-GCV (pink squares) and intact L-Gly-L-Val-GCV (Yellow triangles) after 2h infusion of L-Gly-L-Val-GCV (Mean \pm S.D).....	105
Figure 28. Aqueous humor drug Concentration vs Time profiles of regenerated GCV (Blue diamonds) and intactL-Val-GCV (pink squares) after 2h infusion of L-Val-GCV (Mean \pm S.D).....	106
Figure 29. Cumulative amounts of prodrug, intermediate metabolite and regenerated GCV. Aqueous humor drug Concentration vs Time profiles of cumulative amounts of all prodrugs after 2h infusion in rabbit eyes (Mean \pm S.D). (n = 5)	115
Figure 30. LC-MS/MS spectrum of GCV and its respective ions produced by MRM method. The major ion of GCV was found to be 152.3	133
Figure 31. LC-MS/MS spectrum of L-Val-GCV and its respective ions produced by MRM method.....	134
Figure 32. LC-MS/MS spectrum of L-Tyr-L-Val-GCV and its respective ions produced by MRM method.....	135
Figure 33. Plasma drug log-concentration vs Time profile of GCV (Blue diamonds) after intravenous administration of 10 mg/kg dose of GCV in rats. Data points presented are in Mean \pm S.D. Number of animals used, n=3..	137
Figure 34. Plasma drug log-concentration vs Time profile of GCV (Blue diamonds) after intravenous administration of 10 mg/kg dose of L-Tyr-L-Val-GCV in rats. Data points presented are in Mean \pm S.D. Number of animals used, n=4.	138
Figure 35. Structures of TFT (above) and L-Tyr-L-Val-GCV (below).....	146
Figure 36. In vivo antiviral activity of 1% wt/v TFT (blue), 1% wt/v Try-L-Val-GCV (red) and control/BSA (Green). Five doses of 50 μ l drops were topically administered every day to the HSV-1 infected eyes of New Zealand Albino male rabbits, from PI day 3 to PI day 7. SLE scores were taken from PI day 3 to PI day 10. Total number of animals used for the studies is 30, n=10 for each group.....	151
Figure 37. Survival analysis graph of three groups of rabbits, 10 each, treated with 1% wt/v TFT (blue), 1% wt/v L-Tyr-L-Val-GCV (red), and BSA (green). Five doses of 50 μ l drops were administered per day on PI days 3-7. Survival of animals was observed till day 12.....	152

Figure 38. Models of mean SLE scores of three groups after treatment with BSA (Green), 1% wt/v TFT (blue) and 1% wt/v L-Tyr-L-Val-GCV (red). Three polynomial equations represent the three groups of treatment. 153

Figure 39. The above picture depicts (i) anterior and posterior chambers (left) of anterior segment and (ii) the aqueous humor generation in ciliary body in the posterior chamber and clearance through trabecular meshwork into canal of schlemm in the anterior chamber. Drugs in the anterior segment are eliminated via this route [162]. 158

TABLES

Table	Page
Table 1. Mean percentage of rPCEC cells viable after treatment with GCV, TFT, and all prodrugs. Data represented as mean \pm SD. Number of experiments performed were, n=8.....	46
Table 2. Data showing half maximal inhibitory concentrations (IC50) of amino acids mono and di ester prodrugs against B ^{0,+} . Interaction studies of [³ H] L-Arginine with B ^{0,+} in presence of amino acid monoester and diester prodrugs of GCV. Dose dependent inhibition was performed in vitro on rPCEC cells. Data represented are mean \pm SE. (n=4).....	68
Table 3. Pharmacokinetic parameters of [³ H] L-Arginine. A constant infusion of amino acid was administered for 2h using topical well in rabbit eyes. AUC- area under the curve, Cmax- Maximum concentrations achieved in aqueous humor, Tmax – Time to reach maximum concentrations. Data represented as mean \pm S.D. (n=5).....	76
Table 4. Pharmacokinetic parameters of [³ H] L-Arginine. A constant infusion of amino acid was administered for 2h in presence of cold L-Arginine 1mM and BCH 1mM using topical well in rabbit eyes. AUC- area under the curve, Cmax- Maximum concentrations achieved in aqueous humor, Tmax – Time to reach maximum concentrations. Data represented as mean \pm S.D. (n=5).....	77
Table 5. Pharmacokinetic parameters of [³ H] L-Arginine. A constant infusion of amino acid was administered for 2h in Chloride and sodium ion free buffers, using topical well in rabbit eyes. AUC- area under the curve, Cmax- Maximum concentrations achieved in aqueous humor, Tmax – Time to reach maximum concentrations. Data represented as mean \pm S.D. (n=5).....	78
Table 6. Pharmacokinetic parameters of L-Tyr-GCV and γ -L-Glu-GCV. Drugs were given constant infusion for 2h across the cornea in rabbit eyes. Values presented are for regenerated GCV from both prodrugs (Mean \pm S.E.M). (n=5).....	84
Table 7. HPLC conditions for the analysis of GCV and prodrugs. C8 column was used for the separation of drug peaks. Mobile phases used are various mixtures of Acetonitrile and phosphate buffer at pH 2.5.....	100
Table 8. Pharmacokinetic parameters after 2h infusion of L-Tyr-L-Val-GCV. Values presented are for regenerated GCV and regenerated amino acid intermediate L-Val-GCV (Mean \pm S.E.M). AUC- Area under the curve, Cmax- Maximum concentration in aqueous humor, Tmax- Time to reach maximum concentration, Clast- Concentration of the last sample point in aqueous humor, MRT- Mean residence time, Tlast- Time of last time point, λ_z - Terminal elimination rate constant.....	109
Table 9. Determination of Pharmacokinetic parameters of L-Val-L-Val-GCV after 2h of corneal infusion. Values presented are for regenerated GCV,	

regenerated amino acid intermediate L-Val-GCV and intact L-Val-L-Val-GCV (Mean \pm S.E.M).....	110
Table 10. Determination of Pharmacokinetic parameters of L-Gly-L-Val-GCV after 2h of corneal infusion. Values presented are for regenerated GCV, regenerated amino acid intermediate L-Val-GCV and intact L-Gly-L-Val-GCV (Mean \pm S.E.M).....	111
Table 11. Pharmacokinetic parameters after 2h infusion of GCV. Values presented are for GCV (Mean \pm S.E.M).....	112
Table 12. Determination of Pharmacokinetic parameters of L-Val-GCV after 2h of corneal infusion. Values presented are for regenerated GCV and intact L-Val-GCV (Mean \pm S.E.M).....	113
Table 13. Pharmacokinetic parameters for corneal absorption of L-Tyr-L-Val-GCV, L-Val- L-Val-GCV, L-Gly-L-Val-GCV, L-Val-GCV and GCV. Values presented are for cumulative amounts of prodrug, amino acid metabolite and GCV in mean \pm SEM. (n=5)	119
Table 14. Absorption Rate Constants for corneal absorption of L-Tyr-L-Val-GCV, L-Val- L-Val-GCV, L-Gly-L-Val-GCV, L-Val-GCV and GCV. Values presented are from the mean concentration time profiles of cumulative amounts of GCV from the administration of 4 prodrugs and GCV.....	121
Table 15. GCV and its prodrug(s) calibration curve standards calculated value(s) and percentage accuracy(s).....	127
Table 16. Plasma pharmacokinetic parameters of GCV after oral administration at a dose of 10 mg/kg. Values presented as Mean \pm S.D.....	140
Table 17. Plasma pharmacokinetic parameters of GCV after oral administration of L-Tyr-L-Val-GCV equivalent to dose of 10 mg/kg of GCV. Values presented as Mean \pm S.D.	141
Table 18. SLE Scoring System to measure lesions of epithelial keratitis caused by HSV-1strain Mckrae on Rabbit cornea.....	148
Table 19. Treatment and scoring schedule of three groups of HSV-1 infected rabbits. Inoc.- Inoculation of virus; PI – Post inoculation; SLE – Slit-lamp examination; TFT – Trifluorothymidine, BSA – Control group/placebo, L-Tyr-L-Val-GCV – L-Tyrosine-L-Valine-Ganciclovir	149
Table 20. Table of pharmacokinetic parameters comparing the parent GCV and regenerated GCV from prodrugs	158

ACKNOWLEDGEMENTS

I am truly indebted and thankful to my advisor Prof. Ashim K. Mitra, for his constant support, encouragement, training and intellectual advice. I would like to thank my supervisory committee for their critical review of this work.

I would also like to thank Dr. James Hill from LSU eye center for conducting the *in vivo* antiviral efficacy studies of di-peptide prodrugs. I would like to acknowledge my mentor for in vitro research, Dr. Dhananjay Pal. I would also like extend my gratitude to Drs. Zhu, Samanta and Earla for their collaboration and support in my research. A special thanks to Mrs. Ranjana Mitra for her constant support in the lab.

It is my great pleasure to thank Mrs. Joyce Y. Johnson and Mrs. Sharon Self for their help in administrative works. I would also like to thank Drs. Anand, Boddu, Dey, Gupta, Hariharan, Jain-Vakkalagadda, Janoria, Katragadda, Majumdar, Tirucherai, Mr. Cholkar, Mandava, Ms. Oberoi and Patel, for pursuing research, literary and educational work with me. I would also like to thank my colleagues at school of pharmacy Sridhar, Jignesh, Budda, Kalyan, Kunal, Ripal, Deep, Nilesh, Gayatri, Kalyani, Sandeep, Ramya, Aswani, Piyush, Ravi and all other pharmacy mates for their constant support and friendship.

I would also like to thank my dear friends at UMKC, Dr. Dolla, Mr & Mrs. Jamithireddy, Mr. Ambati, Basetti, Chittoori, Gera, Gollakota, Khaja, Lella, Mettu, Nathani, Neelakanti, Rudraraju, Vooradi Ms. Diana, Mary and Sripriya, and to all other friends whom I couldn't mention here.

Finally, I would like to thank my brothers Ramana & Ravi, and my mother Mrs. Vijaya Laxmi Gunda and my father Mr. Pandu Rangaiah Gunda for their nurture, support, encouragement and love. This wouldn't have been possible without them.

Dedicated to my family

CHAPTER 1

INTRODUCTION

Overview

Herpes Simplex Virus type-1 (HSV-1) induced epithelial and stromal keratitis of the cornea is one of the leading causes of blindness in the United States [1-2]. The drug of choice for the treatment of these viral infections is trifluorothymidine (TFT). Even though TFT is currently the drug of choice for ocular herpes infections, it is reported to be cytotoxic and mutagenic in long term usage [3]. Ganciclovir (GCV), an acyclic guanosine analog exhibits excellent antiviral activity against the herpes family of viruses [4]. It is the drug of choice for the systemic and ocular HCMV infections and it is as effective as ACV against HSV-1 [5]. Drug delivery to anterior and posterior segments of the eye is one of the most challenging tasks currently encountered by ocular drug delivery scientists. Ophthalmic drugs are primarily administered by topical route to treat ocular viral and bacterial infections, glaucoma, inflammations, and immune-suppression. Other routes of ocular drug delivery would be by oral, systemic, intraocular and periocular injections, transscleral and sub-conjunctival pathways.

Statement of the problem

Drugs administered topically have low probability of reaching anterior segment in significant amounts as it has to traverse the corneal and conjunctival epithelia, aqueous humor and lens. Topical solutions of TFT, idoxuridine (IDU) and

vidarabine have high toxicities in long term usage [3]. Even though GCV is effective against corneal herpes infections, its modest aqueous solubility limits the preparation of a formulation as a topical eye solution and its hydrophilic property makes it impermeable across the cornea. Previously in our laboratory, a series of lipophilic prodrugs were prepared to enhance the permeability across the cornea [6]. Even though permeability across the cornea improved, aqueous solubility of the compounds was found to be diminished. As a result these prodrugs could not be formulated as high dose topical solutions [6].

Drug delivery to the anterior segment is important since a large fraction (up to 90%) of the administered dose is washed away through drainage, tears, reflex blinking, and into the naso-lacrimal ducts. In order for a drug to reach therapeutic concentrations in the anterior segment, it has to pass through the anterior segment barriers such as corneal and conjunctival epithelia. Various formulation strategies, including oil solutions, emulsions, nanoemulsions, ointments, and gels have been employed to increase the residence time of the drug on the corneal surface. A conjunctival sack can accommodate a maximal fluid volume of 30 μL . When a 50 μL volume is instilled topically, about 20 μL of drug will be drained away [7]. In order to generate high drug concentrations in the pre-corneal area, a large dose (about 2-3% wt/v) is usually required to be achieved in formulations that are required to achieve 500-600 μM of drug in the pre-corneal area. Fifty percent of the normal human tear film is replaced every 2-20

min. Such a high rate of tear turnover also reduces drug residence in the pre-corneal and pre-conjunctival areas. Therefore, the tear film also acts as a barrier to topical drug absorption [7].

Our earlier reports have shown that hydrophilic GCV is not a substrate for nucleoside/nucleobase transporters present on the cornea and its permeation across the cornea occurs primarily by passive diffusion [6, 8]. Peptide and amino derivatization of relatively hydrophilic molecules, such as GCV, may enhance both aqueous solubility and PEPT and B^{0,+} aided permeation across the cornea.

Objectives

Objectives of the project were:

- ❖ To determine the *in vitro* cytotoxicity of amino acid prodrugs of GCV (L-Tyr-GCV, L-Phe-GCV, L-Glu-GCV, di-L-Phe-GCV, and di-L-Glu-GCV) at 0.2 mM and 1mM concentrations after 24h exposure on rabbit primary corneal epithelial cells (rPCEC) and compare with GCV and TFT.
- ❖ To determine the *in vitro* cytotoxicity of dipeptide monoester prodrugs of GCV (L-Tyr-L-Val-GCV, L-Gly-L-Val-GCV, L-Val-L-Val-GCV) at 0.2 mM and 1mM concentrations after 24h exposure on rabbit primary corneal epithelial cells (rPCEC) and compare with GCV and TFT.
- ❖ To study the *in vitro* interaction of amino acid prodrugs of GCV (L-Tyr-GCV, L-Phe-GCV, L-Glu-GCV, di-L-Phe-GCV, and di-L-Glu-GCV) and [³H] L-

Arginine with sodium dependent large neutral and cationic amino acid transporter ($B^{0,+}$) on rPCEC cells.

- ❖ To determine the *in vivo* absorption across rabbit cornea and aqueous humor kinetics of [^3H] L- Arginine in rabbit eye using anterior chamber microdialysis and well infusion model. Also, to observe the *in vivo* interaction of [^3H] L- Arginine and $B^{0,+}$ transporter in presence and absence of various ions (sodium ions and chloride ions) and inhibitors (cold L-Arginine and BCH).
- ❖ To determine ocular pharmacokinetics of GCV and amino acid monoester prodrugs utilizing microdialysis and well infusion rabbit model.
- ❖ To determine the ocular pharmacokinetics of dipeptide monoester prodrugs of GCV (L-Tyr-L-Val-GCV, L-Gly-L-Val-GCV, L-Val-L-Val-GCV) using microdialysis and well infusion model.
- ❖ To determine the antiviral activity of L-Tyr-L-Val-GCV in HSV-1 induced corneal epithelial keratitis rabbit model. To compare slit-lamp examination (SLE) scores of animals treated with L-Tyr-L-Val-GCV, TFT and control group (BSA).
- ❖ To perform survival analysis of animals after the treatment with L-Tyr-L-Val-GCV, TFT and BSA after administration of 20 doses for 5 day period.

CHAPTER 2

LITERATURE REVIEW

Drug delivery to the eye

Transporter targeted drug delivery can be utilized to deliver drugs across mucosal barriers. Several therapeutic agents are substrates of nutrient transporters present in the biological membranes and tissues. Many nutrients *i.e.*, ions, vitamins, amino acids, peptides, carboxylic acids and metal ions are taken up into the cells *via* specialized mechanisms such as facilitated diffusion, ion channels, carrier mediated transport and receptor mediated endocytosis [9]. Transporters are trans-membrane proteins expressed in most epithelial and endothelial cells. These transporters are designed to transport specific endogenous substrates. For example, amino acid transporters are only capable of transporting amino acids or substances that are structurally similar to amino acids. Drugs such as L-methyldopa and L-dopa are the examples in this category [10]. Among others peptide, monocarboxylate, vitamin, glucose and nucleoside/nucleobase transporters have been utilized for drug delivery purposes [9]. Various tissues, including brain, eye, intestine, kidneys and blood vessels express various transporters.

Eye is a complex organ divided into two, the anterior and the posterior segment (Figure 1). Anterior segment consists of the transparent avascular cornea

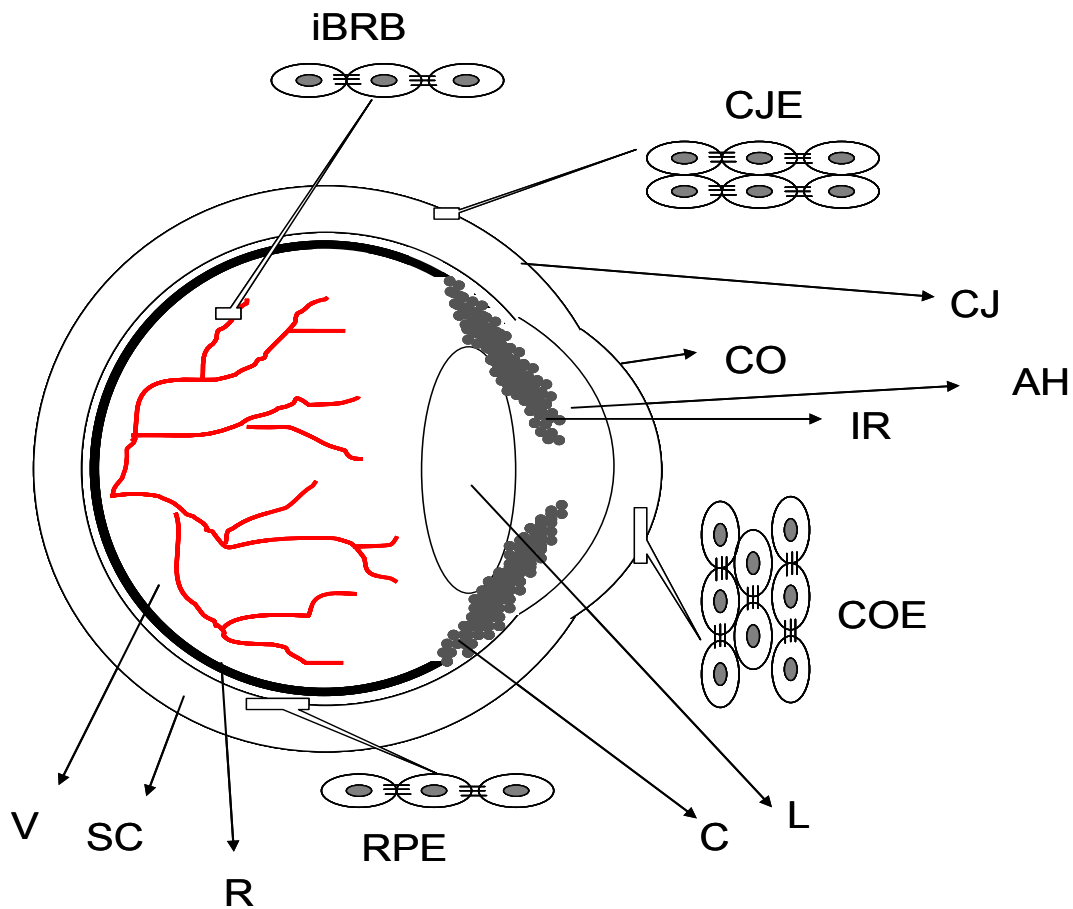


Figure 1. Structure of the Eye.

AH-Aqueous Humor, C- Ciliary Body, CJ- Conjunctiva, CJE- Conjunctival Epithelium, CO- Cornea, COE- Corneal epithelium, iBRB- inner Blood Retinal Barrier (endothelial cells lining the retinal blood vessels), IR- Iris, L- Lens, R- Retina, RPE- Retinal Pigmented Epithelium, SC- Sclera and Choroid, and V- Vitreous.

and lens, vascular iris-ciliary body and conjunctiva covering the outer part of the sclera. Most of the nutrients are supplied to avascular ocular tissues by iris-ciliary body through aqueous humor. Nutrients from blood in the iris-ciliary body are mostly carried into aqueous humor to reach cornea and lens and subsequently are taken up by ion channels, transporters and receptors [11]. Posterior segment of the eye constitutes primarily sclera, choroid, retinal pigmented epithelium (RPE) and neural retina. Nutrients to the retina are mainly supplied by blood vessels in the retina and choroid. RPE on the other hand is a single cell layered epithelium which separates choroid from neural retina, thereby serving as a defensive wall. Intercellular tight junctions prevent the entry of unwanted substances from the choroidal blood into the retina. Similar to the cornea and lens, RPE also receives its nutrient supply through ion channels, transporters and receptors.

With such a complex structure and physiology, the eye poses a major challenge to the delivery of xenobiotics. Some of the anterior segment diseases like uveitis, endophthalmitis, keratitis, conjunctivitis, glaucoma or cataract and posterior segment diseases like retinitis, proliferative diseases *i.e.*, proliferative vitreal retinopathy, diabetic macular edema and age related macular degeneration are commonly treated by intravitreal drug delivery [12].

Major challenges to the topical drug delivery include drug drainage from the pre-corneal area, induced tear flow, corneal and conjunctival epithelia. Drugs used for the treatment of anterior segment diseases are primarily absorbed by

diffusion through the cornea or conjunctiva by either paracellular or transcellular pathways. Both the cornea and conjunctiva possess tight epithelial layers that act as drug diffusion barriers, as these cells are tightly bound to each other with the aid of zonula occludens [7, 13]. On the other hand, blood aqueous barriers (iris-ciliary), RPE and retinal endothelial cells (iBRB) constitute drug absorption barriers to retina from systemic administration. Epithelial cells of the RPE and the endothelial cells on the inner lining of the retinal blood vessels are also lined with tight junctions [14]. To overcome such diffusional resistance, drugs to the posterior segment of the eye are administered repeatedly through intravitreal injections or implants. Patient noncompliance, retinal detachment and infections at the site of surgery are some of the problems associated with such procedures [12]. Drugs administered to the eye either diffuses by paracellular or transcellular pathways. In the paracellular diffusion processes, drugs or endogenous substances diffuse through the tortuous intercellular spaces. In the transcellular diffusion processes, drugs diffuse through the lipoidal cellular membrane (Figure 2). Since these paracellular ocular barriers express tight junctions, many hydrophilic macromolecules *i.e.*, antibodies, peptides, proteins, oligonucleotides, DNA fragments, genes can not readily diffuse. Therefore most molecules diffuse through transcellular pathways requiring optimal lipophilicity in order to cross mucosal membranes *via* transcellular diffusion. Zhang W et al. developed a mathematical model to determine ocular bioavailability in the anterior chamber.

Solute molecular radius, octanol/water distribution coefficient, clearance and tear fluid hydrodynamics were considered to predict bioavailability in the anterior chamber. Their results reveal that bioavailability is primarily determined by lipophilicity of the solutes[15]. Kawazu K *et al.* suggested the involvement of efflux pumps on the tear-side [16] by studying the transport of lipophilic cyclosporine across the rabbit primary corneal epithelial cultures. Dey *et al.* also reported on molecular and functional expression of P-gp and its role in limiting ocular bioavailability of antibacterial drug erythromycin [17-18].

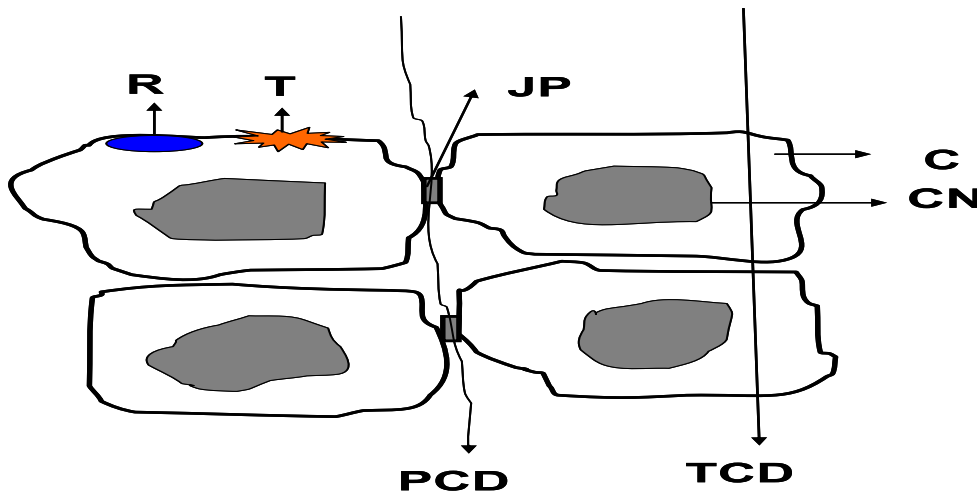


Figure 2. Picture depicts drugs diffusing across the model ocular barrier by para and trans cellular routes. C- Cell, CN- Cell Nucleus, JP- Junction Proteins, PCD- Paracellular Drug Diffusion, R- Receptor, T- Transporter and TCD- Transcellular Drug Diffusion

These studies suggest that efflux transporters also play a major role in the ocular bioavailability of drugs.

Anatomy and physiology of the eye as a barrier to ocular drug delivery

Human eye is generally divided into anterior and posterior segments. The anterior segment of the eye consists of (i) Cornea (ii) Conjunctiva (iii) Iris-Ciliary Body (iv) Lens and the posterior segment consists of (i) Neural retina (ii) Sclera (iii) Choroid (iv) Vitreous humor (v) Retinal pigmented epithelium (RPE)

Cornea:

Cornea has an average vertical diameter of 11.5 mm and a horizontal diameter of 12 mm in mammals[19] with a thickness of about 300-500 μm . It mainly consists of 5 layers.

- 1) Epithelium: Epithelium is the outer most layer of the cornea consisting of 5-6 layers of columnar cells including 2 layers of surface cells, 2-3 rows of wing cells and one layer of basal cells.
- 2) Bowman's layer: It is the non-cellular superficial layer of the stroma.
- 3) Stroma: It is the thickest layer of the cornea which makes up to 90% of the corneal thickness. It mostly constitutes water, collagen and few interspersed keratocytes.
- 4) Descemet membrane: This layer of the cornea is composed of collagen fibrils. It separates stroma from endothelium.

5) Endothelium: It constitutes a single layer of hexagonal cells.

Corneal epithelial cells are bridged together by junctional proteins, called zonula occludens that form “tight junctions” to primarily offer resistance to paracellular drug transport.

Conjunctiva:

The conjunctiva is a highly vascular mucous membrane covering the external part of sclera exposed to the outer environment, referred to as the bulbar conjunctiva, lining the inner side of the eyelids, referred to as the palpebral conjunctiva, and the transition portion forming the junction between the posterior eyelid and the eyeball, referred to as the fornix. Conjunctiva constitutes three layers, epithelium, substantia propria and submucosa. The conjunctival epithelium is stratified and contains goblet cells which secrete “mucin”, an important component of pre-corneal tear layer to protect and nourish cornea. Among all three layers, epithelium plays a major role as a barrier to drug transport into the eye.

Iris-ciliary body/Blood aqueous barriers (BAB):

Iris and ciliary body constitute the BAB that restricts the entry of solutes and drug molecules into posterior as well as anterior chambers of the eye. A systemically administered drug has to cross iris endothelium, stroma, and epithelium, in order to reach the posterior chamber. If a drug has to reach posterior chamber from ciliary body, the molecules must traverse ciliary

microvessels, stroma and two layers of ciliary epithelium. One of two layers of the epithelium is pigmented and the other is non-pigmented. Both iris endothelium and non-pigmented ciliary epithelium exhibit cellular tight junctions which restrict the paracellular transport of molecules.

Lens:

The lens is the transparent part of eye behind the iris that helps to focus light on the retina. It is a firm, gel like, convex shaped tissue composed of three layers *i.e.*, the capsule, nucleus and cortex. The outer epithelial layer enveloping the underlying fibers is referred as the capsule. Compactly arranged fibers in the center form nucleus and the periphery of the lens is called cortex. Lens is held in position by suspension ligaments called zonules that are connected to the ciliary body. Lens is considered almost impermeable in relation to drug delivery to the posterior segment *via* topical route.

Retinal pigmented epithelium (RPE) & inner blood retinal barrier (iBRB):

Retina is the seven layered sensory tissue that lines the back of the eye. Primarily, it is divided into the neural retina and the retinal pigmented epithelium (RPE). Neural retina is comprised of 7 layers including a layer of optic nerve fibers, ganglion cells, inner plexiform layer, inner nuclear layer, outer plexiform layer, outer nuclear layer and a layer of photoreceptor cells (bacillary layer). Center of the retina is called fovea that contains a high density of cones making it a region of the highest visual acuity. These layers are involved in signal

transduction to the optic nerve. RPE separates neural retina and choroid. It is a continuous, uniform, monolayer of hexagonal shaped low-cuboidal cells derived from neuroepithelium extending throughout the retina. The RPE plays an important role in forming the outer blood retinal barrier and supporting the function of photoreceptors. Functions of RPE also include absorption of light, metabolism of vitamin A, phagocytosis of rod and cone outer segments. RPE cells are bound together by tight junctional complexes that differentiate cells into two portions, the apical portion facing the neural retina and the basolateral portion facing the choroid. The apical microvilli of RPE closely oppose the outer segments of photoreceptor cells[20]. The basolateral portion has convoluted infoldings that increase the surface area for absorption of nutrients from choroid side. Inner neural retina is separated from blood supply by the endothelial cells of retinal blood vessels. RPE and endothelial layer simultaneously act as the Blood Retinal Barrier (BRB) of the eye to restrict the drug movement.

Efflux pumps:

Multidrug resistance in humans is mainly due to the efflux pumps belonging to ATP-Binding cassette (ABC) super family. There are two main efflux proteins; P-glycoprotein (P-gp) and multidrug resistance (MDR) associated proteins (MRPs).

P-glycoprotein:

P-gp is a versatile xenobiotic efflux pump. Several classes of drugs which

are structurally and pharmacologically unrelated are substrates for P-gp including anticancer drugs, steroids, protease inhibitors, cardiac drugs etc. P-gp is expressed in different tissues in eye. It has been reported that P-gp is expressed in the retinal capillary endothelial cells [20], retinal pigmented epithelial cells [21], ciliary nonpigmented epithelium [22], conjunctival epithelial cells [22], and iris and ciliary muscle cells [20]. A study was performed in our laboratory using quinidine as a model substrate and verapamil as inhibitor of P-gp. Intravitreal concentration of quinidine was increased two folds in the presence of verapamil indicating the importance of P-gp in ocular disposition of drugs [23]. In RT-PCR and western blot analysis, Dey S *et al.* found that P-gp belonging to the MDR1 family is expressed in the rabbit corneal epithelium [17]. Their RT-PCR experiments also suggested the presence of P-gp mRNA in human cornea [17]. Study also showed that ocular bioavailability of antibiotic erythromycin was enhanced in the presence of P-gp inhibitors such as cyclosporine A, quinidine and verapamil [18].

Multidrug Resistance Protein (MRPs):

MRP is an integral membrane glycolphosphoprotein belonging to the super family of ATP-binding cassette transmembrane transporter proteins. The MRP family contains at least seven members: MRP-1 and its six homologs, known as MRP2-7. MRPs expel out some of the drugs to protect the cell as an act of defense mechanism. A functional and biochemically active MRP was identified in human RPE cells [24]. MRP1 was reported in rabbit conjunctival epithelial

cells [25]. In previous reports from our laboratory, MRP2 was identified and studied for its role in rabbit primary corneal epithelial cells and its mRNA was also identified in the human cornea. Other MRPs in ocular tissues have not yet been identified.

Physicochemical properties of drug affecting permeability across ocular barriers

The drug permeability prediction across the ocular tissues is important in the development of new drugs and drug delivery strategies. To provide models that broadly predict permeability, it is imperative to understand the effect of various physicochemical properties of the drug such as lipophilicity, molecular charge, radius and size on its transport across ocular barriers [26].

Cornea is composed of 5 to 6 layers of columnar epithelium with tight junction proteins. On the other hand, passive diffusion is the primary route for hydrophilic drugs to permeate into the cornea. Thus the lipoidal nature of the corneal epithelium presents a major barrier to the entry of hydrophilic drugs like ACV and GCV. In human eyes, bioavailability is predicted to range between 1 and 5% for lipophilic molecules (octanol/water distribution coefficient >1) and to be less than 0.5% for hydrophilic molecules (octanol/water distribution coefficient <0.01). But chemical modifications were carried out to improve the partition coefficient of hydrophilic drugs by acyl-ester prodrug design and results showed improved permeability across corneal epithelium. But one of the major disadvantages is, achieving the desired lipophilicity often required compromising

on the aqueous solubility of the molecule. For a compound to be effective topically and to be formulated into eye drops, it must possess sufficient hydrophilicity and at the same time exhibit sufficient permeability across the cornea to reach 3–5 times the minimum inhibitory concentration levels. Thus, in general, there is a trend that indicates the increase in permeability with increase in partition coefficient of the drug. Cornea provides an effective barrier to compounds larger than 10 Å and cannot cross the membrane at measurable rates. Also, there is no apparent dependence of corneal permeability on molecular radius for compounds with small molecular radii. But for macromolecular peptides like thyrotropin-releasing hormone (TRH), p-nitrophenyl beta-cellopentaoside (PNP) and luteinizing hormone-releasing hormone (LHRH), there was a trend observed with increasing molecular size [27]. Ionization state of the drug molecule can also affect its permeability across corneal epithelium. *In vitro* corneal transport experiments showed that the permeability of the unionized pilocarpine species was twice that of the ionized species [28]. Thus the lipoidal epithelial layer of the corneal membrane appears to be a predominant barrier to the transport of polar species. Conjunctiva offers an attractive route to deliver drugs to the posterior segment of the eye because of the large surface area relative to cornea. But the conjunctival epithelium is similar to corneal epithelium when it comes to restricting the entry of molecules across the membrane. The limited data available on conjunctiva shows no clear dependence on distribution coefficient and a

possible dependence on molecular size. But one would expect conjunctival permeability to show a preference for lipophilic molecules, as it is a cellular tissue. Also, in general, conjunctiva appears to have similar or greater permeability than cornea. On the posterior segment of the eye, the RPE functions as a protective barrier against the entry of xenobiotics into the neural retina and vitreous from the systemic circulation. Pitkanen *et al.* studied the effects of solute molecular weight and lipophilicity on the permeability across a RPE-choroid preparation from bovine eyes [29]. Carboxyfluorescein, fluorescein isothiocyanate (FITC)-labeled dextrans with molecular masses from 4 to 80 kDa and β -blockers exhibiting a wide range of lipophilicity was chosen as permeation markers. Results showed that the RPE-choroid preparation was 35 times more permeable to carboxyfluorescein (376 Da) than to FITC-dextran (80 kDa) [29]. The permeabilities of lipophilic β -blockers were up to 8 and 20 times higher than that of hydrophilic atenolol and carboxyfluorescein, respectively. Indeed, with increasing drug partition coefficients, the vitreal concentrations as well as the rate of vitreal penetration of different antibiotics increased [29].

Therefore, knowing the effect of physicochemical properties of the drug on permeation across barriers can lead to the development of theoretical models that in turn can be broadly applied to predict permeability of new drugs and lead to novel drug delivery strategies.

A prodrug approach to targeted drug delivery

Antibiotics under the chemical classification of beta-lactams, macrolides, fluoroquinolones and cephalosporins are indicated in the treatment of various ocular infections and are substrates of both efflux and influx transporters. Thirty one beta-lactams and cephalosporins are substrates of PEPT1 and PEPT2 on renal SKPT cells with varying affinities [30]. Beta-lactams were also found to be substrates of PEPTs on LLC-PK1 cells [31]. Efflux of grepafloxacin and levofloxacin is mediated by P-gp on the caco-2 cells [32].

Another mode of utilizing transporters would be to design prodrugs by conjugating promoieties to target nutrient transporters. Such chemical modification could yield better pharmaceutical, pharmacological and pharmacokinetic properties. For example, L-Val-acyclovir, a prodrug of ACV, has higher oral bioavailability compared to the parent drug [33-34]. Prodrugs, in general, are absorbed readily across mucosal membranes and undergo bioreversion with the aid of intracellular enzymes into their active parent drugs (Figure 3). Mitra *et al.* designed various dipeptide prodrugs of ACV and GCV to target peptide transporter on the cornea and retina to facilitate higher permeability and bioavailability of these poorly permeable drugs [35-36]. Such prodrug design not only resulted in higher aqueous solubility and ocular bioavailability but also enhanced in vitro antiviral activity of the compounds against herpes family of viruses.

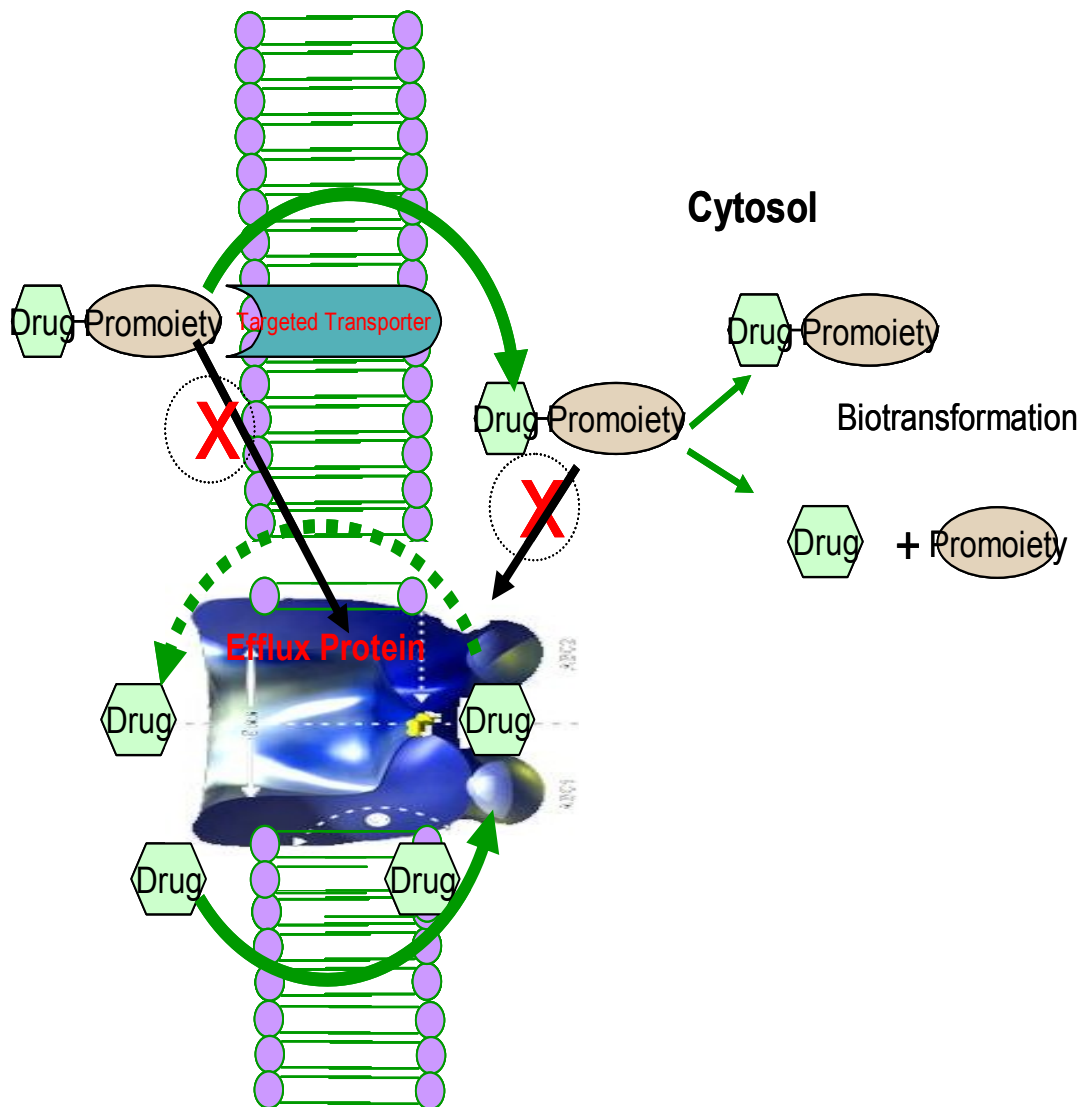


Figure 3. Circumvention of P-gp by prodrug derivitazation

Experiments with rabbit epithelial and stromal keratitis models showed that these prodrugs have superior antiviral activity compared to the currently marketed 1% wt/v topical eye drops of TFT[35-37]. Katragadda *et al.* demonstrated the utility of peptide transporter in circumventing P-gp mediated drug efflux across the rabbit cornea. Quinidine, a model P-gp substrate, when chemically linked to L-valine amino acid and dipeptide L-valine-L-Valine, it not only demonstrated a high affinity for peptide transporter on the cornea but also circumvented drug efflux by P-gp [38].

Transporters in the ocular tissues:

Several articles reported the existence of influx and efflux transporters on the ocular tissues. A detailed description of various transporters, their utility and the potential in delivering drugs to the eye are given below (Figure 4).

Peptide transporters:

Peptide transporters are specialized systems that translocate various di and tri-peptides across biological membranes. These proteins are mainly classified into two subtypes, PEPT1 and PEPT2. These transporters have broad substrate specificity and recognize various drugs, such as L-Val-acyclovir, beta-lactams and cephalosporins, etc. Peptide transporters are expressed in blood-ocular barriers [39], corneal epithelium [40], and vitreous side of the retina. Dipeptide prodrugs of ACV and GCV were found to be substrates of PEPT on the cornea

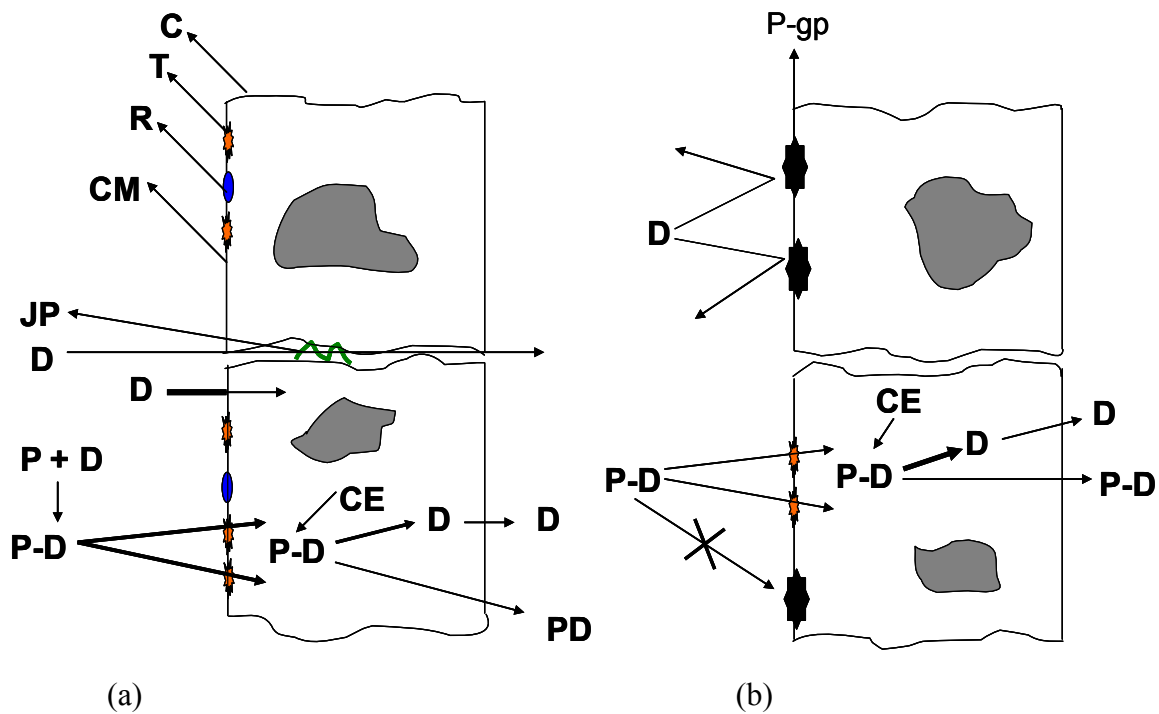


Figure 4. transporter targeted prodrug strategy

C- Cell, CE- Cellular Enzymes, CM- Cell Membrane, D- Drug, JP- Junction Proteins, PD- Prodrug, P-gp- P-Glycoprotein, R- Receptor and T- Transporter. (a) depicts the diffusion of drugs, D, by paracellular and transcellular route. A promoiety, P, is attached to drugs to make prodrugs, PD, which are targeted to nutrient transporters. (b) depicts drugs, D, substrates of P-gp are effluxed out of the cells. PD strategy can also be targeted to transporters to circumvent P-gp. Later, these PD is converted to D by cellular enzymes, CE.

[35-36]. Some of these novel antiviral agents were also found to have higher solubility activity was mainly attributed to their higher cell membrane permeability and intracellular availability. These dipeptide prodrugs were converted to their parent drugs by enzymatic hydrolysis by various enzymes present in the eye, *i.e.*, peptidases and cholinesterases. Peptide transporter present on the tear side of the corneal epithelium can be utilized in the delivery of various other drugs such as cephalosporins. Cephalexin, a cephalosporin antibiotic, was also found to be transported across rabbit retina *via* peptide transporter [41]. A model dipeptide, glycylsarcosine, was also found to be transported across blood-ocular barriers with the aid of an oligopeptide transport system [39]. In conclusion, peptide transporters could be utilized to target drugs to both anterior and posterior segments of the eye.

Amino acid transport systems:

Amino acid transporters are classified based on their affinity for cationic, anionic and neutral amino acids [42]. These transporters are also classified based on their dependency on sodium ion co-transport.

A Na^+ independent, facilitative transport system, LAT1, was identified and functionally characterized on rabbit cornea. LAT1 was also identified on human cornea [43]. A Na^+ , Cl^- , and energy-dependent carrier for L-Arginine, $\text{B}^{0,+}$, was also identified on rabbit corneal epithelium and human cornea [44]. Amino acid prodrugs of ACV were designed in an attempt to increase the aqueous

solubility and corneal permeability of ACV [45]. Other amino acid transporters such as Na⁺ dependent, neutral amino acid exchanger ASCT1, was also identified and functionally characterized on rPCEC cells and rabbit cornea [46].

Lee *et al.* suggested the presence of L-Glycine receptor and transporter in the bullfrog retinal müller cells [47]. Tomi *et al.* reported that L-leucine, a substrate of LAT1, was influxed by a carrier mediated process in rat retina [48]. Expression of LAT 1 protein in TR-iBRB2 and primary cultured human retinal endothelial cells and immunostaining results confirmed the presence of LAT1 in the rat retinal capillaries [48]. Neuronal glutamate transporter EAAC1 was found to be expressed in cultured retinal pigment epithelial (RPE) and retinoblastoma cells [49]. Foscarnet and L-Dopa are examples of substrates of amino acid transporters. Targeting amino acid transporters is a promising strategy to enhance ocular bioavailability of drugs.

Monocarboxylate (MCT) transporters:

MCT is involved in the translocation of monocarboxylic acids such as lactate, and ketone bodies. At least 9 isoforms of MCTs have been identified [50]. These transporters are highly expressed in cells with higher rates of glycolysis such as retina. RPE is involved in transporting lactic acid from retinal side to the choroid. MCT1 and MCT3 were found in rat RPE and MCT2 in retinal capillaries. Rat cornea expresses MCT1 and MCT2 [51]. Hosoya *et al.* observed MCT1-mediated transport of L-lactic acid at the inner blood-retinal barrier [52].

A polarized expression of various monocarboxylate transporters was found on human retinal pigment epithelium [53]. Majumdar *et al.* [54] also observed functional activity of monocarboxylate transporters on ARPE-19. ELISA studies indicated the presence of MCT1, 4 and 8. Salicylic acid, valproic acid and ceftibutine are substrates of these transporters. MCTs on the cornea, RPE and BRB could be utilized to target both drugs and prodrugs for delivery.

Vitamin transporters:

Vitamins like folic acid, ascorbic acid (AA), riboflavin and biotin are taken up into the cells *via* specialized transport systems known as vitamin transporters which remain relatively unexplored in the eye. There are several reports suggesting the presence of L-ascorbic transporter on the lens epithelium [55]. Lam K.W *et al.* studied the transport of AA and dehydroascorbic acid in SV-40 transformed retinal pigmented epithelium [56], which indicate the presence of specialized transport systems for vitamin C. Folic acid is another vitamin which is translocated across biological membranes *via* folate transporters (FTRs) and receptors (FRs). A polarized distribution of FTR-1 (apical side) and FR-alpha (basolateral side) was observed in the RPE. These two proteins function together to ferry folic acid from choroid to the retina [57-58]. Riboflavin transporter is another transport system present on the human-derived retinoblastoma cell line. This influx protein is also one of the potential transporters for drug and prodrug design [59].

Other transporters:

Several other transporters such as nucleoside/nucleobase transporters [8, 60-61], organic anion transporters (OATs), organic cation transporters (OCTs) and glucose transporters may be targeted for drug delivery to cornea and retina.

Ocular herpes infections, treatments and utility of GCV

Human eye is one of the frequent organs of target to herpes simplex virus (HSV) infections. Pathogenesis of HSV infections leads to the occurrence of various ocular disorders such as epithelial keratitis, anterior uveitis, retinitis, conjunctivitis, dermatitis of eyelids etc. Most common manifestation of HSV is the corneal epithelial keratitis. These infections are classified into primary, latent or recurrent or secondary infections [62-64]. HSV type 1 is found to be prevalent in the ocular manifestations. Other genital-ocular infections are uncommonly caused by HSV type 2 viruses. These infections are also found in neonates and infants that transmitted through infected mothers. Conditions such as keratitis, uveitis, cataract or glaucoma are the most common causes of morbidity and/or visual loss. Recurrent infections in cornea following primary infections may cause epithelial keratitis. Sometimes stromal layer and endothelium may also be involved in the recurrent infections. Some of the risk factors associated with recurrent infections include UV light, stress, immunosuppressive agents, surgical trauma, corneal grafts, fever, etc [63, 65-66]. Recurrent infections occur frequently in epithelium, stroma or endothelium after corneal transplants.

Several drugs are used to treat HSV infections, including TFT, ACV (ACV), famcyclovir, cidofovir, idoxuridine (IDU), L-Valacyclovir (L-Val-ACV), L-Valganciclovir (L-Val-GCV), vidarabine etc. Thymidine analogues, such as IDU and TFT, involve in the polymerization of viral DNA resulting in defective viral replication [64]. Purine analogues, such as vidarabine, inhibit DNA polymerase by getting incorporated into viral DNA. Non-selective affinity of IDU, TFT and vidarabine to host DNA is the primary cause of corneal epithelial cell toxicity. Long term treatment with thymidine analogues also causes surface ocular toxicity [64]. ACV, a guanosine analogue, is phosphorylated to a monophosphate by virus enzyme HSV thymidine kinase and then to a triphosphate by host cellular enzymes. This triphosphate inhibits the HSV DNA polymerase stalling viral replication. Three percent ACV is available as topical ophthalmic ointment for the treatment of corneal epithelial infections. Multiple studies suggest that GCV is also very effective for the treatment of HSV 1&2. GCV is administered intravenously and as implants for the treatment of CMV retinitis in immune-compromised patients and is also indicated for CMV diseases in bone marrow transplant and organ transplant recipients.

GCV is also a guanosine analogue structurally similar to ACV (Figure 5). GCV is available as sodium salt marketed as Cytovene[®] and Cymevene[®] (Roche). It is also available as ocular inserts marketed under the name Vitrasert[®] (Bausch

and Lomb). A prodrug of GCV, L-Val-GCV, is also available for improved oral bioavailability. Topical GCV gel (1.5 mg/g) is marketed as Virgan[®] and Zirgan[®].

GCV is selectively phosphorylated by viral thymidine kinases to a monophosphate and subsequently into a triphosphate by host enzymes [67]. GCV

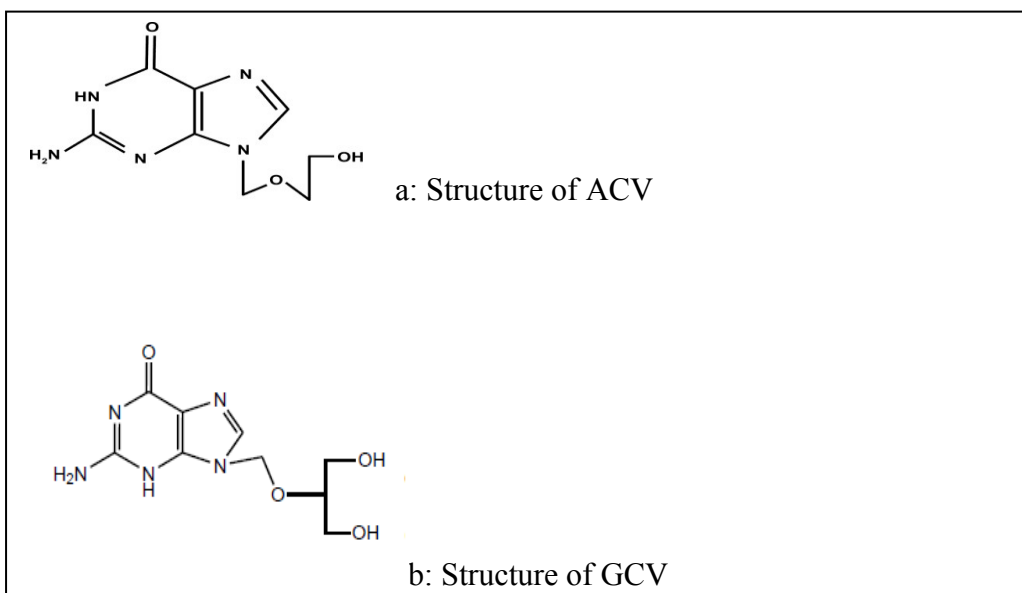


Figure 5. Chemical structures of (a) Acyclovir and (b) Ganciclovir

triphosphate is an active metabolite which elicits its action by arresting replication of virus through DNA polymerase inhibition [67]. GCV has more selective affinity to viral thymidine kinase compared to ACV, which is a rate limiting factor in conversion of thymidine analogues to respective monophosphates [5, 68-70]. GCV was found to be as effective as ACV and other antiviral agents for the treatment of HSV induced epithelial keratitis [62].

Effect of pre-corneal events on ocular bio-availability

The pre-corneal pocket or cul-de-sac can accommodate 6-7 μL of lacrimal fluid. An additional volume of 3 μL can be added without much overflow rendering the total capacity to ~ 10 μL [71-72]. A total volume of 30 μL can be retained in the pre-corneal area if the head is held upright without blinking the eye lids. Generally, the volume of drug solution administered is about 50 μL , even though commercially available eye-dropper dosage volume varies between 24 μL and 56 μL [73-74] depending on the size of the tip diameter. Following a 50 μL of topical eye drop administration, only 10 μL is retained in the pre-corneal area assuming an entire lacrimal fluid displacement. Therefore only 20% of the dose is available for absorption. In addition to the low retention, approximately within 5 minutes, a 16% per minute of tear turnover [75] reduces the dose to 8% of the initial 50 μL dose. Soon after topical drug administration, an additional reflex tearing is observed that further reduces the amount or concentration of the drug available for ocular absorption. In contrast, orally administered dose is retained in the intestinal lumen for significant amount of time enhancing the rate and extent of absorption. For this reason, fraction of dose (F) absorbed across the intestine is greater than eye. Administration of local anesthetics prior to the dosing may reduce reflex tears and in turn can enhance ocular drug absorption [76-78]. Zimmerman *et al.* and Huang *et al.* [79-80] suggested that blinking rate of the eye and occlusion of the naso-lacrimal duct may improve efficacy of the glaucoma

drugs. This study reported that, digital compression of the nasal canthal area and continuous eyelid closure may help retain the drug in the pre-corneal area and in turn can enhance ocular drug absorption. Another study performed by White *et al.* [81] provided correlation of eye blinking to the rate of technetium pertechnetate clearance. In this study dose was administered twice to the same eye, once with normal blinking and once with eye lids closed. After 2 minutes, half-life of drug in the blinking eye was about 93 ± 10 seconds compared to 1290 ± 578 seconds in the closed eye. But with 3- 5 minutes data, it was observed that half-life of technetium in the tear film is not significantly different between the two experiments [81]. An increase in the hypotensive response of pilocarpine is also observed when naso-lacrimal occlusion was performed. A single drop of 2% wt/v pilocarpine in subjects with naso-lacrimal occlusion elicits similar response relative to 4% wt/v pilocarpine dose without any occlusion [82]. A similar effect is observed with 1.5% wt/v carbachol administration with naso-lacrimal occlusion to 3% wt/v carbachol. Timolol maleate 0.5% wt/v was administered in subjects with and without naso-lacrimal occlusion. The peak aqueous humor concentrations in subjects with occlusion are observed to be 70% more than subjects without occlusion even though T_{max} in both studies was 1h, suggesting the higher rate of absorption in subjects with occlusion. Increase in the absorption rate can be attributed to higher drug concentrations in precorneal area due to lower rate of clearance from the pre-corneal compartment [83].

Several human studies were performed to correlate the effect of drop size on rate of drainage through canaliculi. An increase in the drop size from 1 μL to 10 μL and from 5 μL to 15 μL did not affect the rate of drainage. However, increase in the drop size to 20 μL altered the rate of drainage while the overflow from the pre-corneal area had altered the net effect [84-88]. Brown *et al.* compared the mydriatic effect of two 8 μL drops of 10% wt/v phenylephrine to two 32 μL drops of 2.5% wt/v phenylephrine. This study concluded that the mydriatic effect of phenylephrine after high concentration- low drop volume dosing was found to be slightly higher than the low concentration-high volume dosing. This result suggests a minimal effect of canaliculi drainage rate on drop size [89].

In another study, administration of two drops in rabbits was found to have little effect on the tear drug concentration. When two drops were administered at a distance of 1 min and 3 min apart, tear concentrations were found to increase only by 10% and 20% respectively [90]. A similar experiment was performed in 2 different groups of 50 human volunteers [86]. Tropicamide, 0.125% wt/v, or phenylephrine, 2.5% wt/v, was administered to volunteers, 2 drops in one eye and one drop in the control eye. Dilation of pupils was measured at 20 and 60 min in the tropicamide treated group and at 30 and 90 min in the phenylephrine treatment group. The mean dilation in tropicamide treatment group after 20 min were observed to be 2.2 ± 0.75 mm and 1.4 ± 0.72 mm in two drop and single drop

treated eyes respectively. Mean dilation after 60 min were measured to be 3.16 ± 0.83 mm and 2.34 ± 0.75 mm in two drop and one drop treated eyes, respectively. A similar trend was observed in the phenylephrine treatment group. The dilation was 33% in the two drops treated eyes. This contrast in rabbits and humans could be attributed to the difference in tear turnover rates, which are 7.1% and 16% respectively. In addition to the difference in tear turnover rates, rabbits also have nictitating membranes that are absent in humans. These nictitating membranes may prolong the contact time of drug in the rabbits, rendering the second drop redundant or effect minimally. In a study by Miller and O'Connor [91], the effect of nictitating membrane on residence of drug in the pre-corneal area was observed. Fluorescein concentrations in the tear film was observed over prolonged periods in rabbits with nictitating membranes, compared to the group of rabbits without any membrane.

Protein binding also can alter bio-availability. Human tears contain about 0.7% wt/v of proteins including 0.4% wt/v of albumin. In a study performed by Mikkelsen *et al.* an addition of 3% wt/v bovine serum albumin to the rabbit tears reduced the miotic effect of 0.025 M pilocarpine nitrate similar to a 0.00025 M concentration [92-93]. Elevated protein levels in disease states, such as conjunctivitis, might also affect drug binding, bio-availability and therapeutic response. Formulation excipients, such as cetylpyridinium chloride and benzalkonium chloride, can also compete for protein binding sites [94-95]. These

cationic surfactants bind to the same binding sites as of cationic drugs, such as pilocarpine, and in turn raise unbound drug concentrations in the lacrimal fluid. A rise in drug concentration can result in increased therapeutic response [95]. Such effect may not be observed if the excipients and active ingredient carry opposite charges. Permeation of anionic prednisolone phosphate is not altered in the presence of cationic benzalkonium chloride [96]. Flow chart below depicts the effects of precorneal events on the ocular pharmacokinetics (Figure 6).

Anterior segment pharmacokinetics following topical administration

The intraocular absorption mechanisms of topically applied drugs may determine the strategies that can be utilized to optimize ocular drug delivery. Cornea is considered one of the major pathways by which drugs are absorbed into the globe. In an experiment performed by Doane *et al.* absorption of hydrocortisone and pilocarpine through the cornea were blocked. The amounts of these drugs in the iris ciliary were found to be decreased by 40 and 5 times respectively [97]. This study not only confirmed that cornea is the major route of drug absorption into the anterior segment but also indicated the partial drug entry through conjunctiva and sclera. Topical route of administration is mainly utilized to treat diseases of anterior chamber. As mentioned earlier, drug accumulation is almost negligible in the posterior segment following topical administration.

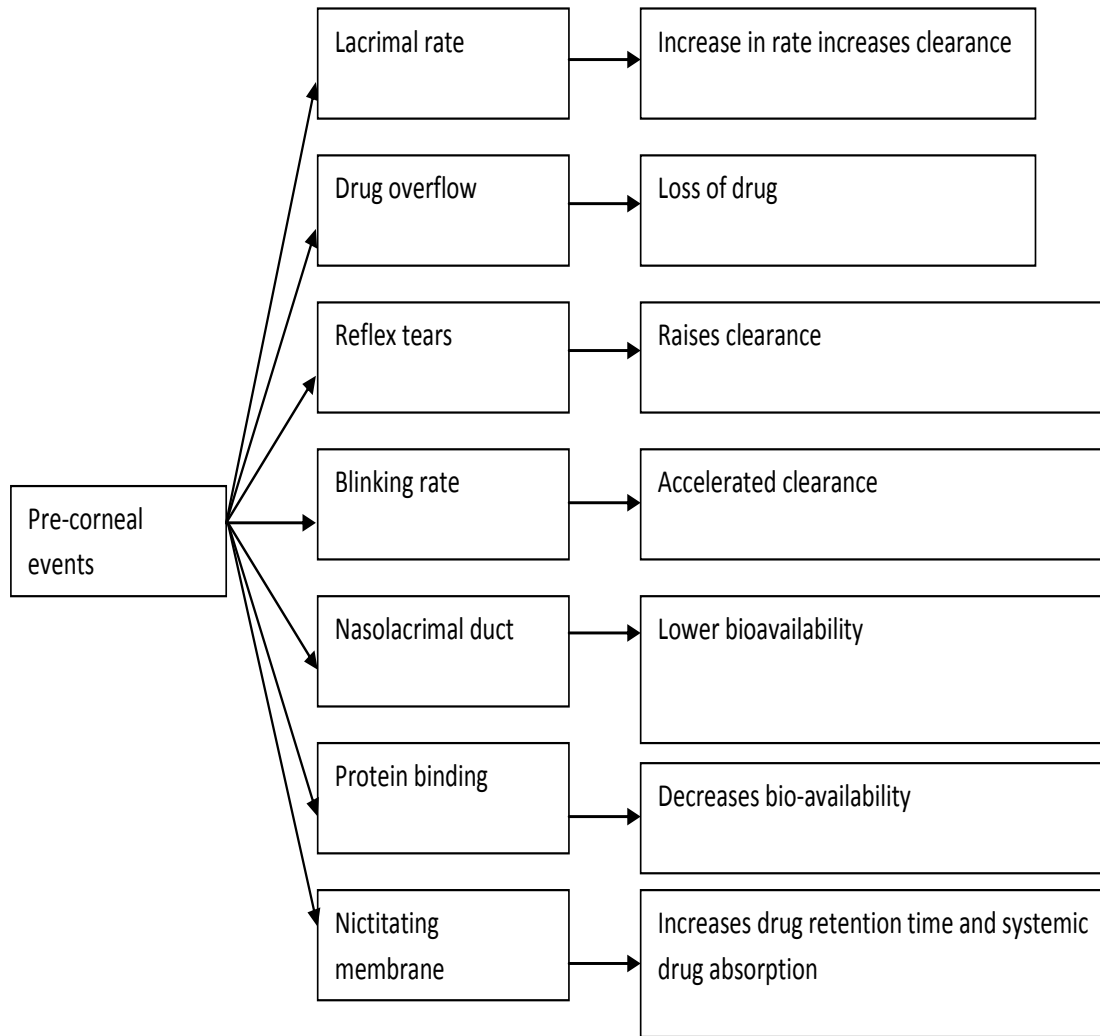


Figure 6. Flow chart below depicts the effects of precorneal events on the ocular pharmacokinetics

Hence it is necessary to sample the aqueous humor in the anterior chamber as opposed to the vitreous humor in the posterior segment of the eye following topical route of administration.

Aqueous humor is the central compartment of the eye similar to the blood in the body. It is the circulating fluid of the eye through which most of the drugs are distributed to the various tissues such as cornea, lens and iris ciliary body, etc. Drug concentrations in the central compartment, in this case aqueous humor, have been correlated to the concentrations in peripheral tissues in the anterior chamber. Moreover, collection and processing of fluid samples is relatively convenient compared to the tissues.

Predicting optimal dosage regimen for ocular drug delivery is one of the most complex processes. Ocular pharmacokinetic study of drugs is a difficult process due to the inaccessibility of internal tissues of the human eye. Rabbit models are often used to study toxicity, pharmacokinetics and pharmacodynamics of drugs and formulations applied to the eye. Irrespective of the models, continuous sampling of ocular fluids is a major constraint. Unlike blood, volume of ocular fluids is comparatively low for serial sampling. Further contributing to the difficulty in assessing ocular pharmacokinetics of drugs is the fact that a single rabbit eye must be used for a single time point [98]. Even though ocular tissues can be collected and analyzed for drug concentrations, minimum variability in pharmacokinetic profile can only be achieved by sacrificing 6-20

eyes per time interval. To achieve statistically valid parameters, such as absorption rate constant (K_a), volume of distribution (V_d) and clearance (Cl), a minimum of 10 sufficiently spaced time intervals are required. About 120-150 animals are required to complete a single dose pharmacokinetic study from which valid information can be obtained. Apart from using large number of animals, an assumption is made that a representative pharmacokinetic profile will result if a sufficient set of consecutive non-continuous intervals is employed.

Evidence exists to indicate absorption rate of drugs across the cornea is slower than the rate of elimination from the eye, complicating the assignment of slopes. Failure to recognize parallel first order non-absorptive processes such as drainage from the eye can result in an over estimation of transcorneal absorption rate constant [99-100]. Whenever multiple tissues and fluids are simultaneously measured for drugs a number of barriers and compartments can be identified in describing the pharmacokinetics of the eye (Figure 7).

Makoid *et al.* described the ocular disposition of pilocarpine using a four compartment classical model represented by a four exponential equation yielding eight equation parameters. These polyexponential equations have been applied to the rabbit eye to determine the pharmacokinetic parameters [101-105]. Various other models used in studying ocular pharmacokinetics have also been determined. The Figure 8 depicts few of the compartmental models in predicting

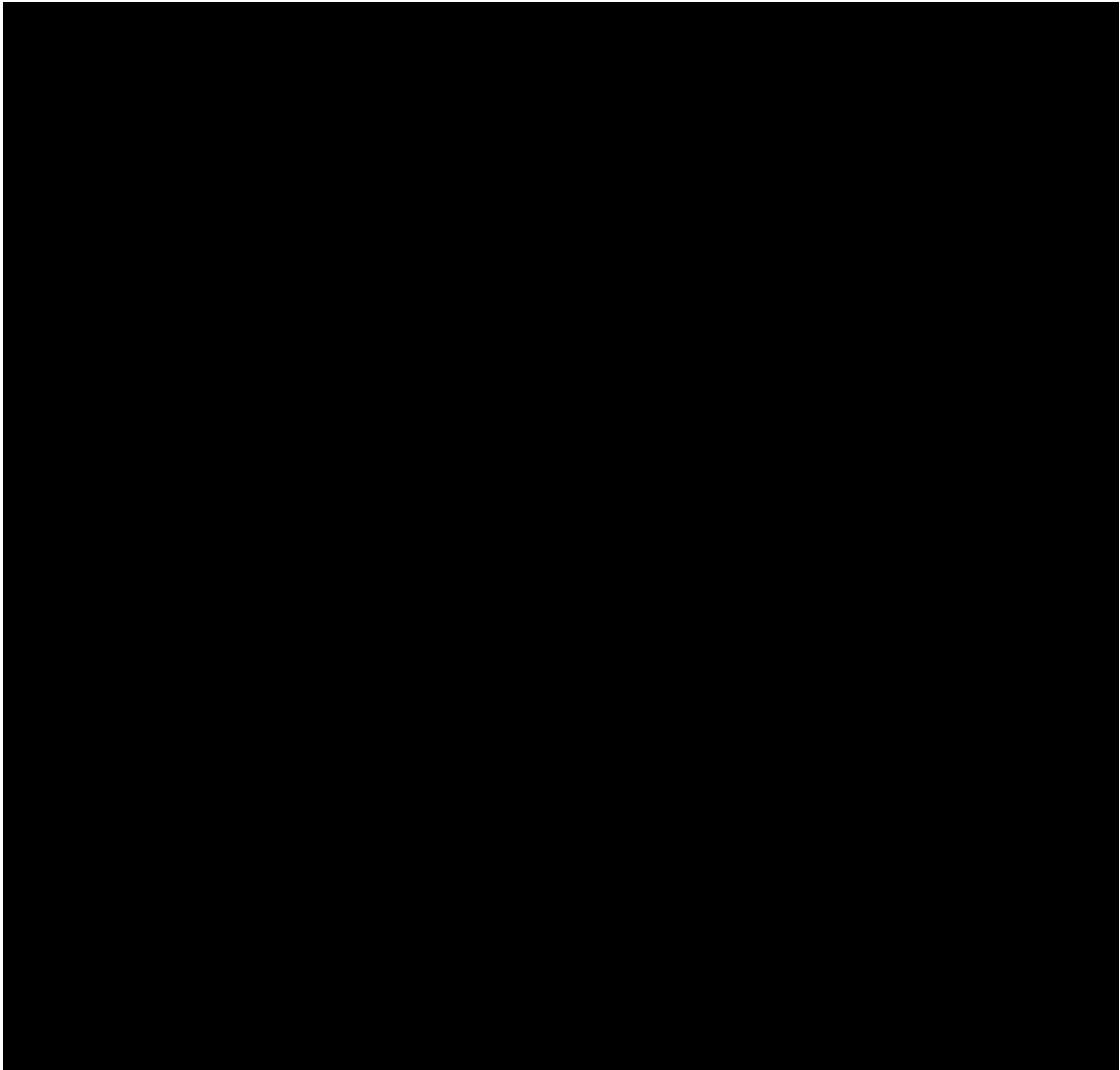
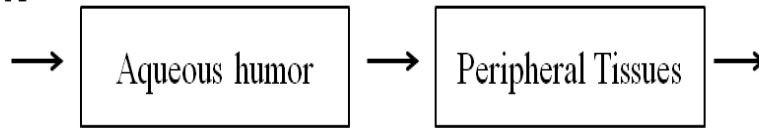
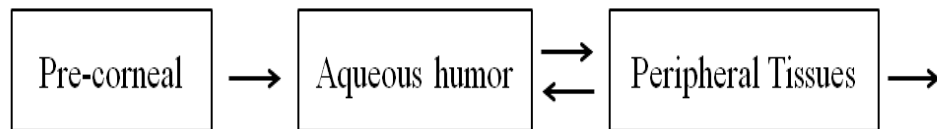


Figure 7. : Model depicting precorneal and intraocular drug movement following topical dosing.

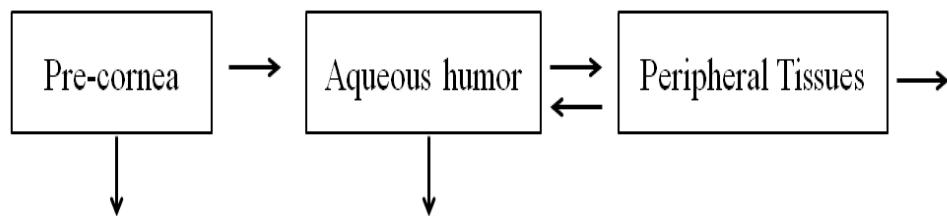
Scheme A



Scheme B



Scheme C



Scheme D

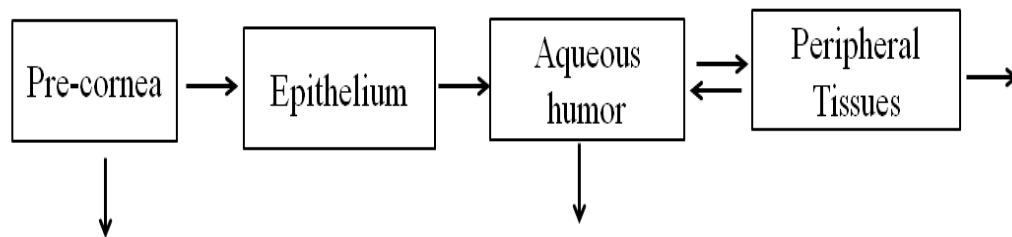


Figure 8. Above schemes (A to D) are various compartmental models which are frequently used to explain ocular pharmacokinetics

ocular pharmacokinetics across various tissues and ocular fluids which are considered as separate physiological compartments.

Eller *et al.* [106] developed a procedure to estimate the absorption rate constant into the aqueous humor. Constant concentration of drug was maintained on the cornea of anesthetized rabbits to eliminate the pre-corneal effects and apply simpler equations independent of modeling. A zero order infusion/input of drug was maintained through the use of a plastic cylinder that was placed over the cornea. Rate of absorption, volume of distribution and rate of elimination were determined independent of peripheral compartments. A known volume of drug solution was retained on the cornea over a period of time to estimate the absorption rate constant (k_a), and clearance in anterior chamber. Below equations were derived to estimate absorption rate constant (k_a), anterior chamber clearance (Cl_o), and volume of distribution at steady state (V_{ss}) (Equations 1 to 4).

Equation 1

$$k_a = \frac{V_A \left(\frac{dC_a}{dt} \right)_i}{C_w V_w}$$

Equation 2

$$Cl_o = \frac{K_0 T}{AUC}$$

Equation 3

$$K_0 = \left(\frac{dC_a}{dt} \right)_i V_A$$

Equation 4

$$V_{ss} = \frac{K_0 T \text{AUMC}}{(\text{AUC})^2} - \frac{K_0 T^2}{2(\text{AUC})}$$

k_a = first-order absorption rate constant

K_0 = rate constant of zero-order input

V_A = Volume of aqueous humor

V_w = Volume of drug solution in the well

V_{ss} = Volume of distribution at steady state

$(dC_a/dt)_i$ = rate of appearance of drug in aqueous humor in the initial data points

Cl_o = Ocular clearance

C_w = Concentration of drug in the infusion well

T = Time of infusion

AUC = Area under the drug concentration V_s time curve

AUMC = Total area under first-moment curve (plot of $C_t - t$)

i = initial time of infusion

This model can be used to determine rate of absorption across various membranes of the eye. However in this model, accumulation of drugs in the ocular tissues was not quantified, but the loss of drug from the well was quantified to deduce pharmacokinetic parameters. This method has limited potential due to the reliance on the large number of animals. Inter individual variability in the data makes pharmacokinetic analysis difficult. Mitra *et al.* developed a microdialysis technique to collect samples directly from the anterior segment of the eye. A combination of well model and microdialysis was utilized to study absorption mechanism of various prodrugs. Microdialysis is a technique to perform continuous *in vivo* sampling of drugs in extracellular matrix. A microdialysis probe is a semi permeable dialysis membrane, implanted into aqueous or vitreous humor and is continuously perfused with isotonic buffer

solution. Xenobiotics can diffuse across the membrane into inner chamber of the probe from the external matrix; from there it is collected as dialysate at the end of the tubing outside matrix. The use of microdialysis has resulted in more precise pharmacokinetic analysis with a need for fewer animals than conventional sampling. Several studies have shown the utility of microdialysis in evaluating pharmacokinetics of ophthalmic medications. A combination of well model and microdialysis can provide precise prediction of ocular absorption, minimize inter individual variability, and reduce the number of subjects for an ocular pharmacokinetic study.

Dey *et al.* and Hariharan *et al.* studied ocular kinetics of erythromycin using well model and anterior segment microdialysis [18, 107]. Absorption rate constants of erythromycin were determined using Eller *et al.* equation. Absorption rates were also determined in presence of testosterone. This model proved to be very effective in studying both transporter activity and drug interactions. An accurate prediction of rate of absorption and rate of elimination were determined. Slow absorption rate of erythromycin through cornea and faster clearance was observed showing the flip-flop nature of kinetics in the anterior chamber. This model proved to very effective in determining the absorption rate, clearance and distribution of various amino acid and dipeptide prodrugs of ACV and GCV [108-110].

CHAPTER 3

CYTOTOXICITY ASSAYS OF AMINO ACID AND DI-PEPTIDE PRODRUGS OF GCV ON RABBIT PRIMARY CORNEAL EPITHELIAL CELLS (RPCEC)

Rationale

A series of amino acid mono-esters and di-esters, and di-peptide monoester of GCV were synthesized [35, 111] to enhance the pharmaceutical properties of GCV and to target amino acid and peptide transporters on the rabbit cornea. In previous studies from our laboratory, these prodrugs showed variable chemical and enzymatic stabilities. *In vitro* antiviral studies on HSV 1 & 2, VZV, and CMV were also performed to evaluate their efficacies. Some of the prodrugs showed either equivalent or better anti viral properties than GCV and ACV [112]. In this chapter, a series of cell proliferation studies will be performed to evaluate the cytotoxic effects of these prodrugs and will be compared with the parent drug molecule GCV and the current anti-HSV standard drug TFT. Since the rationale of this dissertation was to develop a therapy for the HSV infections of the cornea, all the *in vitro* cell culture studies were performed on rabbit Primary Corneal Epithelial Cells (rPCEC).

Methods and materials

Cell proliferation assay:

Cell proliferation assays were performed to examine the cytotoxicity of GCV and its prodrugs, L-Glu-GCV, L-Phe-GCV and L-Tyr-GCV, Di-L-Phe-

GCV, Di-L-Glu-GCV, L-Val-GCV, L-Val-L-Val-GCV, L-Gly-L-Val-GCV and L-Tyr-L-Val-GCV and compared against TFT. For this assay, CellTiter 96 Aqueous nonradioactive cell proliferation assay kit (Promega, Madison, WI) was used. This assay is a colorimetric method for determining the number of viable cells in proliferation. The method comprises of a novel tetrazolium compound, 3-(4,5-dimethylthiazol-2-yl)-5-(3-carboxymethoxyphenyl)-2-(4-sulfophenyl)-2H-tetrazolium (MTS) and an electron coupling reagent, phenazine methosulfate (PMS). MTS is bio-reduced by cells into formazan that is soluble in tissue culture medium. The conversion of MTS into the water soluble formazan is accomplished by dehydrogenase enzymes found in metabolically active cells. The quantity of formazan produced, as measured by the amount at 490 nm absorbance, is directly proportional to the number of viable cells in culture.

Rabbit primary corneal epithelial cells (rPCEC) were plated in 96-well plates and the seeding density was optimized at 1.25×10^4 cells/well. Solutions of GCV, its prodrugs, and TFT of different concentrations, 0.2mM, 1mM and 5mM, were prepared in the culture medium. Hundred microliters of drug solution in culture medium was added in each well. The cells were incubated with the drug solutions for 24 in a humidified 5% CO₂ atmosphere. The effect of the compounds on the proliferation of these cells was observed with a change in the drug concentration. Proliferation of rPCEC in the presence of GCV and its prodrugs were compared against TFT. Proliferation of the cells in the presence of

all drug solutions were also compared with a positive control (without drug) and these values were all corrected for with a negative control (without cells). The cell proliferation assays were conducted according to the manufacturer's protocol. Exactly after 24h of incubating the cells with drug solutions, 20 μ L of the MTS/PMS solution was added to each well. The plate was then incubated for another 4 h at 37°C in a humidified 5% CO₂ atmosphere to allow for the dye to interact with the cells. The absorbance of the solutions was read at 490 nm with an automated 96-well microplate reader. Because the amount of formazan produced is directly proportional to the number of viable cells in culture, percentage of viable cells was calculated for drug treated wells against positive control.

Statistical Analysis:

Cell proliferation assays were conducted in sets of eight experiments (n=8) to address the variability. Results are expressed as mean \pm standard deviations (SD). ANOVA was performed at a statistical significance of $p < 0.05$.

Results

Estimation of cytotoxicity utilizing cell proliferation assay:

Cell proliferation assays were carried out to estimate the cytotoxicity of GCV and TFT solutions (Figure 9) at three concentrations of 0.2mM, 1mM and 5mM. After 24h of exposure, rPCEC cells showed approximately 95-100% of cell viability at 0.2 mM and 1mM concentrations of GCV. At 5mM concentration of

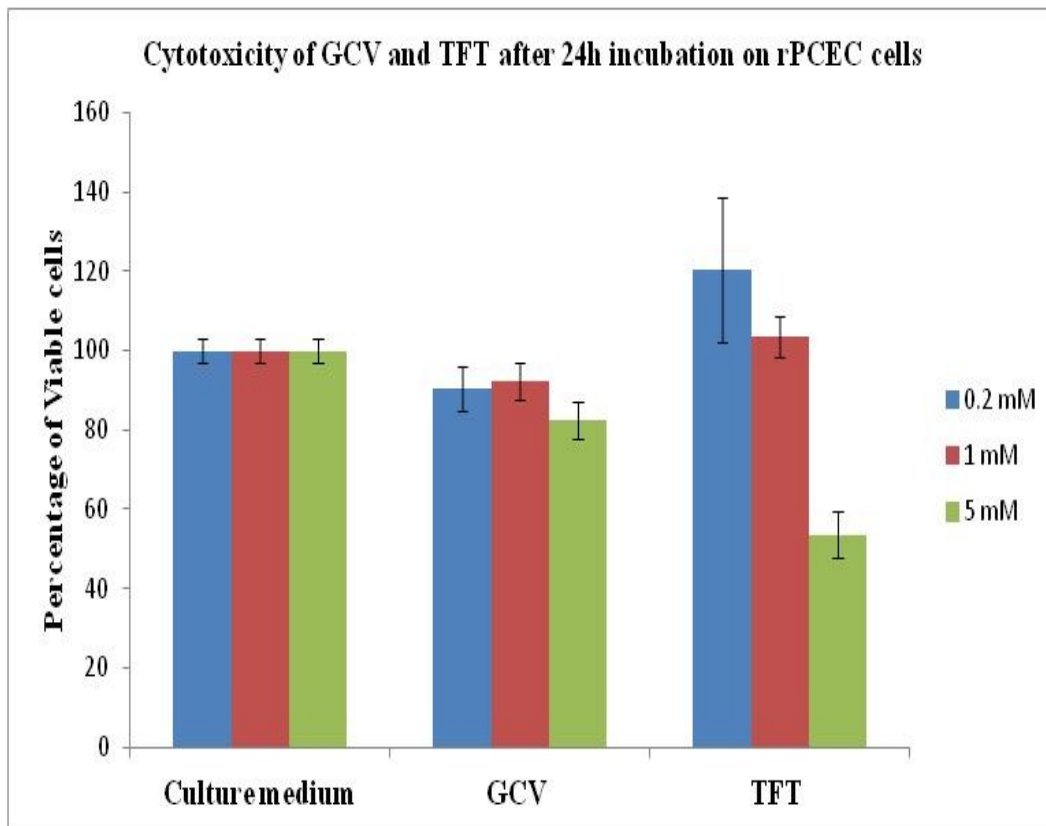


Figure 9. Cytotoxicity studies performed on rPCEC cells after the incubation of ganciclovir (GCV) and trifluorothymidine (TFT) at 0.2 (blue), 1 (Burgundy) and 5 (Green) mM concentrations for 24h.

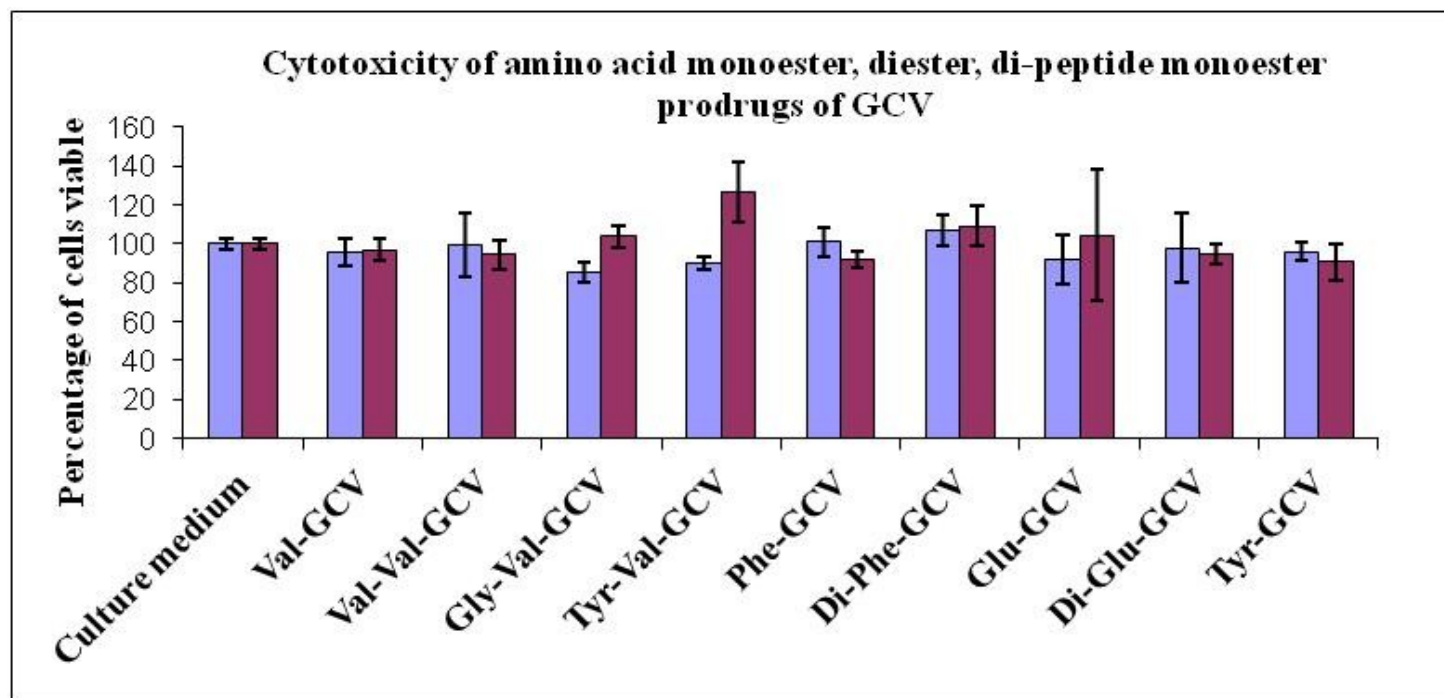


Figure 10. Cytotoxicity assays performed on rPCEC cells after the treatment with amino acid monoester and amino acid di-ester prodrugs, and di-peptide monoester prodrugs of GCV for 24h. All the amino acids were L-isomers. Concentrations of prodrugs used were 0.2 mM (Blue) and 1 mM (Burgundy). Number of experiments performed were, $n = 8$. Error bars represent mean \pm SD.

Table 1. Mean percentage of rPCEC cells viable after treatment with GCV, TFT, and all prodrugs. Data represented as mean \pm SD. Number of experiments performed were, n=8.

Drug/ Prodrug	0.2 mM	1 mM	5 mM
Culture medium/ control	100 \pm 3	100 \pm 3.1	100 \pm 2.9
GCV	90.5 \pm 5.8	92.2 \pm 4.7	82.5 \pm 4.7*
TFT	120.5 \pm 18.2	103.6 \pm 5.3	53.6 \pm 5.9*
L-Val-GCV	95.9 \pm 7.3	97.1 \pm 5.4	ND
L-Val-L-Val-GCV	99.3 \pm 16.6	94.4 \pm 7.2	ND
L-Gly-L-Val-GCV	85.3 \pm 4.9 ^ψ	104 \pm 5.5	ND
L-Tyr-L-Val-GCV	90 \pm 3.1 ^ψ	126.6 \pm 15.7 ^π	ND
L-Phe-GCV	101.2 \pm 7.6	91.9 \pm 4.1	ND
Di-L-Phe-GCV	107.1 \pm 7.8	109 \pm 10.2	ND
L-Glu-GCV	92.2 \pm 12.6	104.4 \pm 33.8	ND
Di-L-Glu-GCV	97.9 \pm 4.8	94.6 \pm 4.9	ND
L-Tyr-GCV	96.2 \pm 4.4	90.7 \pm 9.7	ND

Ψ - $p < 0.05$, between the control and 0.2 mM

Π - $p < 0.05$, between the control and 1 mM

* - $p < 0.05$, between the control and 5 mM

GCV, 80-85% cell viability was observed when compared with the control group. When rPCEC cells were incubated with 0.2 mM and 1mM concentrations of TFT, 90-120% of cells were observed to be viable. However, at 5 mM concentrations, only 55% cells were found to be viable (Table 1). Approximately half of the cells were found to be dead at this concentration of TFT.

Cytotoxicity of amino acid monoester and di-ester prodrugs and di-peptide monoester prodrugs of GCV were studied. All the prodrugs were used at 0.2 mM and 1mM concentrations. After 24 h exposure to the prodrugs, rPCEC cells did not indicate any inhibition of cell proliferation (Figure 10). Approximately, 90-120% cells were viable with all the amino acid and di-peptide prodrugs (Table 1).

Discussion and conclusions

Cell proliferations assays performed on rPCEC cells were found to be a significant tool of decision making in designing further experiments. Studies conclude that all the prodrugs were found to be non-cytotoxic at the concentrations used even after 24h incubation period. Most of the drug solution applied topically to eye will be lost either because of the overflow from the cul-de-sac, or reflex blinking or dilution and drainage through tears or drainage through the naso-lacrimal duct. Almost 90% of the drug solution is lost within 10-15 min of administration. If we take that into account, for a given 50 μ L drop of 1% wt/v of drug which is equivalent to 500 μ g, about 450 μ g is lost within 10-50

min. Remaining 50 μg of drug is available for absorption through cornea, conjunctival blood circulation and eye lids. If a 500 μg or 50 μL of 1% wt/v of drug/pro-drug is administered to the eye, only 50 μg will be available to exhibit either toxicity or efficacy. The rPCEC cells in these experiments are treated with up to 1 mM concentrations of prodrugs, which are higher than the concentrations expected to stay in the cul-de-sac after 10-15 min post topical administration. Multiple doses are given each day, few drugs such as TFT are administered up to 9 times a day, so the closest mimicking experiment could be to treat the cells for 24h. This experiment gives an approximation of how safe these drugs are at given concentrations and exposure times. A direct extrapolation from *in vitro* to *in vivo* would be a concoction for a disaster, so we could only conclude that these prodrugs are safe at these concentrations and time. In the future, designing an experiment involving time based repeated exposures/administrations at expected/calculated concentrations would give a better understanding of drug/prodrug toxicities in the eye.

CHAPTER 4

ANTERIOR CHAMBER PHARMACOKINETICS OF L-ARGININE AND L-AMINO ACID MONOESTER AND DIESTER PRODRUGS OF GCV IN RABBIT EYES AND THEIR INTERACTION WITH B⁰⁺ TRANSPORTER ON THE RABBIT CORNEA AND RABBIT PRIMARY CORNEAL EPITHELIAL CELLS (RPCEC)

Rationale

Herpes simplex virus (HSV) is one of the common causes for corneal keratitis [1-2]. Two common types of viruses, HSV-1 and HSV-2, infect both the epithelium and stroma of the cornea which are associated with ulceration, inflammation and possibly blindness [1-2]. One percent topical solution of TFT is currently available as a drug of choice against HSV-1 and HSV-2 induced infections of the eye. However, one of the major problems associated with TFT is its cytotoxicity restricting its use for a prolonged period of time [3]. In superficial herpes keratitis the efficacy of a 3% wt/wt ophthalmic ointment of ACV applied 5 times a day for up to 14 days has been studied. However, ACV ointment has not been approved in United States for clinical purpose. ACV ointment has not been indicated against stromal keratitis or when the deeper ocular tissues are involved possibly because of poor permeability of ACV across cornea. ACV is relatively hydrophilic in nature which could be the primary reason for the low permeability across cornea. Cornea is a complex tissue with highly lipoidal epithelium on the serosal side with tight junctions. Beneath the epithelium lies the stroma

constituting 90% of water, which makes it hydrophilic in nature. Drugs, in order to cross the complex cornea require optimal lipophilicity.

GCV, structural analog of ACV demonstrated excellent antiviral activity against HSV-1 and 2 as well as HCMV. It was found to be as effective as ACV against HSV-1 and HSV-2 [5]. Even though GCV has good antiviral activity against HSV [113], its limited corneal permeability and poor solubility makes it a bad choice for the treatment of HSV keratitis [6]. A 0.15% wt/wt gel of GCV was found to be well tolerated and as effective as 3% wt/wt ACV ointment. However, this gel causes transient blurring of the vision when applied topically which resulted in a limited acceptance of this ophthalmic formulation. Lipophilic Acyl-ester prodrugs of GCV were synthesized in an attempt to formulate topical solution of GCV for HSV keratitis [6]. Although, permeability of GCV was found to increase, the solubility of the prodrugs was lower than GCV. In an attempt to increase the solubility of these compounds, Hydroxypropyl- β -Cyclodextrins (HP- β -CD) were employed. Despite the higher solubility and chemical stability with HP- β -CD, concentrations of above 5% wt/v were found to be toxic to the eye [114].

Recently a significant work has been published on nutrient transporters and their use in drug delivery. Transporters such as amino acid transporters, peptide transporters, vitamin transporters etc have been reported to be present on

the corneal epithelium [8, 40, 43-44, 59, 115]. Amino acid transporters are the most widely classified transporters. These are mainly divided into cationic, anionic and neutral amino acid transporters. These are also sub classified based on their sodium ion, chloride ion and potassium ion dependency in transport/co-transport of amino acids in to the cells through the plasma membranes. So far, ASC, B^{0,+} and LAT amino acid transporters were found to be present on the cornea [43-44, 46]. B^{0,+} is a sodium dependent neutral and cationic amino acid transporter. This transporter translocates both neutral and cationic amino acids across the corneal epithelium. A co-transport of sodium and chloride ions also takes place along with the transport of one amino acid. Previously from our lab, Jain-Vakkalagadda *et al.* has demonstrated the presence of B^{0,+} on the corneal epithelium using in vitro models [44].

Topical infusion model is an adaptation of the model published by Eller *et al.* in 1985 [106]. In this model, a drug filled well is placed over the cornea for a period of 2hr. A constant infusion of drug is given through the cornea to minimize the effects of tear dynamics, drug drainage from the eye pocket and the drug absorption through the other tissues such as nictitating membrane and the conjunctiva. Previously, several pharmacokinetic models had been proposed for topically applied drugs to determine their absorption rate, distribution and the elimination of drugs for topically applied drugs. These models either had failed to

assign absorption, distribution and elimination rates accurately or propose very complex compartmental models [100-105]. Corneal infusion model was first proposed by Eller *et al.* where the author collected samples from the well and determined the absorption rates of by measuring drug disappearance from the well [106]. Tirucheraï *et al.* and Dey *et al.* from our laboratory have developed a topical infusion model by combining Eller *et al.* model and microdialysis techniques to accurately determine the corneal absorption rates of drugs [18, 116].

In this chapter, *in vivo* functional activity of B^{0,+} was studied using L-Arginine as a natural substrate for the transporter. Amino acid mono and di ester prodrugs of GCV, γ -L-Glutamate-GCV, L-Tyrosine-GCV and γ -L-Phenylalanine-GCV (Figure 11) were studied for their *in vitro* uptake using rPCEC for their affinity towards B^{0,+} and their anterior chamber kinetics using topical infusion method. Cytotoxicity of these prodrugs was examined *in vitro* employing rPCEC.

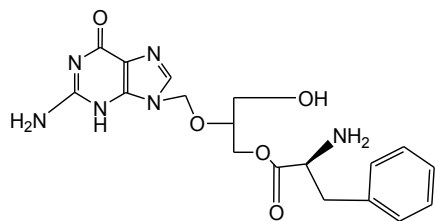
Materials and methods

GCV was obtained as a gift from Hoffman La Roche (Nutley, NJ). All other chemicals were purchased from Sigma Chemical Company (St Louis, MO), unless otherwise mentioned, and used without further purification. Linear probes (MD-2000, 0.32 x 10 mm, polyacrylonitrile membrane and 0.22 mm tubing) used for aqueous humor sampling were obtained from Bio Analytical Systems (West

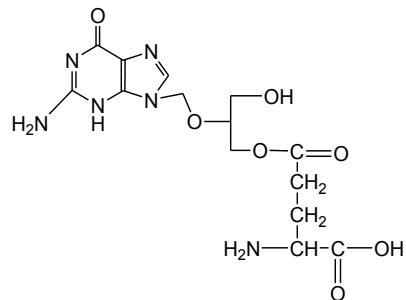
Lafayette, IN). A microinjection pump (CMA/100), for pumping isotonic buffer was purchased from CMA Microdialysis, (Acton MA). Ketamine hydrochloride was obtained from Fort Dodge Animal Health. Rompun (xylazine) was obtained from Bayer Animal Health. Topical wells were custom made by Hansen Ophthalmic Development Corporation, Iowa City, IA) according to special instructions.

Uptake Studies:

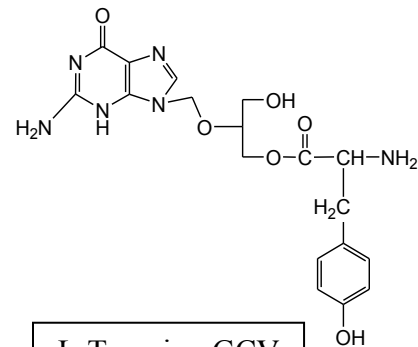
Uptake experiments of [³H] L-Arginine were conducted 10-12 days post-seeding of rPCEC. The medium was aspirated and the cells were rinsed twice (once in 10 minutes) with Dulbecco's phosphate buffered saline (DPBS; pH 7.4), containing 130 mM NaCl, 2.5 mM KCl, 7.5 mM Na₂HPO₄, 1.5 mM KH₂PO₄, 1 mM CaCl₂, 0.5 mM MgSO₄, and 5 mM glucose. Uptake was initiated by incubating the cells with 1 mL of [³H] L-Arginine in DPBS (pH 7.4) for a period of 30 minutes. This served as control. Cells were also incubated with 1 mL of [³H] L-Arginine and prodrugs of GCV in DPBS (pH 7.4) for a period of 30 minutes. At the end of incubation period, the drug solution was aspirated and cells were rinsed twice with 1 mL of ice-cold stop solution (210 mM KCl, 2 mM HEPES) to arrest the cellular uptake. Finally, the cells were lysed with 1 mL of 0.3% wt/v NaOH containing 0.1% wt/v Triton-X solution and left overnight. Five hundred microliters of the solution from each well was then transferred to



L-Phenylalanine-GCV

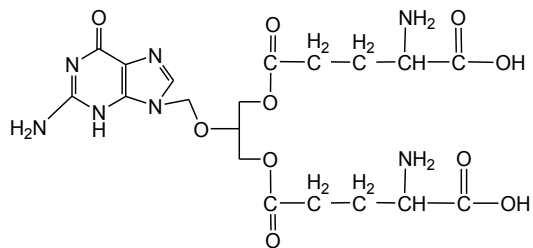


γ -Glutamate-GCV

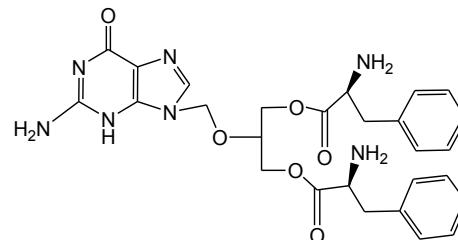


L-Tyrosine-GCV

54



Di - γ -Glutamate-GCV



Di-L-Phenylalanine-GCV

Figure 11. Structures of mono and di-ester amino acid prodrugs of GCV.

scintillation vials and 5 mL of scintillation cocktail was added in each vial. Cellular radioactivity was quantified using a scintillation counter (Model LS-9000; Beckman Instruments Inc., Fullerton, CA). Twenty microliters of the cell lysate from each well was utilized to measure protein content in each sample using Bradford's method (Bio-Rad protein assay kit, Hercules, CA).

Anterior Chamber Microdialysis:

New Zealand albino male rabbits weighing between 5.0 - 5.5 lbs were obtained from Myrtle's Rabbitry (Thompson Station, TN). The animals were kept under anesthesia throughout the experiment with ketamine HCl (35 mg/kg) and xylazine (3.5 mg/kg) given intramuscularly every hour. The animal experiments were conducted according to the approved protocol IACUC, UMKC. Before implanting the linear microdialysis probes, pupils were dilated with two drops of 1% wt/v tropicamide. The linear probe was then implanted in the anterior chamber using a 25-gauge needle. It was inserted across the cornea just above the corneal scleral-limbus so that it traverses through the center of the anterior chamber to the opposite end of the cornea as evidenced by microscopic examination. The sample-collecting end of the linear probe was inserted carefully into the bevel edge end of the needle. The needle was slowly retracted leaving the probe with the dialyzing membrane in the middle of the anterior chamber. The outlet of the probe was fixed to prevent any disturbances during sample

collection. The probe was perfused with isotonic phosphate buffer saline (pH 7.4) at a flow rate of $2.4 \mu\text{L min}^{-1}$ using a CMA/100 microinjection pump. After probe implantation, the animals were allowed to stabilize for 2 h before the initiation of any study. This duration has been shown to be sufficient for the restoration of intraocular pressure and replenishment of the aqueous humor originally lost during probe implantation [116]. After the 2 h stabilization, eyelids of the rabbit were mechanically retracted with Colibri retractors and topical well was placed over the eye such that the well was right on top of the cornea (Figure 12). This positioning allowed the drug solution to be in direct contact with the cornea and exclude the sclera. The outer flange of the topical well was coated with a surgical adhesive to prevent its movement. Subsequent to placing the well, the animals were allowed to stabilize for another 45 min to maintain proper intraocular pressure. After this time period, 200 μL of isotonic phosphate-buffered saline containing drug(s) was added to the well. The drug solution was allowed to diffuse for a period of 120 min after which it was aspirated from the well, which in turn was subsequently removed. The corneal surface was washed with a few drops of distilled water. Samples were collected every 20 min throughout the infusion and post infusion phases over a period of 8 h. At the end of experiment, euthanasia was performed under deep anesthesia with an intravenous injection of



Figure 12. Corneal infusion well model and microdialysis in rabbit anterior chamber

sodium pentobarbital through the marginal ear vein. Samples obtained in the study were then analyzed by high performance liquid chromatography.

In Vitro Probe Calibration:

Microdialysis probe recovery was determined in an aqueous solution containing a known concentration of the compound maintained at physiological temperature. The probe was continuously perfused at a constant flow rate of 3 $\mu\text{L min}^{-1}$ and samples were collected every 20 minutes. The ratio between the concentration of a substance in solution outside the probe and the dialysate is defined as “recovery”, which usually is expressed as a ratio or percentage. The recovery factor of the probes is an important factor in determining the extracellular concentration of the drug. The recovery of a compound of interest is calculated according to Equation 5.

Equation 5

$$\text{Recovery} = C_{\text{out}}/C_{\text{in}}$$

C_{out} is the concentration in the outflow solution and C_{in} the concentration in the medium. The dialysate concentrations were transformed into the actual anterior chamber concentrations by Equation 6

Equation 6

$$C_{\text{in}} * = C_{\text{out}} */\text{recovery}$$

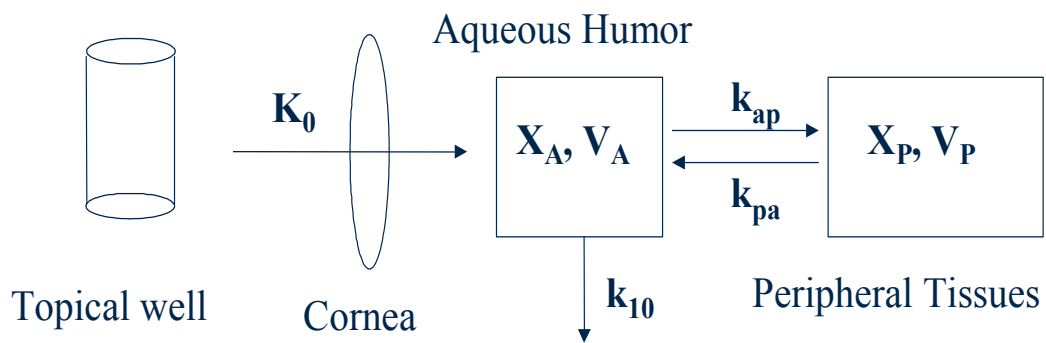


Figure 13. Schematic model representation of a single-dose continuous infusion well model to the rabbit eye

C_{in}^* is the substance concentration in the aqueous humor, and C_{out}^* is the concentration of the compound in dialysate.

Pharmacokinetic data analysis:

A model has been depicted in Figure 13 in which a drug is administered at a constant rate (k_0) to the corneal surface. The disposition of drug in the aqueous humor may be given by

Equation 7

$$\frac{dX_a}{dt} = k_0 - k_{ap}X_a + k_{pa}X_p - k_{10}X_a$$

X_a denotes the amount of drug in the aqueous humor, k_{ap} and k_{pa} are the first order rate constants for the transfer of the drug from the aqueous humor to the peripheral compartment and vice versa. Peripheral tissues are lens, iris ciliary body, k_{10} represents the overall elimination from the aqueous humor. The subscripts a and p refer to the aqueous and peripheral compartments respectively.

The constant input rate is related to the drug in the pre-corneal area by Equation 8

Equation 8

$$K_0 = k_a C_w V_w$$

k_a represents the corneal absorption first order rate constant, C_w is the concentration of the drug in the well, and V_w denotes the volume of the drug solution in the well.

Substituting for K_0 from Equation 8 into Equation 7, and knowing that during initial period of the infusion, concentration of drug in the well (C_w) is much greater than concentration of drug in the aqueous humor (C_a), the first term on the right side of Equation 7 predominates over the second, third and fourth terms. Thus, Equation 7 can be rewritten as Equation 9

Equation 9

$$\left(\frac{dX_a}{dt} \right)_I = k_a C_w V_w$$

The rate of change of drug concentration in the aqueous humor can be expressed according to Equation 10

Equation 10

$$\left(\frac{dC_a}{dt} \right)_I = k_a C_w V_w / V_a$$

V_a is the physiological volume of the aqueous humor (300 μ l). Subscript I represent the initial rate which can be determined from the initial slope of C_a

versus t as determined by aqueous humor microdialysis. Equation 10 may be rearranged as Equation 11 to allow estimation of k_a .

Equation 11

$$k_a = \frac{\left(\frac{dC_a}{dt}\right)_I * V_a}{C_w V_w}$$

If the topical infusion is allowed to continue until steady state is reached, then integration of equation 3 yields Equation 12:

Equation 12

$$C_{ss} = k_0/k_{10} * V_a q = k_a * V_w * C_w / k_{10} * V_a q$$

Thus topical infusion method along with Equation 7-12 permit a rational and reliable determination of ocular pharmacokinetics whereby absorption and disposition can be characterized without using complex compartmental analysis.

Data analysis of *in vitro* uptake experiments:

Dose – dependent inhibition data was fitted to a dose-response relationship given by Equation 13

Equation 13

$$Y = \min + \frac{\max - \min}{1 + 10^{(\text{LogIC}_{50} - x) * H}}$$

IC_{50} is the inhibitor concentration where the rate of ocular absorption is doubled and H is the Hill constant. Data was fitted to Equation **13** using a transformed non-linear regression curve analysis program (GraphPad Prism Version 3.03).

Analytical Procedures:

Tritiated L-Arginine perfusate samples obtained from anterior chamber microdialysis were analyzed using scintillation counter. All other samples of microdialysis were assayed using a reversed phase HPLC. The HPLC system was comprised of a waters pump, an Alcott 1500 series auto sampler and an Agilent 1100 series fluorescence detector. The detector was used at 16 pmt, and the excitation and emission wave lengths used were 265 and 380 respectively. A C8 phenomenex column was used to separate compounds of interest. The mobile phase consisted of a mixture of 15mM phosphate buffer and acetonitrile at pH 2.5. The percentage of organic phase was varied in order to elute compounds of interest. The limits of quantification were found to be GCV, 50 ng mL^{-1} ; γ L-Glu-GCV, 500 ng mL^{-1} ; and L-Tyrosine-GCV, $1 \text{ } \mu\text{g mL}^{-1}$.

Statistical Analysis:

All experiments were conducted at least in 5 rabbits and the results are expressed as mean \pm S.E.M. Student's t-test was applied to determine statistical

significance between the parameters of the prodrugs and GCV with $p < 0.05$ was considered to be statistically significant.

All relevant pharmacokinetic parameters were calculated using non-compartmental analyses of the concentration-time curves of GCV and amino acid monoester prodrugs of GCV with a pharmacokinetic software package, WinNonlin, v2.1 (Pharsight, CA). Data were fitted into a non-compartmental model, with a constant infusion over a period of time. Areas under the plasma concentration time curves (AUCinfinity) were determined by the linear trapezoidal method with extrapolation. The slopes of the terminal phase of plasma profiles were estimated by log-linear regression and the terminal rate constant (λ_z) was derived from the slope. The terminal plasma half-lives were calculated from the equation: $t_{1/2} = 0.693 / \lambda_z$.

Results

Dose dependent inhibition of [^3H] L-Arginine uptake across rPCEC cultures:

Our purpose of this study was to deliver amino acid prodrugs of GCV through amino acid transporter, $\text{B}^{0,+}$, present on cornea. A dose dependant uptake (Figure **14**) and inhibition of [^3H] L-Arginine absorption in presence of γ -L-Glu-GCV, L-Phe-GCV, L-Tyr-GCV, di-L-Phe-GCV and di-L-Glu-GCV was examined (Figure **15**). All the prodrugs inhibited uptake of [^3H] L-Arginine in a dose-dependent manner (**Table 2**). Inhibitory concentration (IC_{50}), values were

calculated for all the prodrugs. The data was fitted to a modified log [Dose]-response curve fit to yield IC_{50} values. K_m and V_{max} of L-Arginine were calculated to be 17.05 mM and 2.1 Picomol mg^{-1} of protein min^{-1} respectively (Figure 14). Half maximal inhibitory concentrations (IC_{50}) values of γ -L-Glu-GCV, L-Phe-GCV, L-Tyr-GCV, di-L-Glu-GCV, and di-L-Phe-GCV were calculated as 3.5 ± 1.3 , 6.3 ± 1.5 , 8.2 ± 2.4 , 3.6 ± 1.5 , and 2.3 ± 1.2 mM respectively (Table 2). Hill factor was chosen to be 1. Even though di-L-Phe-GCV was found to inhibit the uptake of [3H] L-Arginine more than other prodrugs, they were not considered for corneal absorption and aqueous humor kinetics study because of its low aqueous stability [117-118]. Both γ -L-Glu-GCV and L-Tyr-GCV were continued for further evaluations.

In vivo corneal absorption and anterior chamber pharmacokinetics of [3H] L-Arginine alone and in the presence of inhibitors:

Corneal absorption of [3H] L-Arginine was conducted to determine the *in vivo* functional activity of $B^{0,+}$ transporter present on the corneal epithelial cells. Infusion of [3H] L-Arginine (Figure 16) was carried out both with and without inhibitors. One millimolar solutions of inhibitors, cold L-Arginine (Figure 17) and BCH (Figure 18), were used to inhibit the corneal absorption of [3H] L-Arginine. AUClast of [3H] L-Arginine, in the absence and presence of cold L-Arginine and BCH were found to be 351 ± 73.5 , 27.4 ± 15.9 and 43.83 ± 6.5

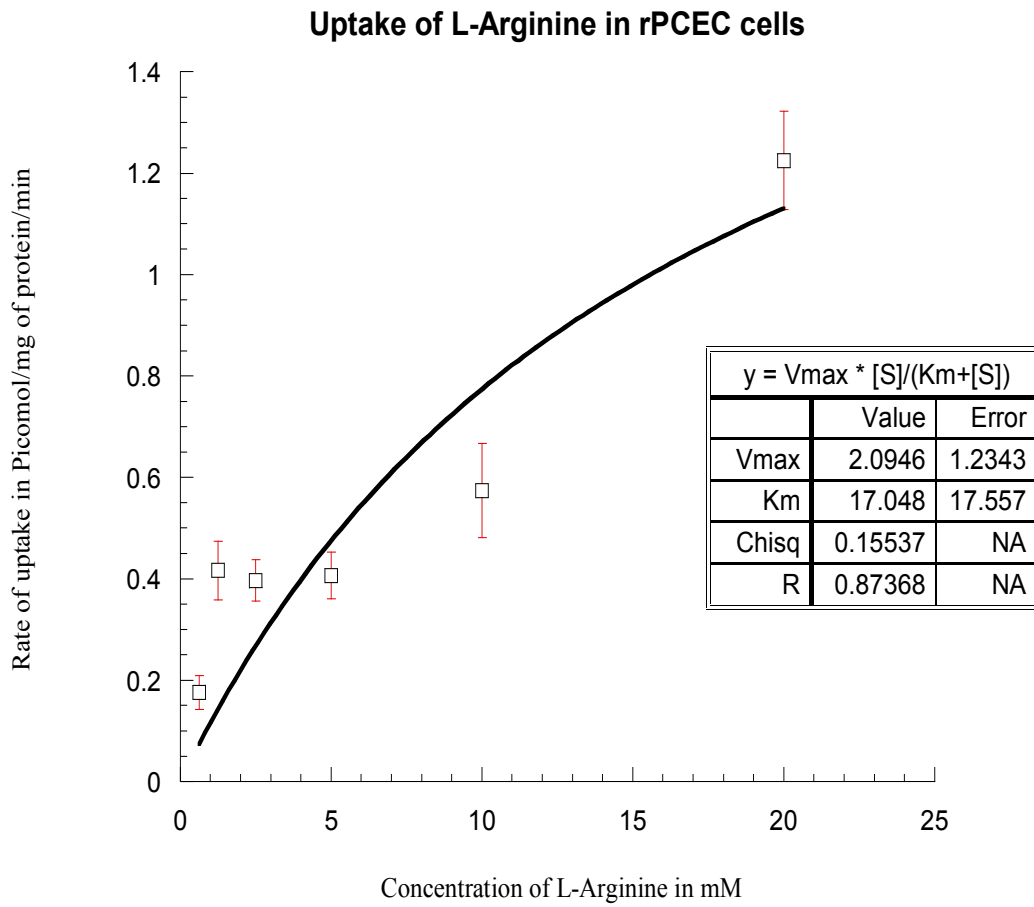


Figure 14. Saturation kinetics of [³H] L-Arginine uptake in rPCEC cells. Data is represented by mean ± SD. (n=4)

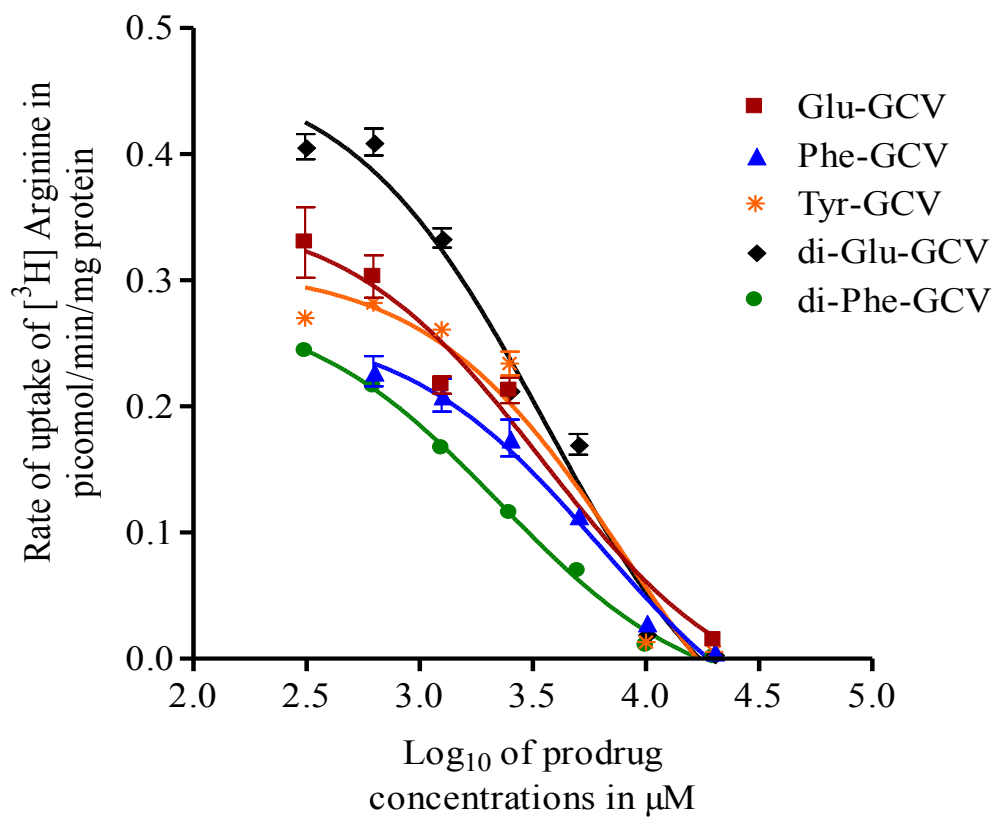


Figure 15. Interaction studies of [³H] L-Arginine with B^{0,+} in presence of amino acid monoester and di-esters prodrugs of GCV. Dose dependent inhibition was performed *in vitro* on rPCEC cells. Data represented are mean ± SE. (n=4)

Table 2. Data showing half maximal inhibitory concentrations (IC50) of amino acids mono and di ester prodrugs against B⁰⁺. Interaction studies of [³H] L-Arginine with B⁰⁺ in presence of amino acid monoester and diester prodrugs of GCV. Dose dependent inhibition was performed *in vitro* on rPCEC cells. Data represented are mean ± SE. (n=4)

Prodrug	IC50 (mM) mean ± SE	R ²
L-Glu-GCV	3.494 ± 1.2888	0.9924
L-Phe-GCV	6.315 ± 1.4686	0.9946
L-Tyr-GCV	8.151 ± 2.4016	0.982
di-L-Glu-GCV	3.618 ± 1.4521	0.9912
di-L-Phe-GCV	2.263 ± 1.1676	0.9983

pico mol* min mL⁻¹ respectively(

Table 3 and Table 4). In the absence of chloride ion and sodium ion in buffer solutions (Figure 19 and Figure 20), AUClast was found to be 62.1 ± 43.1 , and 460.2 ± 65.2 pico mol * min mL⁻¹ (Table 5). In the presence of inhibitors and chloride free buffers AUClast was diminished tremendously indicating the presence of carrier mediated transport of L-Arginine. Also such decrease in AUClast in the presence of BCH and chloride free buffer confirms the presence of B^{0,+} transporter on the rabbit cornea. These results are similar to the ex-vivo transport studies performed across the rabbit cornea by Jain-Vakkalagadda *et al.* [44]. Even though B^{0,+} transporter is a sodium dependent transporter, concentration time profile of [³H] L-Arginine in the absence of sodium ions was found to be almost equal to that of [³H] L-Arginine in IPBS.

AUClast, Tmax and Cmax were also appearing to be equivalent to that of [³H] L-Arginine in IPBS ([³H] L-Arginine in IPBS (

Table 3 and Table 5). This phenomenon could be because of the continuous sodium ion secretion into the infusion well from the cornea, as aqueous humor and cornea are very good source of sodium ions, which could have caused an equilibrium of sodium ions between the cornea and the infusion well with sodium free buffer, resulted in a similar profile to that of the [³H] L-

Arginine in IPBS. Tmax values of control, with cold 1mM L-Arginine, BCH, and chloride free buffers were found to be 80 ± 28 , 160, 140 ± 28 and 153 ± 11 min and Cmax were found to be 2.5 ± 0.7 , 0.15 ± 0.1 , 0.3 ± 0.14 and

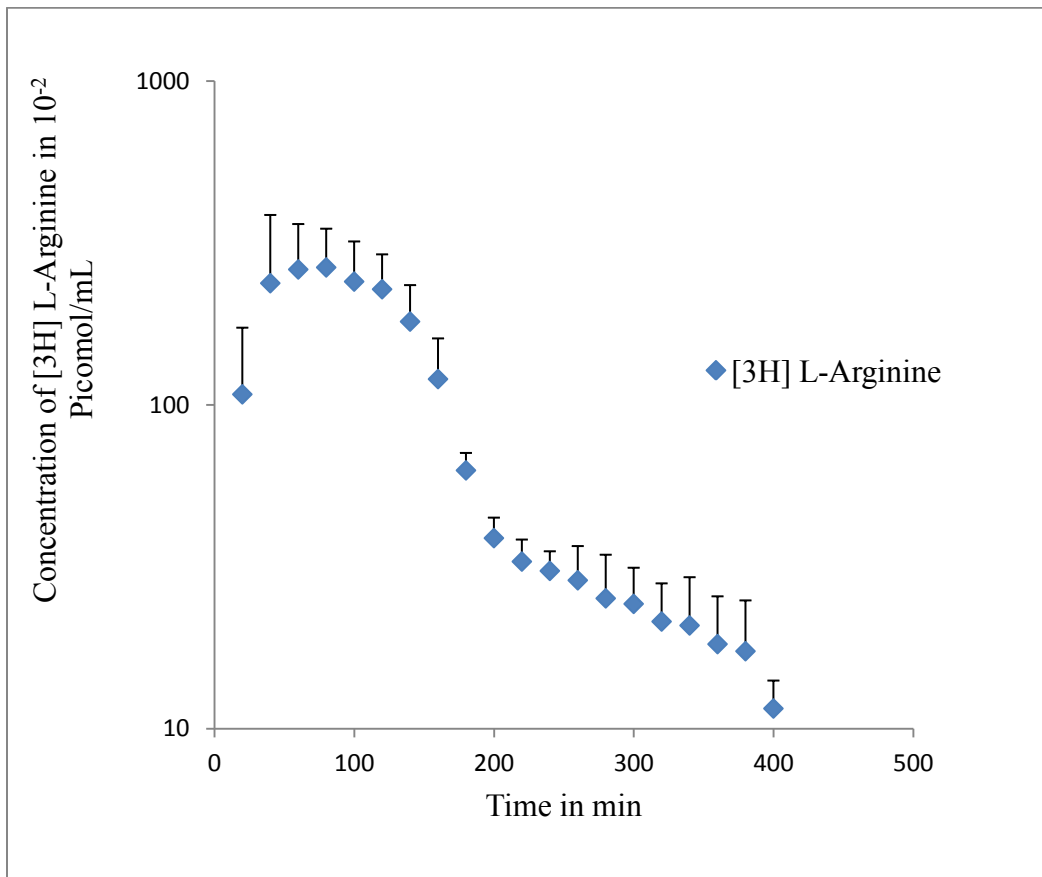


Figure 16. Concentration vs Time profile [³H] L-Arginine (Blue diamonds). Corneal infusion of [³H] L-Arginine was performed using a well, for 2h on New Zealand albino male rabbits under anesthesia. After 2h, infusion was removed to observe distribution and elimination of the amino acid for 6h. An anterior

chamber microdialysis was performed to collect serial samples of aqueous humor dialysate for 8h.

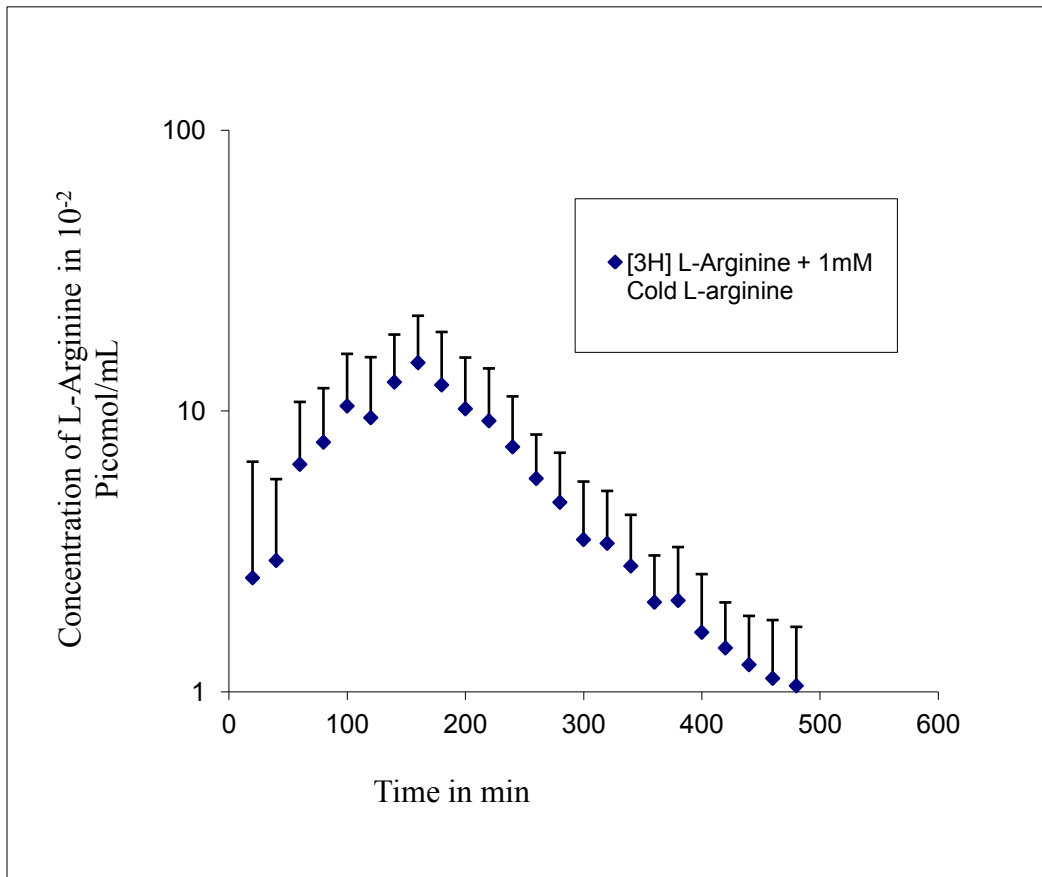


Figure 17. Concentration vs Time profile [³H] L-Arginine inhibition with 1mM cold L-Arginine (Blue diamonds). Corneal infusion of [³H] L-Arginine in presence of 1mM cold L-arginine was performed using a well, for 2h, on New Zealand albino male rabbits under anesthesia. Infusion was performed for 2h to observe the absorption phase. After 2h, infusion was removed to observe distribution and elimination of the amino acid for 6h. An anterior chamber

microdialysis was performed to collect serial samples of aqueous humor dialysate for 8h.

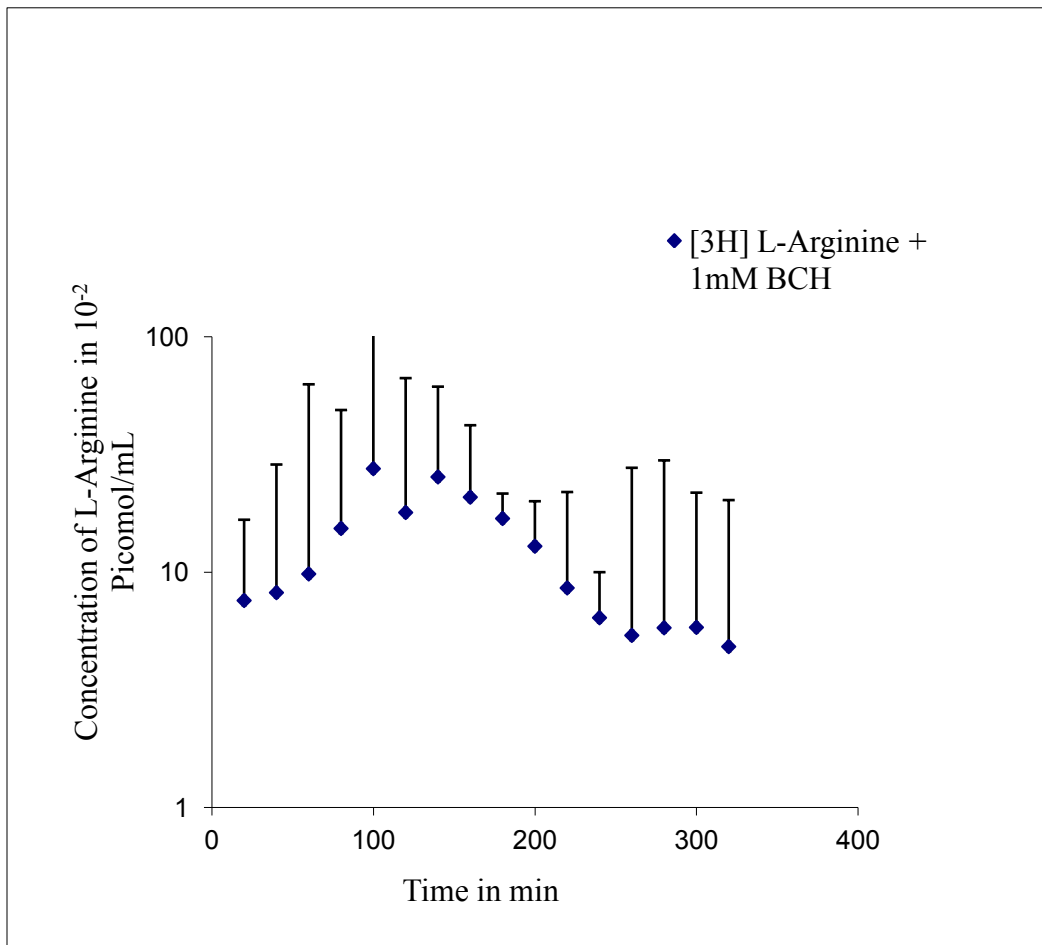


Figure 18. Concentration vs Time profile of [^3H] L-Arginine inhibition with BCH (Blue diamonds). Corneal infusion of [^3H] L-Arginine in presence of 1mM BCH was performed using a well, for 2h, on New Zealand albino male rabbits under anesthesia. Infusion was performed for 2h to observe the absorption phase. After 2h, infusion was removed to observe distribution and elimination of the amino acid for 6h. An anterior chamber microdialysis was performed to collect serial samples of aqueous humor dialysate for 8h.

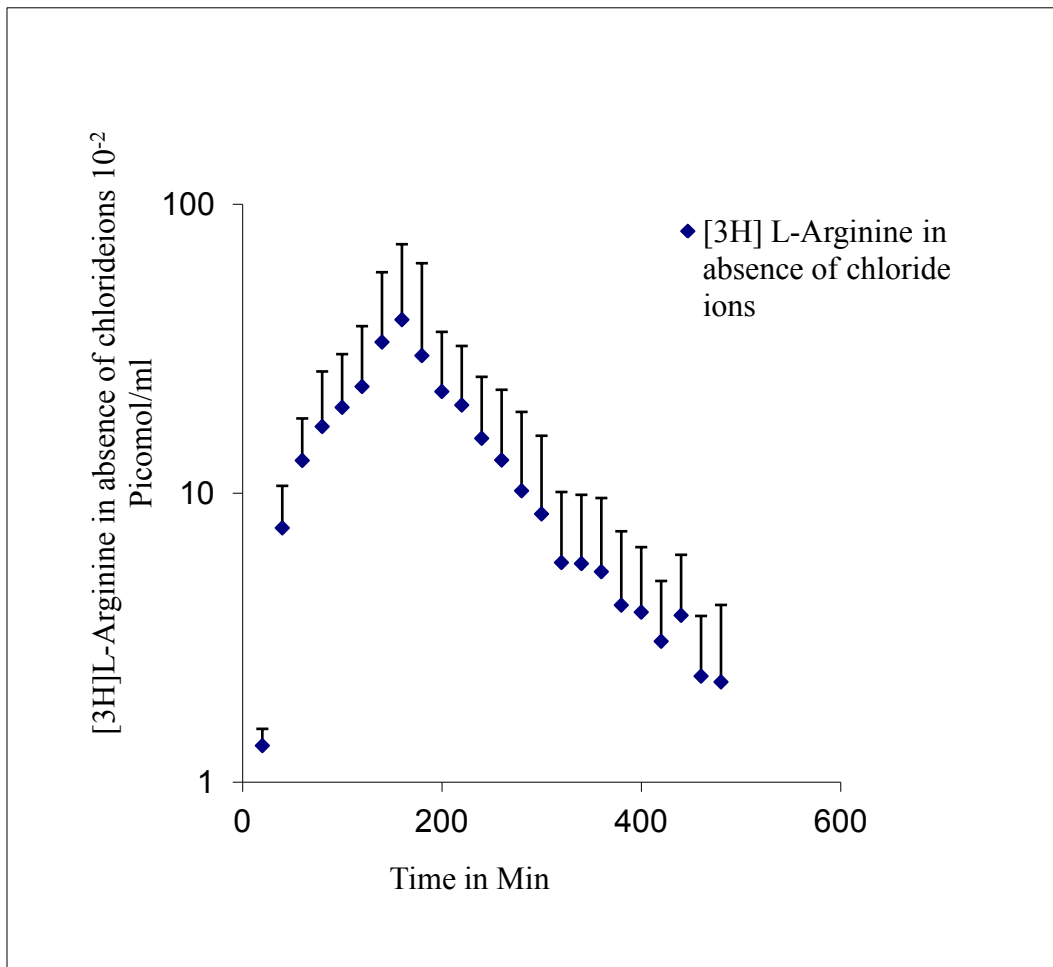


Figure 19. Concentration vs Time profile $[^3\text{H}]$ L-Arginine in presence of chloride ion free buffer (Blue diamonds). Corneal infusion of $[^3\text{H}]$ L-Arginine in absence of chloride ions was performed using a well, for 2h, on New Zealand albino male rabbits under anesthesia. Infusion was performed for 2h to observe the absorption phase. After 2h, infusion was removed to observe distribution and elimination of the amino acid for 6h. An anterior chamber microdialysis was performed to collect serial samples of aqueous humor dialysate for 8h.

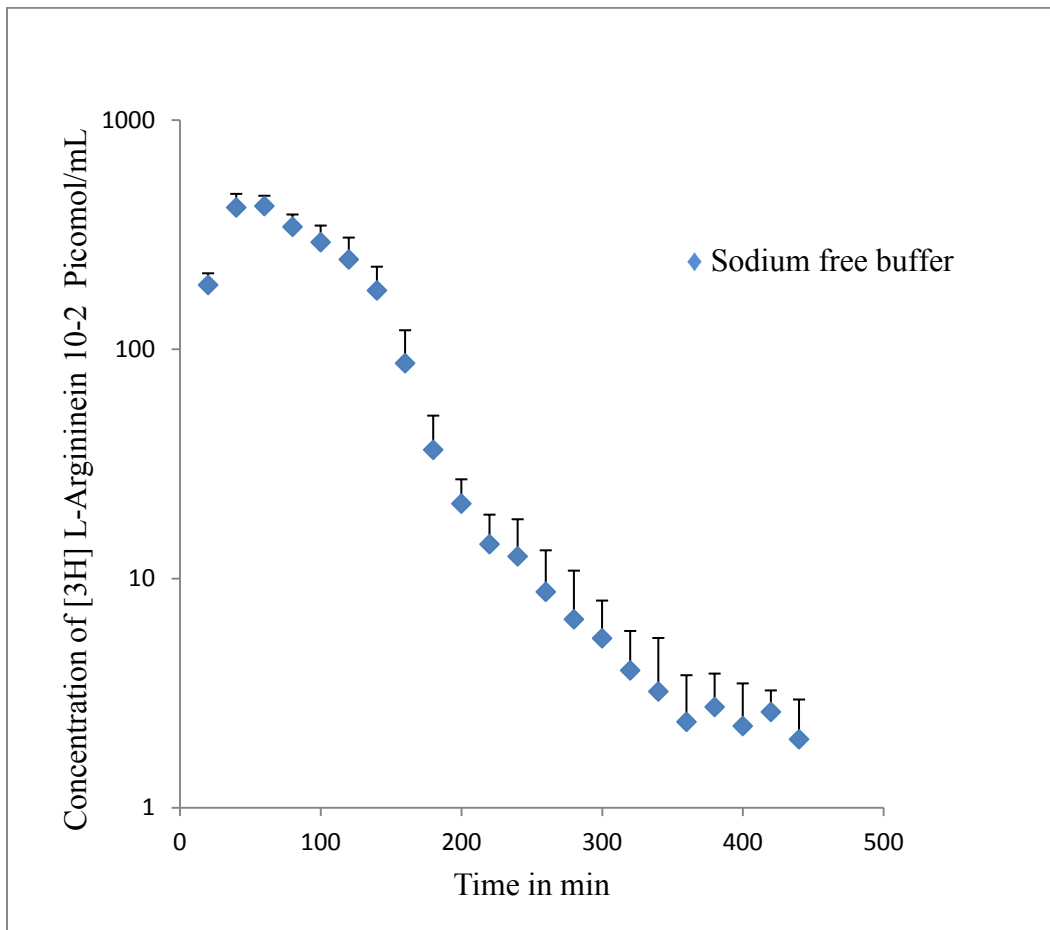


Figure 20. Concentration vs Time profile [³H] L-Arginine in presence of sodium ion free buffer (Blue diamonds). Corneal infusion of [³H] L-Arginine in absence of sodium ions was performed using a well, for 2h, on New Zealand albino male rabbits under anesthesia. Infusion was performed for 2h to observe the absorption phase. After 2h, infusion was removed to observe distribution and elimination of the amino acid for 6h. An anterior chamber microdialysis was performed to collect serial samples of aqueous humor dialysate for 8h.

0.43 ± 0.32 Pico mol mL^{-1} respectively. Shift in the T_{max} and increase in the C_{max} suggests the presence of a carrier mediated process. Overall results suggest the *in vivo* functional presence of $B^{0,+}$ transporter on the cornea.

Anterior chamber pharmacokinetics and corneal absorption of γ -L-Glu-GCV and L-Tyr-GCV monoester prodrugs:

Corneal absorption studies of γ -L-Glu-GCV and L-Tyr-GCV monoester prodrugs were carried out for 8h. Different solutions of prodrugs ($200\mu\text{L}$ each) were administered *via* infusion onto the rabbit cornea for 2h using a corneal well. AUC_{∞} of γ -L-Glu-GCV and L-Tyr-GCV were found to be 44683 ± 11813 and 90587 ± 15891 $\text{min} \cdot \text{nmol mL}^{-1}$ respectively (Table 6). C_{max} of γ -L-Glu-GCV and L-Tyr-GCV were found to be 204 ± 65 and 380 ± 59 nmol mL^{-1} , with MRT of 193 ± 9 and 210 ± 12 min, and λ_z $0.50 \pm 0.05 * 10^{-2}$ and 0.49 ± 0.07 min^{-1} respectively. Elimination rate constants were almost equivalent to that of GCV. In both the experiments prodrugs were not observed in the aqueous humor.

Discussion and Conclusion

Cationic and neutral amino acid transporters carry and translocate cationic and neutral amino acids into the cell membranes. Such systems are classified into four transporters, y^+ , $b^{0,+}$, y^+L , and $B^{0,+}$ [9]. While y^+ is specific only for cationic amino acids, the rest of the three transporters accept a wide a range of amino acids, from cationic to neutral amino acids. But they act differently during

Table 3. Pharmacokinetic parameters of [³H] L-Arginine. A constant infusion of amino acid was administered for 2h using topical well in rabbit eyes. AUC- area under the curve, Cmax- Maximum concentrations achieved in aqueous humor, Tmax – Time to reach maximum concentrations. Data represented as mean ± S.D. (n=5)

PK parameters	DPBS [³ H]L-Arginine (mean ± S.D)
AUC _{last} (Picomol *min mL ⁻¹)	351 ± 73.5
Tmax (min)	80 ± 28.28
Cmax (Picomol mL ⁻¹)	2.5 ± 0.7

Table 4. Pharmacokinetic parameters of [³H] L-Arginine. A constant infusion of amino acid was administered for 2h in presence of cold L-Arginine 1mM and BCH 1mM using topical well in rabbit eyes. AUC- area under the curve, Cmax- Maximum concentrations achieved in aqueous humor, Tmax – Time to reach maximum concentrations. Data represented as mean ± S.D. (n=5)

PK parameters	Inhibitors 1mM	
	L-Arginine (mean ± S.D)	BCH (mean ± S.D)
AUClast (Picomol *min mL ⁻¹)	27.4 ± 15.9	43.83 ± 6.5
Tmax (min)	160	140 ± 28.3
Cmax (Picomol mL ⁻¹)	0.15 ± 0.1	0.3 ± 0.14

Table 5. Pharmacokinetic parameters of [³H] L-Arginine. A constant infusion of amino acid was administered for 2h in Chloride and sodium ion free buffers, using topical well in rabbit eyes. AUC- area under the curve, Cmax- Maximum concentrations achieved in aqueous humor, Tmax – Time to reach maximum concentrations. Data represented as mean ± S.D. (n=5)

PK parameters	Buffers	
	Chloride Free Buffer (mean ± S.D)	Sodium Free Buffer (mean ± S.D)
AUClast (Picomol *min mL ⁻¹)	62.1 ± 43.1	460.2 ± 65.2
Tmax (min)	153 ± 11.5	55 ± 10
Cmax (Picomol mL ⁻¹)	0.43 ± 0.32	4.25 ± 0.14

co-transport of certain metal ions, like sodium and potassium ions, and chloride. The transporter $b^{0,+}$ is sodium independent transporter, where as $B^{0,+}$ is sodium and chloride ion dependent. It is also specifically inhibited by BCH. In our earlier reports, we suggested the presence of the $B^{0,+}$ transporters on the corneal epithelium. We also have reported that this transporter does not transport cationic amino acids in the absence of sodium and chloride ions. RT-PCR results also suggested the presence of this transporter on the rabbit cornea [44]. In this manuscript, we have demonstrated the *in vivo* functional activity of $B^{0,+}$ transporter on the rabbit cornea. Previously, Eller *et al.* studied the absorption of carbonic anhydrase inhibitors across the rabbit cornea using a well model [106]. In this study we have modified model by combining it with a microdialysis technique. This model provides accurate data with the use of a few animals compared to the conventional methods which require a large number of animals for a single profile.

In the presence of cold L-Arginine, AUClast of [3 H] L-Arginine was found to be reduced by 8 times. A similar result was observed when BCH was added as a specific inhibitor during the absorption of [3 H] L-Arginine across cornea. Eight to ten times decrease in both AUClast and Cmax was observed.

Corneal absorption of [3 H] L-Arginine was found to be carrier mediated process. When the chloride and sodium dependency experiments were conducted

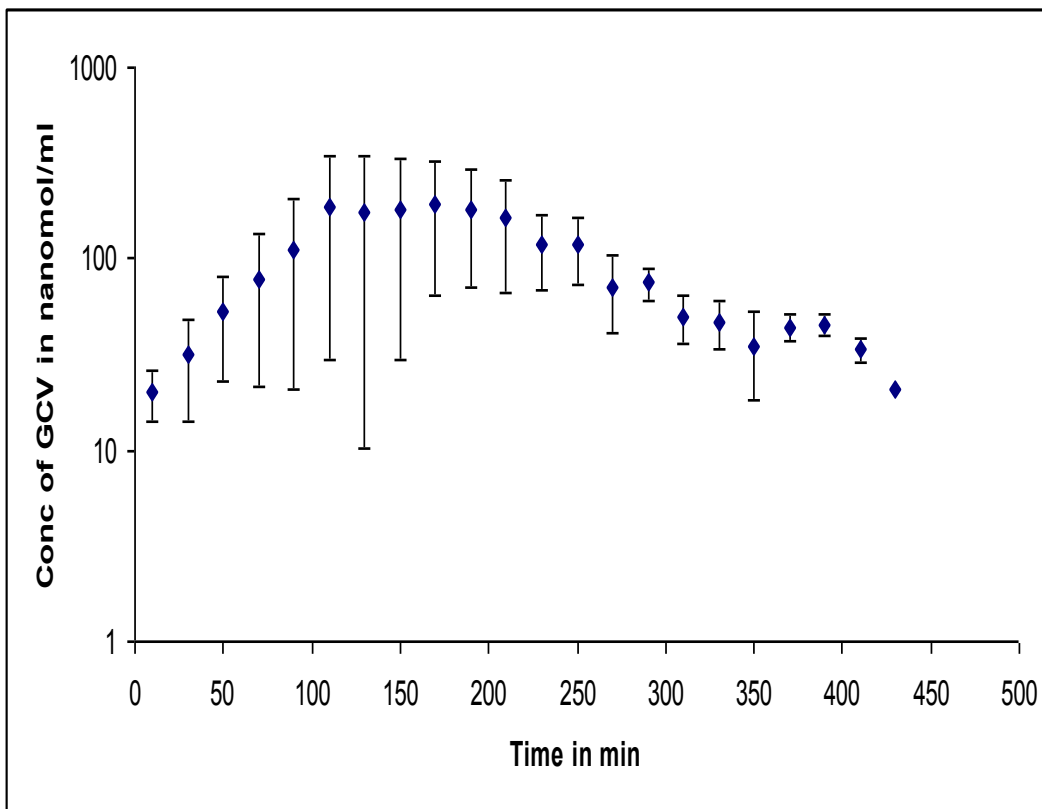


Figure 21. Corneal absorption and anterior chamber pharmacokinetics γ -L-Glu-GCV. A 2h infusion of γ -L-Glu-GCV administered using well model. Anterior chamber microdialysis was performed to collect aqueous humor dialysate containing bio-reversed GCV. Data points are represented as mean \pm SD. Number of animals used were, n=5.

a different pattern was observed compared to ex vivo results. It is a well established phenomenon that transport of L-Arginine takes place in the presence of sodium and chloride ions. As expected, depletion of chloride ions reduced the AUClast and Cmax values almost by 5 times. However, corneal absorption of L-Arginine in the absence of sodium ions was not affected during *in vivo* studies (Table 5). This could be because of the continuous sodium ion secretion from the corneal membrane and aqueous humor into the corneal well. Except for the sodium dependency, transporter exhibits all the characteristics of the B^{0,+} transporter. This suggests that *in vivo* absorption of [³H] L-Arginine taking place *via* B^{0,+}. Such a transport system can be utilized to deliver drugs to the anterior chamber of the eye. Ganapathy et al, has extensively studied the application of transporter targeted drug delivery *via* B^{0,+} [119]. In his study, he observed the ability of B^{0,+} in transporting amino acid prodrugs of ACV and GCV across the cell membranes, and suggested the utility of such a system in drug delivery.

Herpes viral diseases of the anterior segment of the eye are a threat to the vision as these diseases may cause severe damage to the cornea if left untreated. GCV, a relatively hydrophilic drug, possesses good antiviral activity against the herpes group of viruses. It was also found to be very active against HSV-1 and 2 types of viruses [113]. Currently it is not used against herpes keratitis, mainly due to its lower ocular bioavailability. The cornea, being a complex organ, consists of

three main layers: the corneal epithelium, stroma and the endothelium. Because of high membrane lipid contents and tight intercellular junctions the epithelium does not permit hydrophilic GCV to pass through the cornea to any significant extent. We reported that lipophilic monoester prodrugs of GCV possess enhanced permeability across cornea. Even though permeability of GCV was increased with this approach, it did so at the expense of aqueous solubility [6, 116].

Amino acid monoesters of GCV were found to have good affinity to B^{0,+} transporter. This nutrient transporter ferried the prodrug molecules across corneal epithelium, which in turn were broken down to its amino acid metabolite and parent GCV molecules by esterases and peptidases present in the corneal tissues.

This work represents the continuation of our earlier work on amino acid monoester prodrugs of GCV. The main objective of this study was to evaluate cytotoxicity, active uptake, corneal absorption and aqueous humor pharmacokinetic parameters of these amino acid monoester prodrugs, γ -L-Glu-GCV and L-Tyr-GCV and to compare their pharmacological properties with the GCV.

Cell proliferation studies were conducted on rPCEC cultures indicated no cytotoxicity when cells were exposed to GCV and all three amino acid prodrugs up to 1mM concentration (Chapter 3). Inhibition of [³H] L-Arginine uptake was observed in the presence of all five GCV prodrugs, di-L-Phe-GCV has lowest

value of IC₅₀ compared to others. Even though di-L-Phe-GCV has the maximum inhibition of [³H] L-Arginine uptake, it has very poor aqueous stability [117-118], it was not considered for further *in vivo* evaluations. Both L-Tyr-GCV and γ -L-Glu-GCV were studied for pharmacokinetic behavior. AUC of L-Tyr-GCV was found to be double that of γ -L-Glu-GCV (Table 6). C_{max} were found to be 380 ± 59 and 204 ± 65 nmol mL⁻¹ respectively for Try-GCV and γ -L-Glu-GCV. Absorption of Try-GCV resulted in twice the C_{max} in the anterior chamber compared to and γ -L-Glu-GCV (Table 6). Elimination rate constants and MRT (mean residence time) of the prodrugs remained unchanged, which are approximately equivalent to that of GCV, possibly because of complete hydrolysis of prodrugs into their parent molecule GCV. Elimination process of amino acid monoester prodrugs could be different because of the presence of amino acid transporters on the blood aqueous barriers. But in this case no prodrugs were observed in the aqueous humor, so the elimination of parent drug was only observed.

In this study we have established the presence of functional activity of B^{0,+} transporter on the rabbit cornea. Corneal absorption of L-Arginine was found to be dependent on chloride ions and BCH. This is the first report of *in vivo* functional activity of any transporter on the cornea. Amino acid monoester prodrugs γ -L-Glu-GCV, L-Phe-GCV and L-Tyr-GCV can be transported through

Table 6. Pharmacokinetic parameters of L-Tyr-GCV and γ -L-Glu-GCV. Drugs were given constant infusion for 2h across the cornea in rabbit eyes. Values presented are for regenerated GCV from both prodrugs (Mean \pm S.E.M). (n=5)

PK parameters	GCV regenerated from L-Tyr-GCV	GCV regenerated from γ -L-Glu-GCV Mean \pm S.E.M
AUCinfinity (min*nmol mL ⁻¹)	90587 \pm 15891	44683 \pm 11813
Cmax (nmol mL ⁻¹)	380 \pm 59	204 \pm 65
Tmax (min)	150 \pm 27	137 \pm 21
Clast (nmol mL ⁻¹)	30 \pm 4	33 \pm 7
MRT (min)	210 \pm 12	193 \pm 9
$\lambda_z \cdot 10^2$ (min ⁻¹)	0.49 \pm 0.07	0.50 \pm 0.05
Tlast	430 \pm 10	410 \pm 9

$B^{0,+}$ transporter across rabbit cornea. Among the prodrugs studied L-Tyr-GCV demonstrated maximum corneal absorption and better pharmacokinetic profile. In conclusion, we predict that L-Tyr-GCV can be developed as next generation candidate for herpes keratitis.

CHAPTER 5

ANTERIOR CHAMBER PHARMACOKINETICS OF DI-PEPTIDE MONOESTER PRODRUGS OF GCV IN RABBIT EYES AND ABSORPTION OF PRODRUGS TARGETING PEPT1 TRANSPORTER ON THE RABBIT CORNEAL EPITHELIUM

Rationale

Herpes Simplex Virus type-1 (HSV-1) induced epithelial and stromal keratitis of the cornea is one of the leading causes of blindness in the United States [120-122]. The drug of choice for the treatment of these viral infections is TFT as 1% wt/v topical solution. Even though IDU was the first antiviral used for the treatment of corneal keratitis [123], its use was reduced because of low aqueous solubility and ocular toxicity [124]. Toxicity of IDU was mainly attributed to its non-specificity towards viral and human kinases. Acyclovir, drug of choice for systemic HSV infections, is a hydrophilic drug molecule with low aqueous solubility that prohibits its use as topical solution for the treatment of corneal herpes infections. Three percent ACV ointment was used topically in the eye for the treatment of herpes infections in Europe, but not in United States [124-126]. Even though 1 % wt/v TFT is currently the drug of choice for ocular herpes infections, it is reported to be cytotoxic and mutagenic in long term usage [127]. GCV, an acyclic guanosine analog exhibits excellent antiviral activity against the herpes family of viruses [128-129]. It is the drug of choice for the systemic and ocular HCMV infections and it is as effective as ACV against HSV-1 [130]. In

1983, Smee *et al.* suggested its potential as an anti-HSV-1 agent [131]. GCV is also found to be extremely effective against HSV-1 in rabbits and humans. Even though GCV is effective against corneal herpes infections, its modest aqueous solubility limits the preparation of a formulation as a topical eye solution and its hydrophilic property makes it impermeable across the cornea. A 0.15% wt/wt gel of GCV was found to be as effective as 3% wt/wt ACV ointment and was also better tolerated relative compared to ACV ointment [132-133]. A few attempts have been made in our laboratory to formulate topical eye drops of GCV. Lipophilic acyl-ester prodrug strategy was utilized to improve its corneal permeation [114]. Even though permeability across the cornea was found to be improved, aqueous solubility of the compounds diminished. As a result these prodrugs could not be formulated as 3% wt/v topical solutions. In one of the previous reports from our laboratory, cyclodextrins were used to increase the solubility of these lipophilic acyl ester prodrugs of GCV. This strategy of using prodrugs and cyclodextrins together was effective to a certain degree but inclusion of more than 5% wt/v cyclodextrins in the formulation resulted in corneal toxicity [134].

Recently, nutrient transporters are being targeted for efficient delivery of drugs across cell membranes. Previously published reports from our laboratory have demonstrated utilization of such strategies [135-136]. Transporters such as

peptide (PEPT1, PEPT2), amino acid ($B^{0,+}$, $b^{0,+}$ and LAT), folate and other vitamin transporters as well as transferring and insulin receptors can be good targets for drug delivery. Peptide transporters (PEPT1 and PEPT2) have been so far the most widely utilized [137-138]. Several drugs including cephalosporins, L-Val-ACV and L-Val-GCV are substrates of peptide transporters [139-141]. Oral bioavailabilities of L-Valine linked antiviral agents have improved significantly. These L-Valine ester prodrugs, after oral administration, were broken down into their parent drugs by enzymes such as peptidases and esterases present in intestinal mucosa and blood. Our earlier reports have shown that hydrophilic GCV is not a substrate for nucleoside/nucleobase transporters present on the cornea and its permeation across the cornea occurs primarily by passive diffusion[60]. Peptide derivatization of hydrophilic molecules, such as GCV, may enhance both aqueous solubility and PEPT aided permeation across the cornea.

Our previous research demonstrated the utilization of peptide transporter for transcorneal delivery of GCV [35]. In those studies, dipeptide monoester prodrugs of GCV were synthesized and their superior aqueous solubility and stability were shown. Inhibition studies of radio labeled gly-sar and gly-pro with these prodrugs demonstrated their affinity towards the peptide transporter on the cornea. These derivatives also demonstrated higher antiviral efficacies. In vitro and *in vivo*, against HSV-1, HSV-2, VZV and HCMV relative to parent drug .

Topical infusion model has been developed by modifying a method published by Eller *et al.* in 1985 [106]. In this model, a constant concentration of the drug is maintained on the cornea so that the effects of tear turnover, fluid dynamics, conjunctival absorption are eliminated. Several pharmacokinetic models have been proposed to determine absorption, distribution and elimination of drugs applied topically to the eye [99, 101, 142]. All these models either fail to provide absorption, distribution or elimination rate constants accurately or utilized very complex multi compartment pharmacokinetic analysis. To accurately predict transcorneal absorption of drugs and reduce the complexity in pharmacokinetic modeling. Tirucherai *et al.* and Dey *et al.* have developed a topical infusion model based on Eller's model and microdialysis sampling techniques [18, 116]. The overall objective of this manuscript is to determine corneal absorption and aqueous humor kinetics of dipeptide monoester prodrugs of GCV, such as L-Val-GCV, L-Val-L-Val-GCV, L-Gly-L-Val-GCV and L-Tyr-L-Val-GCV (Figure 22) by a topical infusion model with rabbit as the animal model.

Material and methods

GCV was obtained as a gift from Hoffman La Roche (Nutley, NJ). All other chemicals were purchased from Sigma Chemical Company (St Louis, MO), and used without further purification. Linear probes (MD-2000, 0.32 x 10 mm, polyacrylonitrile membrane and 0.22 mm tubing) used for aqueous humor

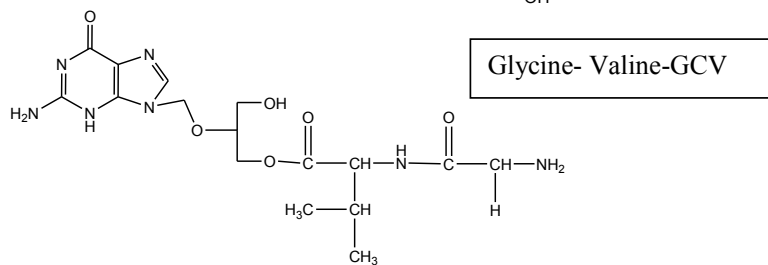
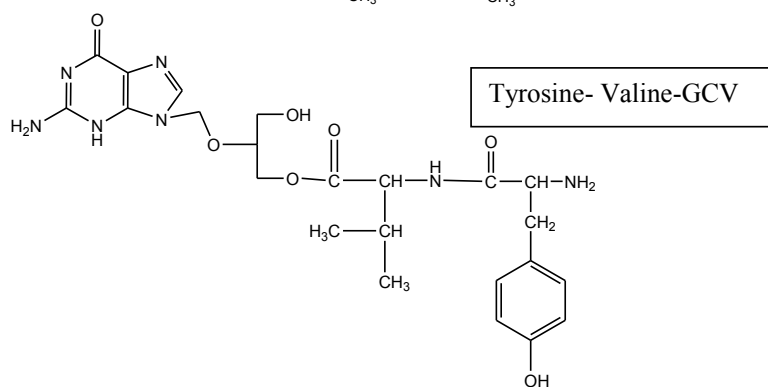
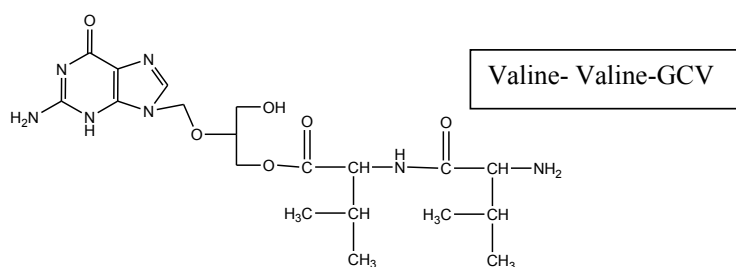
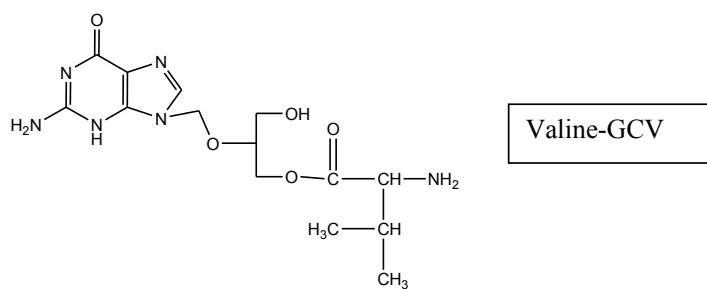


Figure 22. Structures of peptide prodrugs of GCV. L-Valine-GCV, L-Valine- L-Valine-GCV, L-Tyrosine-L-Valine-GCV, and L-Glycine-L-Valine-GCV (from top to bottom in order)

sampling were obtained from Bio Analytical Systems (West Lafayette, IN). A microinjection pump (CMA/100), for pumping isotonic buffer was procured from CMA Microdialysis, (Acton, MA). Ketamine hydrochloride was obtained from Fort Dodge Animal Health and Rompun (xylazine) was obtained from Bayer animal Health. Topical wells were custom made by Hansen Ophthalmic Fort Dodge Development Corporation (Iowa City, IA) according to special instructions. All the prodrugs were synthesized in our laboratory [35].

Animal model:

New Zealand albino rabbits weighing between 5-6 lbs were employed as an animal model. All studies involving rabbits were conducted according to the Association for Research in Vision and Ophthalmology (ARVO) Statement for the Use of Animals in Ophthalmic and Vision Research. Rabbits were kept under anesthesia throughout the experiment using ketamine hydrochloride (35 mg/kg) and xylazine (3.5 mg/kg) given intramuscularly every 40 minutes. Pupils were dilated with 1% wt/v tropicamide solution to avoid contact with the probe while implanting. The linear probe was implanted into the aqueous humor using a 25G needle in the right eye of the animal. The needle was inserted across the cornea just above the corneal-scleral limbus so that it traverses through the center of the anterior chamber to the other end of the cornea. The sample-collecting end of the linear probe was inserted carefully into the bevel end edge of the needle. The

needle was slowly retracted leaving the probe with the dialysis membrane in the middle of the anterior chamber. The outlet of the probe was then fixed to prevent any disturbance during sample collection.

The probes were perfused with pH 7.4 IPBS at a flow rate of $3 \mu\text{l min}^{-1}$ using the CMA/100 microinjection pump. After probe implantation, the animals were allowed to stabilize for two hours. This duration has been shown to be sufficient for the restoration of intraocular pressure and replenishment of the aqueous humor lost during probe implantation [143]. Following the two hours stabilization period, the eyelids of the rabbits were mechanically retracted with Colibri retractors. Subsequent to eyelid retraction, the topical well was placed over the eye such that the central portion formed a well allowing the each drug/prodrug solution to remain in direct contact with the cornea, with exclusion of the sclera. The outer flange of the topical well was coated with surgical adhesive to prevent its movement. During all these manipulations, care was taken to avoid contact with the entry and exit ports of the aqueous humor microdialysis probe.

Subsequent to placing the well, the animals were allowed to stabilize for another 45 minutes. Following this interval, 200 μl of IPBS containing GCV (at saturation solubility) and 0.43% wt/v solutions of prodrugs L-Val-GCV, L-Val-L-

Val-GCV, L-Gly-L-Val-GCV and L-Tyr-L-Val-GCV were added to the well. The compounds were allowed to diffuse for a period of 2 hours across the cornea. Following this period, drug solution was aspirated from the well and the well removed. The corneal surface was washed clean with a few drops of distilled water. The experiment was continued for six hours after removal of the topical well. Samples were collected every 20 minutes throughout the infusion and the post infusion phases.

In vitro probe calibration:

Dialysate concentrations of the analytes are only a measure of the concentrations in the extra cellular space. The ratio between the concentration of a substance in the outflow solution and the undisturbed concentration of the same substance in solution outside the probe is defined as “recovery”, expressed as a ratio or a percentage [144]. The recovery factor of the probes is an important factor in determining the extracellular concentrations of the drug. An in vitro recovery technique is appropriate for ocular microdialysis since aqueous humor is primarily aqueous (>95%) in nature.

Recovery was determined in an aqueous solution containing a known concentration of the compounds. The probe was continuously perfused at a constant flow rate of $3 \mu\text{l min}^{-1}$ and samples collected every 20 minutes. Before

each time point a donor sample was taken and used as a standard for the respective recovery sample. The recovery of the compound of interest was calculated according to Equation 14

Equation 14

$$\text{Recovery} = C_{\text{out}}/C_{\text{in}}$$

C_{out} is the concentration in the outflow solution and C_{in} is the concentration in the medium.

After determining the recovery of the compound, dialysate concentrations were transformed into the actual anterior chamber concentration utilizing Equation 15.

Equation 15

$$C_i^* = C_{\text{out}}^*/\text{recovery}$$

C_i^* is the substance concentration in the aqueous humor and C_{out}^* is the concentration of the dialysate [145].

The recovery of the linear probe was between 14-27% for all the compounds studied. There was no significant variation in the recovery of the probes with time over the experimental time period.

Theoretical considerations and data treatment:

A model has been considered in which a drug is administered at a constant rate to the corneal surface. As shown in (Figure 23).

The disposition of drug in the aqueous humor may be given by Equation 16

Equation 16

$$\frac{dX_a}{dt} = k_o - k_{ap}X_a + k_{pa}X_p - k_{10}X_a$$

X_a denotes the amount of drug in the aqueous humor, k_{ap} and k_{pa} are the first order rate constants for the transfer of the drug from the aqueous humor to the peripheral compartment and vice versa. Peripheral tissues are lens, iris ciliary body, k_{10} represents the overall elimination from the aqueous humor. The subscripts a and p refer to the aqueous and peripheral compartments respectively.

The constant input rate is related to the drug in pre-corneal area by Equation 17

Equation 17

$$k_0 = k_a C_w V_w$$

k_a represents the corneal absorption first order rate constant, C_w is the concentration of the drug in the well, and V_w denotes the volume of the drug solution in the well.

Substituting for k_0 from Equation 17 into Equation 16, and knowing that during initial period of the infusion, concentration of drug in the well (C_w) is much greater than concentration of drug in the aqueous humor (C_a), the first term on the right side of Equation 16 predominates over the second, third and fourth terms. Thus, Equation 16 can be rewritten as Equation 18

Equation 18

$$\left(\frac{dX_a}{dt}\right)_I = k_a C_w V_w$$

The rate of change of drug concentration in the aqueous humor can be expressed according to Equation 19

Equation 19

$$\left(\frac{dC_a}{dt}\right)_I = k_a C_w V_w / V_a$$

V_a is the physiological volume of the aqueous humor (300 μ l). Subscript I refer to the initial rate which can be determined from the initial slope of C_a versus t as determined by aqueous humor microdialysis. Equation 19 may be rearranged as Equation 20 to allow estimation of k_a .

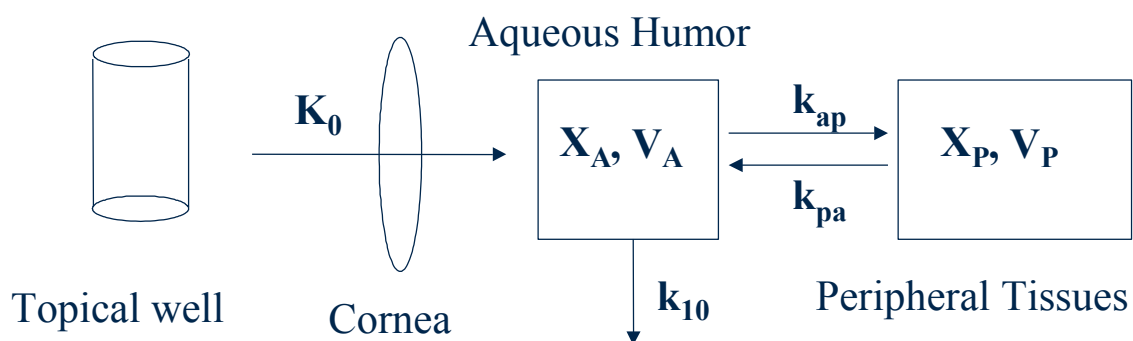


Figure 23. Depiction of the experimental and compartmental model. Drug is administered at a constant rate onto the corneal surface (K_0). Elimination rate from the central compartment is represented by k_{10} , and inter-compartmental the distribution rates are described by k_{ap} and k_{pa} .

Equation 20

$$k_a = \frac{\left(\frac{dC_a}{dt}\right)_I * V}{C_w}$$

If the topical infusion is allowed to continue until steady state is reached, then integration of Equation 16 yields Equation 21:

Equation 21

$$C_{ss} = k_0/k_{10} * V_{aq} = k_a * V_w * C_w/k_{10} * V_{aq}$$

Thus topical infusion method along with Equation 16-21 permit a rational and reliable determination of ocular pharmacokinetics whereby absorption and disposition can be characterized without using complex compartmental analysis [144].

Analytical Procedures:

All samples were assayed using a reversed phase HPLC (Table 7). The HPLC system was comprised of a waters pump, an Alcott 1500 series auto sampler and an Agilent 1100 series fluorescence detector. The detector was used at 16 pmt, and the excitation and emission wave lengths used were 265nm and 380nm respectively. A C8 phenomenex column was used to separate compounds of interest. The mobile phase consisted of a mixture of 15mM phosphate buffer and acetonitrile at pH 2.5. The percentage of organic phase was varied in order to

elute compounds of interest. The limits of quantification were found to be GCV, 50 ng mL⁻¹; L-Val-GCV, 500 ng mL⁻¹; L-Gly-L-Val-GCV, 2 µg mL⁻¹; L-Val- L-Val-GCV, 1µg mL⁻¹; and L-Tyr-L-Val-GCV, 2 µg mL⁻¹. Ion pairing agent octane sulfonic acid was added to the mobile phase to get better separation of L-Gly-L-Val-GCV and L-Val-GCV (Table 7).

Statistical Analysis:

All experiments were conducted at least in 5 rabbits and the results are expressed as mean ± S.E.M and the graphs were plotted in Microsoft excel and expressed as mean ± S.D. Student's t-test was applied to determine statistical significance between the parameters of the prodrugs and GCV with $p < 0.05$ was considered to be statistically significant. All relevant pharmacokinetic parameters were calculated using non-compartmental analyses of the concentration-time curves of GCV, L-Val-GCV and the dipeptide monoester prodrugs of GCV with a pharmacokinetic software package, WinNonlin, v5.1 (Pharsight, CA). Data was fitted into a non-compartmental model, with a constant infusion over a period of time. Areas under the plasma concentration time curves (AUC_{infinity}) were determined by the linear trapezoidal method with extrapolation. The slopes of the terminal phase of plasma profiles were estimated by log-linear regression and the terminal rate constant (λ_z) was derived from the slope. The terminal plasma half-lives were calculated from the equation: $t_{1/2} = 0.693 / \lambda_z$.

Table 7. HPLC conditions for the analysis of GCV and prodrugs. C8 column was used for the separation of drug peaks. Mobile phases used are various mixtures of Acetonitrile and phosphate buffer at pH 2.5.

Prodrug	Aqueous phase (pH-2.5)	Organic Phase	Mobile phase	Retention times		
				Aq : Org	GCV	L-Val-GCV
GCV	15mM KH ₂ PO ₄	Acetonitrile	99 : 1	4.8	-	-
L-Val-GCV	15mM KH ₂ PO ₄	Acetonitrile	98 : 2 ^a	5.2	12	-
L-Val-L-Val-GCV	15mM KH ₂ PO ₄	Acetonitrile	97 : 3	4.1	9	22
L-Gly-L-Val-GCV	15mM KH ₂ PO ₄	Acetonitrile	98 : 2 ^a	5.2	11	18
L-Tyr-L-Val-GCV	15mM KH ₂ PO ₄	Acetonitrile	99 : 1	3.9	5.0	-

a - indicates the use of 1% wt/v octane sulphonic acid as ion pairing agent in the mobile phase.

Results

GCV and all its prodrugs were infused across the cornea at a dose equimolar to 0.43% wt/v GCV solution (saturation concentration). All the cumulative GCV concentrations of prodrugs reached steady state concentrations at least after 1h of infusion (Figure 24 - 27) with the exception of L-Val-GCV monoester (Figure 28) which showed a linear absorption profile. All the peptide prodrugs were broken down sequentially into their amino acid prodrug and parent drug. L-Val-GCV was the common amino acid metabolite observed for all dipeptide monoester prodrugs. Areas under the curve concentration time profiles (AUCinfinity) of regenerated GCV were found to be 367081 ± 31873 , 74709 ± 16336 , 26123 ± 5810 , 51923 ± 5519 and $42259 \pm 6862 \text{ min} \cdot \text{nmol mL}^{-1}$ for L-Tyr-L-Val-GCV, L-Val- L-Val-GCV, L-Gly-L-Val-GCV, L-Val-GCV and GCV respectively (Table 8 - 12). Means of AUCinfinity of regenerated GCV from L-Tyr-L-Val-GCV, L-Val- L-Val-GCV and L-Val-GCV administration were found to be 8.6, 1.8 and 1.2 fold higher respectively relative to GCV. Cmax (maximum concentration) of GCV regenerated from L-Tyr-L-Val-GCV, L-Val- L-Val-GCV, L-Gly-L-Val-GCV, L-Val-GCV and GCV were 996.25 ± 160.49 , 112.61 ± 20 , 81.31 ± 11.31 , 389.4 ± 33.1 and $201.02 \pm 30.55 \text{ nmol mL}^{-1}$ respectively (Table 8 – 12). Cmax of regenerated GCV from L-Tyr-L-Val-GCV and L-Val-GCV were found to be 4.9 and 1.9 times higher than Cmax of GCV.

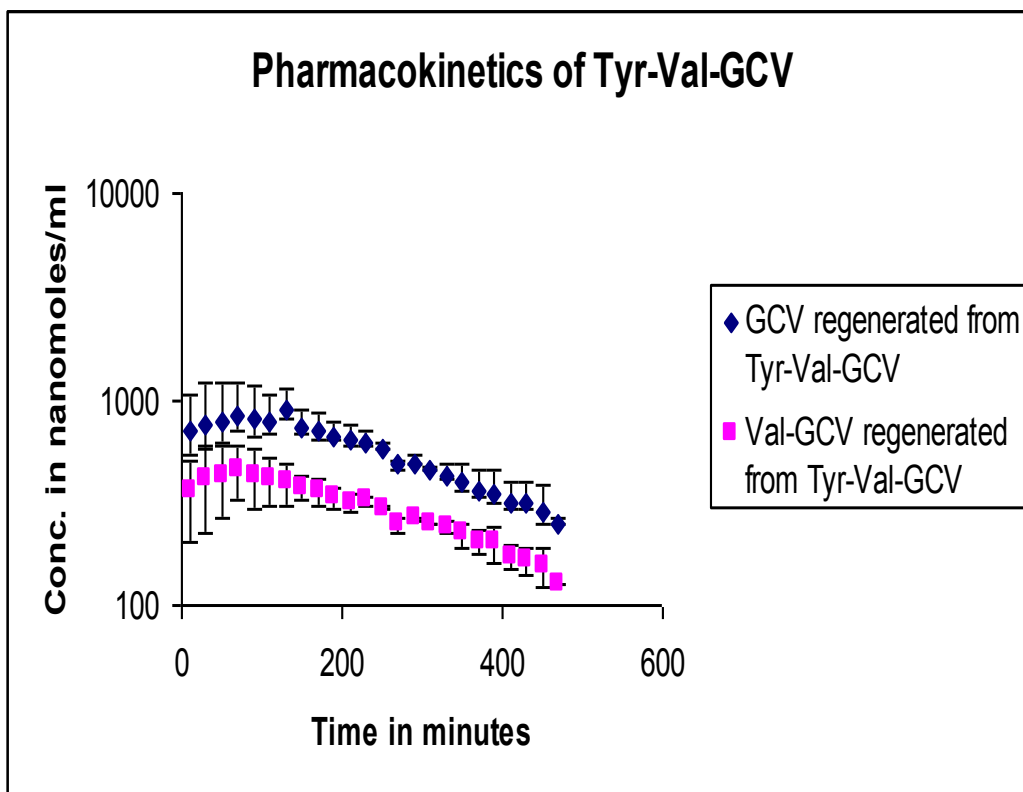


Figure 24. Aqueous humor drug Concentration vs Time profiles of regenerated GCV (Blue diamonds) and L-Val-GCV (pink squares) after 2h infusion of L-Tyr-L-Val-GCV (Mean \pm S.D).

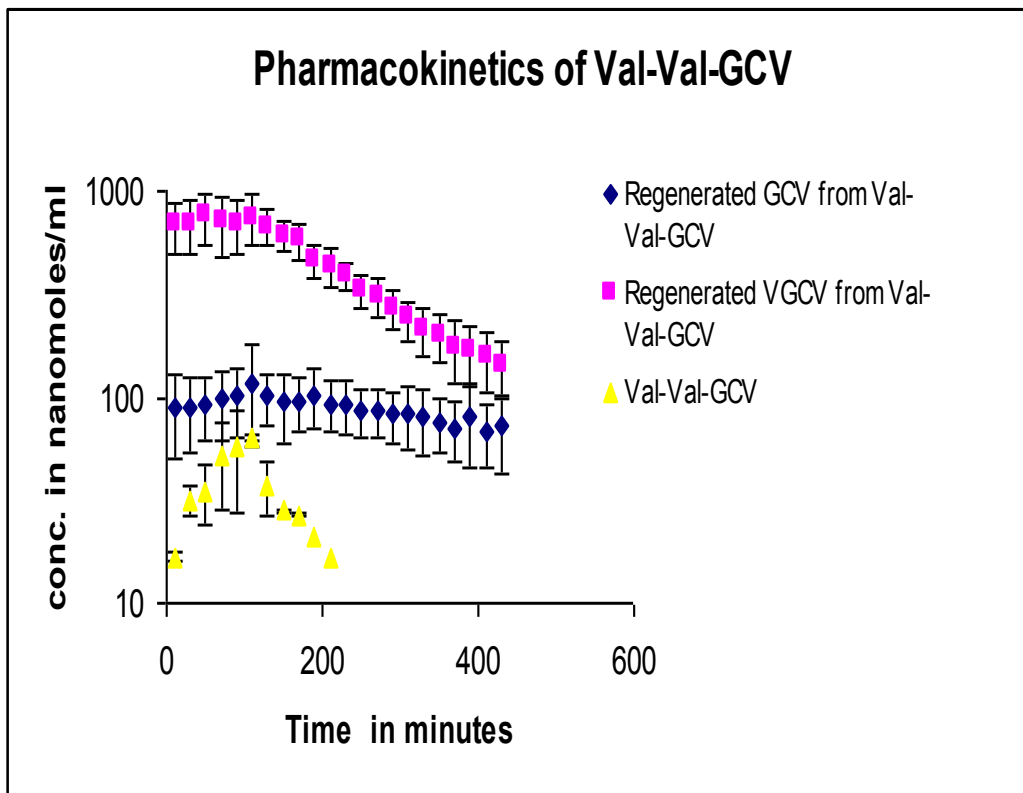


Figure 25. Aqueous humor drug Concentration vs Time profiles of regenerated GCV (Blue diamonds) and L-Val-GCV (pink squares) and intact L-Val-L-Val-GCV (Yellow triangles) after 2h infusion of L-Val-L-Val-GCV (Mean \pm S.D).

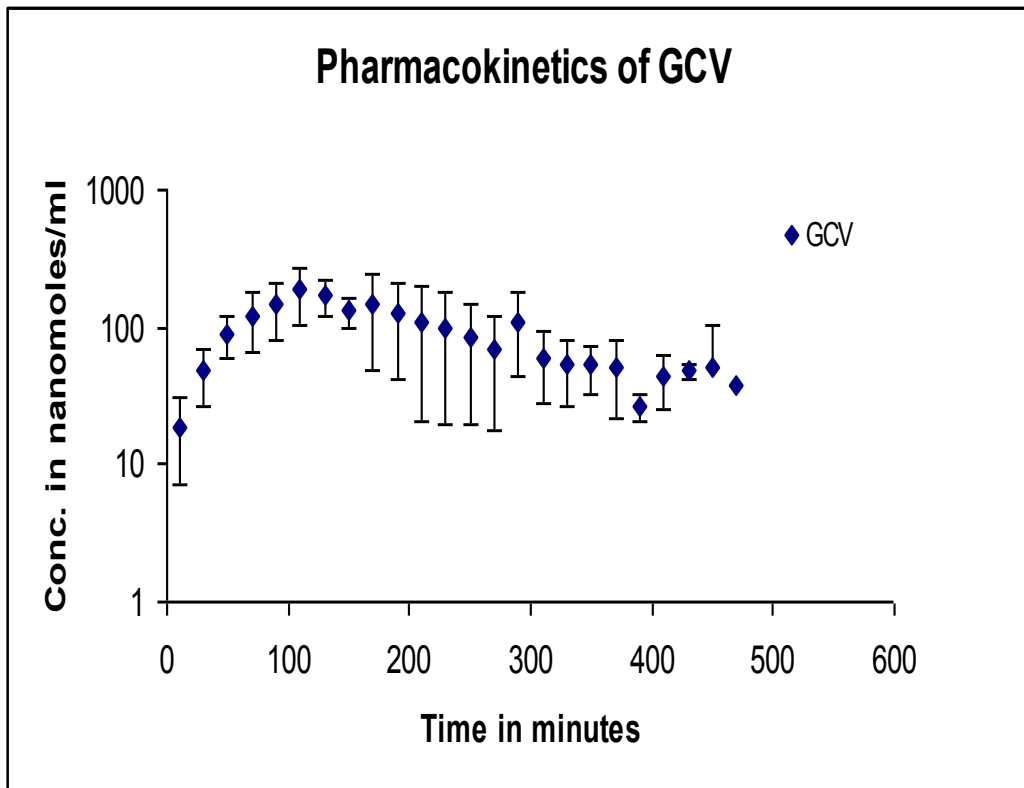


Figure 26. Aqueous humor drug Concentration vs Time profiles of GCV (Blue diamonds) after 2h infusion of GCV (Mean \pm S.D).

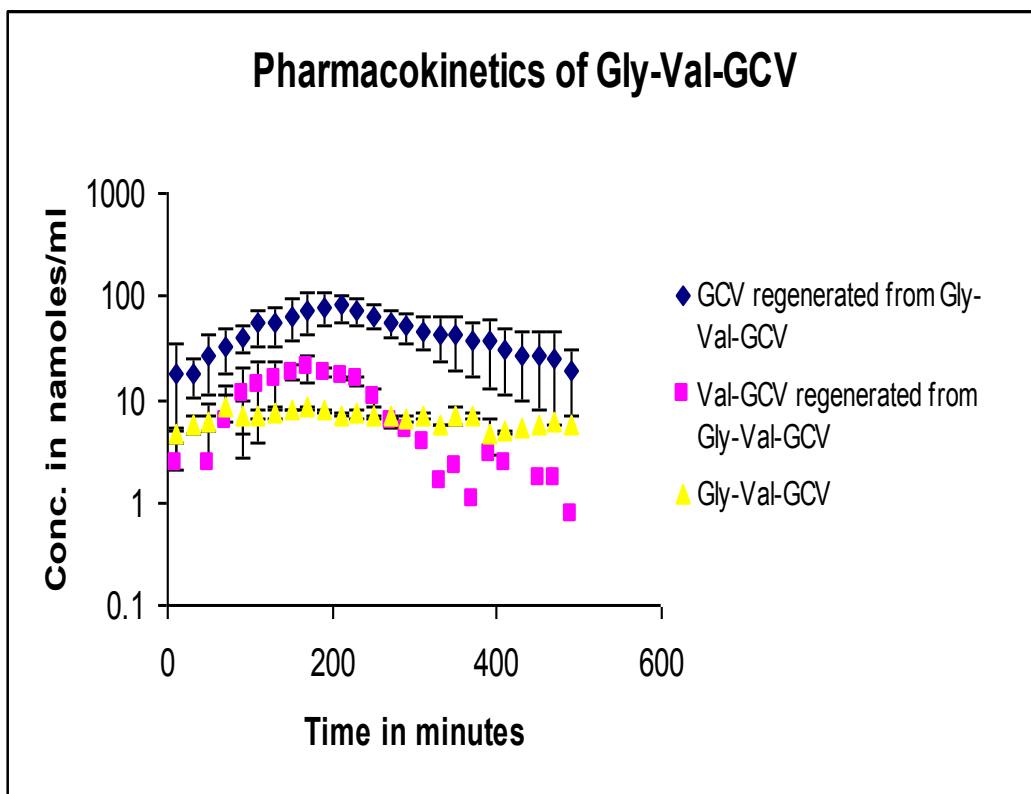


Figure 27. Aqueous humor drug Concentration vs Time profiles of regenerated GCV (Blue diamonds) and L-Val-GCV (pink squares) and intact L-Gly-L-Val-GCV (Yellow triangles) after 2h infusion of L-Gly-L-Val-GCV (Mean \pm S.D).

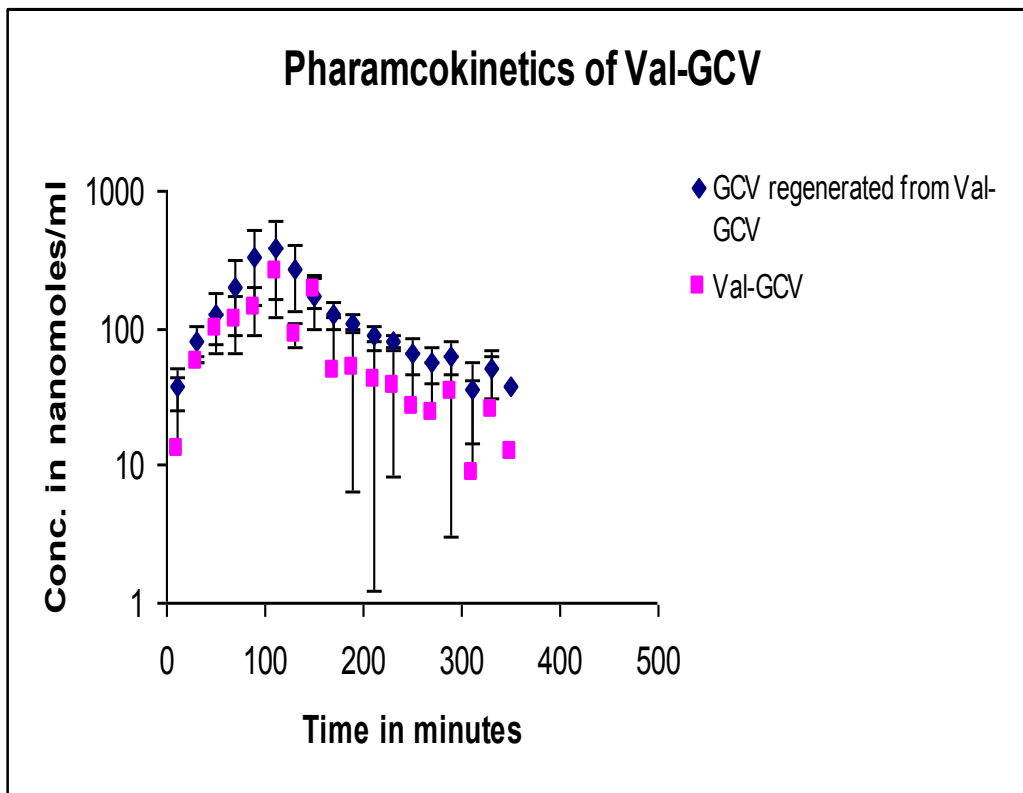


Figure 28. Aqueous humor drug Concentration vs Time profiles of regenerated GCV (Blue diamonds) and intact L-Val-GCV (pink squares) after 2h infusion of L-Val-GCV (Mean \pm S.D).

T_{max} values of regenerated GCV from prodrugs were found to be 70, 130 ± 9, 200 ± 6, 110 and 150 ± 15 min for L-Tyr-L-Val-GCV, L-Val- L-Val-GCV, L-Gly-L-Val-GCV, L-Val-GCV and GCV respectively (Table 8 - 12). Such differences in the T_{max} values might be due to the fact that all of these prodrugs have different lipophilicity values and different conversion rates of prodrugs in the corneal tissues. L-Gly-L-Val-GCV is relatively lesser lipophilic whose T_{max} was observed at 200 min. This could be because L-Gly-L-Val-GCV might have got entrapped in the lipophilic epithelium and slowly got converted to L-Val-GCV and GCV, and then sequentially was released into the aqueous humor. Terminal elimination (λ_z values) rates of regenerated GCV from all the prodrugs were found to be similar except for L-Val- L-Val-GCV. AUC_{infinity} values of the amino acid metabolite L-Val-GCV regenerated from L-Tyr-L-Val-GCV, L-Val- L-Val-GCV, L-Gly-L-Val-GCV and L-Val-GCV administration were found to be 153021 ± 20146, 228391 ± 17329, 3627 ± 594 and 26797 ± 2516 min*nmol/mL respectively (Table 8 - 12). AUC_{infinity} values of amino acid metabolites regenerated from prodrugs L-Tyr-L-Val-GCV and L-Val- L-Val-GCV were found to be 5.7 and 8.5 folds higher than L-Val-GCV. C_{max} values of L-Val-GCV were found to be 460 ± 63, 797 ± 92, and 21 ± 4.3 and 258 ± 11 nmol mL⁻¹ from L-Tyr-L-Val-GCV, L-Val- L-Val-GCV, L-Gly-L-Val-GCV and L-Val-GCV respectively (Table 8 - 12). Most importantly, the maximum aqueous humor concentrations of L-Val-GCV, after L-Tyr-L-Val-GCV and L-Val- L-Val-GCV

infusion, were 1.7 and 3 fold higher than L-Val-GCV respectively. λ_z values for L-Val-GCV regenerated from L-Tyr-L-Val-GCV, L-Val- L-Val-GCV, L-Gly-L-Val-GCV and L-Val-GCV were observed to be 0.0044 ± 0.0002 , 0.004175 ± 0.0006 , $0.0111 \pm .005$ and $0.0078 \pm 0.0006 \text{ min}^{-1}$ respectively (Table 8 - 12).

T_{max} values of L-Val-GCV from these prodrugs varied from 70 to 190 min. AUC_{∞} values of cumulative amounts of GCV, after L-Tyr-L-Val-GCV, L-Val- L-Val-GCV and L-Val-GCV administration, were observed to be 536278 ± 41753 , 301370 ± 13401 and $82112 \pm 4214 \text{ min} \cdot \text{nmol mL}^{-1}$ and were 12, 7, and 1.9 times higher than GCV (Table 13). AUC_{∞} values of cumulative amounts of GCV generated from L-Tyr-L-Val-GCV and L-Val- L-Val-GCV administration resulted in 6.5 and 3.6 times increase compared to equimolar dose of L-Val-GCV.

C_{max} values of cumulative amounts of GCV were found to be 1458 ± 223 , 943 ± 82 , 109 ± 16 and $647 \pm 59 \text{ nmol mL}^{-1}$ and λ_z values were observed to be 0.0044 ± 0.0002 , 0.003475 ± 0.0006 , 0.00465 ± 0.001 and $0.0061 \pm 0.0025 \text{ min}^{-1}$ from administration of L-Tyr-L-Val-GCV, L-Val- L-Val-GCV, L-Gly-L-Val-GCV and L-Val-GCV respectively (Table 13). Dipeptide monoester L-Tyr-L-Val-GCV was not detectable at all. However, L-Val- L-Val-GCV was detected in all subjects except for one, and L-Gly-L-Val-GCV was detected in all the animals. Absorption rate constants (k_a) were determined from the cumulative GCV concentration time profiles.

Table 8. Pharmacokinetic parameters after 2h infusion of L-Tyr-L-Val-GCV. Values presented are for regenerated GCV and regenerated amino acid intermediate L-Val-GCV (Mean \pm S.E.M). AUC- Area under the curve, Cmax- Maximum concentration in aqueous humor, Tmax- Time to reach maximum concentration, Clast- Concentration of the last sample point in aqueous humor, MRT- Mean residence time, Tlast- Time of last time point, λ_z - Terminal elimination rate constant.

pk parameters	Regenerated GCV \pm S.E.M	Regenerated L-Val-GCV \pm S.E.M
AUCinfinity (min*nmol mL ⁻¹)	367082 \pm 31837	153022 \pm 20146
Cmax (nmol mL ⁻¹)	996 \pm 160	461 \pm 63
Tmax (min)	70	70
Clast (nmol mL ⁻¹)	272 \pm 7	125
MRT (min)	168 \pm 13	197 \pm 6
Tlast (min)	480 \pm 6	470
$\lambda_z \cdot 10^2$ (min ⁻¹)	0.44 \pm 0.02	0.44 \pm 0.02

Table 9. Determination of Pharmacokinetic parameters of L-Val-L-Val-GCV after 2h of corneal infusion. Values presented are for regenerated GCV, regenerated amino acid intermediate L-Val-GCV and intact L-Val-L-Val-GCV (Mean \pm S.E.M)

pk parameters	Regenerated GCV Mean \pm S.E.M	Regenerated L-Val-GCV Mean \pm S.E.M	L-Val-L-Val-GCV Mean \pm S.E.M
AUCinfinity (min*nmol mL ⁻¹)	74709 \pm 16336	228392 \pm 17329	12226.4 \pm 2782.3
Cmax (nmol mL ⁻¹)	112.61 \pm 20	797 \pm 92	61 \pm 101
Tmax (min)	130 \pm 9	80 \pm 16	103 \pm 14
Clast (nmol mL ⁻¹)	61 \pm 11	140 \pm 17	24 \pm 3
MRT (min)	206 \pm 3	161 \pm 8	115 \pm 13
Tlast (min)	430	440 \pm 8.9	197 \pm 27
$\lambda_z \cdot 10^2$ (min ⁻¹)	0.18 \pm 0.04	0.42 \pm 0.06	0.56 \pm 0.14

Table 10. Determination of Pharmacokinetic parameters of L-Gly-L-Val-GCV after 2h of corneal infusion. Values presented are for regenerated GCV, regenerated amino acid intermediate L-Val-GCV and intact L-Gly-L-Val-GCV (Mean \pm S.E.M)

pk parameters	Regenerated GCV Mean \pm S.E.M	Regenerated L-Val-GCV Mean \pm S.E.M	L-Gly-L-Val- GCV Mean \pm S.E.M
AUCinfinity (min*nmol mL ⁻¹)	26123 \pm 5811	3628 \pm 594	4918 \pm 546
Cmax (nmol mL ⁻¹)	81 \pm 11	21 \pm 4	9 \pm 1
Tmax (min)	200 \pm 6	190 \pm 13	240 \pm 44
Clast (nmol mL ⁻¹)	19 \pm 5	1 \pm 0.1	5.3 \pm 0.3
MRT (min)	235 \pm 3.2	182 \pm 3	231 \pm 19
Tlast (min)	490	410 \pm 51	450 \pm 25
$\lambda_z \cdot 10^2$ (min ⁻¹)	0.55 \pm 0.1	1.1 \pm 0.5	0.29 \pm 0.1

Table 11. Pharmacokinetic parameters after 2h infusion of GCV. Values presented are for GCV (Mean \pm S.E.M)

pk parameters	GCV Mean \pm S.E.M
AUCinfinity (min*nmol mL ⁻¹)	42259 \pm 6863
Cmax (nmol mL ⁻¹)	201 \pm 31
Tmax (min)	150 \pm 15
Clast (nmol mL ⁻¹)	33.84 \pm 9.57
Cl (mL min ⁻¹)	0.0864 \pm 0.0124
MRT (min)	114.39 \pm 6.19
Tlast (min)	410 \pm 17.88
$\lambda_z \cdot 10^2$ (min ⁻¹)	0.58 \pm 0.12

Table 12. Determination of Pharmacokinetic parameters of L-Val-GCV after 2h of corneal infusion. Values presented are for regenerated GCV and intact L-Val-GCV (Mean \pm S.E.M).

pk parameters	Regenerated GCV Mean \pm S.E.M	L-Val-GCV Mean \pm S.E.M
AUCinfinity (min*nmol mL ⁻¹)	51923 \pm 5519	26797 \pm 2516
Cmax (nmol mL ⁻¹)	389 \pm 33	257 \pm 11
Tmax (min)	110	110
Clast (nmol mL ⁻¹)	37 \pm 3	13 \pm 2
MRT (min)	139 \pm 4	133 \pm 6
Tlast (min)	350	350
$\lambda_z \cdot 10^2$ (min ⁻¹)	0.6 \pm 0.07	0.78 \pm 0.07

Absorption rate constants (k_a) of the drug and prodrugs were determined according to Equation 20 and Equation 21. Absorption rate constants of L-Tyr-L-Val-GCV, L-Val- L-Val-GCV and L-Val-GCV were observed to be 0.57, 0.26 and 0.43 $\text{min}^{-1} * 10^{-3}$ respectively (Table 13). Absorption rate constants (Table 14) were determined from the mean values of the cumulative amounts of the GCV. GCV, L-Val- L-Val-GCV, L-Tyr-L-Val-GCV and L-Gly-L-Val-GCV achieved C_{ss} at least after 70 min. L-Val-GCV did not achieve steady state. All the drugs followed flip-flop kinetics, as it can be observed from their mean values of elimination rate constants and k_a .

Discussion and Conclusion:

GCV, a relatively hydrophilic drug, possesses good antiviral activity against the herpes group of viruses including HSV-1 and 2 types of viruses [128-129] Currently it is not used against herpes keratitis, mainly due to its lower ocular bioavailability. The cornea, being a complex organ, consists of three main layers: the corneal epithelium, stroma and the endothelium. Because of high membrane lipid contents and tight intercellular junctions the epithelium does not permit hydrophilic GCV to pass through the cornea to any significant extent. We reported that lipophilic monoester prodrugs of GCV possess enhanced permeability across cornea. Even though permeability of GCV was increased with this approach, it did so at the expense of aqueous solubility [6].

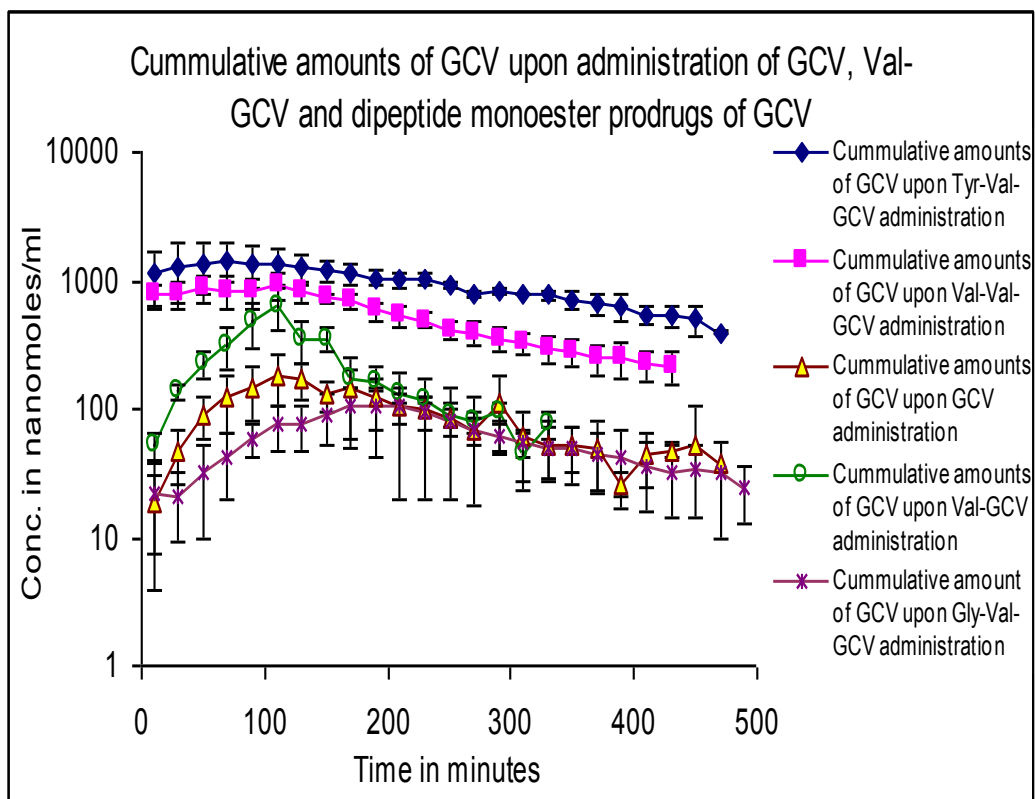


Figure 29. Cumulative amounts of prodrug, intermediate metabolite and regenerated GCV. Aqueous humor drug Concentration vs Time profiles of cumulative amounts of all prodrugs after 2h infusion in rabbit eyes (Mean \pm S.D). (n = 5)

In our earlier publication on dipeptide monoester prodrugs of GCV, it was found that monoester prodrugs L-Tyr-L-Val-GCV, L-Val- L-Val-GCV and L-Gly-L-Val-GCV showed higher solubility and better stability relative to the currently marketed oral prodrug L-Val-GCV. Dipeptide monoester prodrugs exhibited 20-30 times higher lipophilicity along with an additional increase in aqueous solubility [35]. These prodrugs had better in vitro antiviral activity against HSV-1,2 and VZV. L-Val- L-Val-GCV was found to be very effective against corneal epithelial and stromal keratitis [35]. Dipeptide monoesters were found to have excellent affinity to peptide transporter, an influx transporter present on the corneal epithelium. This nutrient transporter ferried the prodrug molecules across corneal epithelium, which in turn were broken down to its amino acid metabolite and parent GCV molecules by esterases and peptidases present in the corneal tissues.

This work represents the continuation of our earlier work on dipeptide monoester prodrugs of GCV [35]. Previously, Eller *et al.* studied the absorption of carbonic anhydrase inhibitors across the rabbit cornea using a well model [106]. In this study we have modified this model by combining it with a microdialysis technique. This model provides accurate data with the use of a few animals compared to the conventional methods which require a large number of animals for a single profile.

Pharmacokinetic data clearly indicate that AUC_{infinity} of the cumulative amounts of GCV regenerated from L-Tyr-L-Val-GCV is 12 times more than GCV alone and 6.5 times more than L-Val-GCV. L-Val- L-Val-GCV was also found to be 7 fold higher than GCV and 3.5 fold higher than L-Val-GCV. A similar trend was observed for C_{max} of L-Tyr-L-Val-GCV and L-Val- L-Val-GCV. Dipeptide monoester L-Tyr-L-Val-GCV was not found in any animal; this suggests that the lipophilic dipeptide monoester ester might be translocated across the corneal epithelium by a peptide transporter as well as by passive transcellular diffusion and may be entrapped in the epithelial layers. Cellular enzymes in the corneal epithelium break L-Tyr-L-Val-GCV into its amino acid metabolite L-Val-GCV and GCV. Because L-Val-GCV and GCV are relatively less lipophilic, these compounds are able to enter the hydrophilic stroma and then into the aqueous humor. Unlike L-Tyr-L-Val-GCV, other prodrugs which are less lipophilic entered the epithelium as well as stroma in lesser quantities and were sequentially bioreversed into L-Val-GCV and GCV both in the epithelium and stroma and in turn were detected in aqueous humor. Elimination of regenerated GCV from all the prodrugs was found to be similar except for L-Val- L-Val-GCV and it accounts for the elimination from aqueous humor as well as the bioreversion into respective metabolites. Significant regeneration of GCV was happening even at the end of the experiment after the administration of L-Val- L-Val-GCV, this

could be the reason for such a different elimination rate observed. AUCinfinity of GCV regenerated from L-Tyr-L-Val-GCV, L-Val- L-Val-GCV and L-Val-GCV was 8.6, 1.8 and 1.2 folds higher and Cmax of regenerated GCV from L-Tyr-L-Val-GCV and L-Val-GCV were 4.9 and 1.9 fold higher than GCV. Both L-Tyr-L-Val-GCV and L-Val- L-Val-GCV exhibited higher AUCinfinity values of regenerated GCV compared to GCV. But Cmax of regenerated GCV was found to be less from L-Val- L-Val-GCV administration than from GCV administration. This observation clearly suggests that L-Tyr-L-Val-GCV displays a more favorable pharmacologic profile relative to L-Val- L-Val-GCV and L-Val-GCV as it is rapidly converted into GCV molecule which is the effective antiviral agent.

Terminal elimination rate constants of regenerated GCV from all the prodrugs slightly differed because there was a constant regeneration as well as elimination of GCV occurring simultaneously. This result can also be confirmed by the different Tlast values of the amino acid intermediate metabolite found in all the groups. Elimination half life of L-Tyr-L-Val-GCV was found to be 157 min as compared to the 18-20 min of currently available drug of choice TFT. As a result of short half life TFT is administered every 2h. With a longer half life of L-Tyr-L-Val-GCV, frequency of drug administration can be significantly reduced. Also, longer MRT (mean residence time) values of regenerated GCV from L-Tyr-L-Val-GCV and L-Val- L-Val-GCV indicate that the mean residence of GCV

Table 13. Pharmacokinetic parameters for corneal absorption of L-Tyr-L-Val-GCV, L-Val- L-Val-GCV, L-Gly-L-Val-GCV, L-Val-GCV and GCV. Values presented are for cumulative amounts of prodrug, amino acid metabolite and GCV in mean \pm SEM. (n=5)

PK parameters	Cumulative amounts of GCV from L-Tyr-L-Val-GCV administration Mean \pm S.E.M	Cumulative amounts of GCV from L-Val- L-Val-GCV administration Mean \pm S.E.M	Cumulative amounts of GCV from L-Gly-L-Val-GCV administration Mean \pm S.E.M	Cumulative amounts of GCV from L-Val-GCV administration Mean \pm S.E.M	GCV Mean \pm S.E.M
AUCinfinity (min*nmol mL ⁻¹)	536278 \pm 41753	301370 \pm 13401	34460 \pm 7022	82112 \pm 4214	42259 \pm 6863
Cmax (nmol mL ⁻¹)	1458 \pm 223	943 \pm 82	109 \pm 16	647 \pm 59	201 \pm 31
Tmax (min)	70	80 \pm 15	190 \pm 13	110	150 \pm 15
Clast (nmol mL ⁻¹)	398 \pm 7	206 \pm 20	25 \pm 5	76 \pm 5	34 \pm 10
Cl (mL min ⁻¹)	0.0064 \pm 0.0005	0.011 \pm 0.0004	0.1092 \pm 0.02	0.041	0.0864 \pm 0.0124
MRT (min)	1378 \pm 6	109 \pm 8	172 \pm 1	73 \pm 2	114 \pm 6
Tlast (min)	470	440 \pm 9	490	330	410 \pm 18
$\lambda_z \cdot 10^2$ (min ⁻¹)	0.44 \pm 0.02	0.35 \pm 0.06	0.47 \pm 0.1	0.61 \pm 0.25	0.58 \pm 0.12

molecule is longer in the aqueous humor. Absorption rate constant L-Tyr-L-Val-GCV was about 6 times higher than GCV. This also suggests that L-Tyr-L-Val-GCV is entering the cornea at higher rates as well at higher amounts compared to GCV, as it has higher lipophilicity as well as affinity to peptide transporter on the rabbit cornea.

In conclusion, L-Tyr-L-Val-GCV and L-Val- L-Val-GCV exhibited superior corneal absorption and bioavailability in comparison with GCV and L-Val-GCV following topical administration. This result might be due to enhanced absorption of these drugs *via* both transcellular passive diffusion and hPEPT1 mediated transport across corneal epithelium. L-Gly-L-Val-GCV did not appear to be a better candidate. AUCinfinity of regenerated GCV from L-Tyr-L-Val-GCV was higher compared to GCV and L-Val-GCV which suggests L-Tyr-L-Val-GCV has the best and most therapeutically desirable pharmacologic profile.

Table 14. Absorption Rate Constants for corneal absorption of L-Tyr-L-Val-GCV, L-Val- L-Val-GCV, L-Gly-L-Val-GCV, L-Val-GCV and GCV. Values presented are from the mean concentration time profiles of cumulative amounts of GCV from the administration of 4 prodrugs and GCV.

Drug/Prodrugs	Absorption rate constants	
	Ka*10 ³ (min ⁻¹)	Half life t _{1/2} (min)
L-Tyr-L-Val-GCV	0.57	-
L-Val- L-Val-GCV	0.26	124
L-Gly-L-Val-GCV	0.04	239
L-Val-GCV	0.43	89
GCV	.09	119

CHAPTER 6

PHARMACOKINETICS AND METHOD DEVELOPMENT OF GANCICLOVIR AND ITS DIPEPTIDE MONOESTER PRODRUGS IN SPRAGUE DAWLEY RATS USING HIGH PERFORMANCE LIQUID CHROMATOGRAPHY COUPLED MASS SPECTROMETRY

Rationale

GCV, a nucleoside analog of 2'-deoxyguanosine is an effective agent for the treatment of herpes simplex virus (HSV) infections [113, 131]. In cells infected with HSV, viral thymidine kinase phosphorylates GCV to the corresponding monophosphate (MP) [146]. Cellular kinases then convert GCV-MP into the triphosphate (TP), which competitively inhibits DNA polymerase-catalyzed incorporation of dGuo-TP into DNA [147]. GCV-TP is incorporated into the end of a growing chain of viral DNA with concomitant loss of pyrophosphate [148-149]. In contrast to ACV, GCV does not appear to serve as a chain terminator but is incorporated internally into DNA strands [146]. This causes a decrease in the rate of DNA synthesis and disrupts viral replication [147]. The specificity of GCV arises because it is an excellent substrate for viral kinases, whereas it is a poor substrate for endogenous mammalian kinases [150-151]. The ability of GCV-TP to inhibit replication has stimulated a suicide gene therapy approach for the treatment of human tumors [151-155]. Transfection of an HSVtk gene into mammalian cells results in the efficient conversion of GCV to GCV-MP. As with virally infected cells, subsequent conversion to GCV-TP then

provides a substrate to compete with dGuo-TP for incorporation into elongating DNA. The decreased rate of DNA synthesis and incorporation of GCV-TP into DNA then inhibit host cell DNA replication. A critical component of this approach involves the ability to rapidly and specifically monitor plasma levels of GCV so that appropriate pharmacokinetic models can be constructed and optimal dosing strategies be developed. GCV exhibits excellent antiviral activity against the herpes family of viruses. It is the drug of choice for systemic and ocular HCMV infections and is as effective as ACV against HSV-1. Even though GCV has advantages of antiviral property, it has very low permeability across various physiological barriers, including blood aqueous and blood retinal barriers, and intestinal epithelial cells. It also exhibits relatively low aqueous solubility.

A few attempts have been made in our laboratory to identify derivatives of GCV, especially for topical drug delivery to the eye. Lipophilic acyl ester prodrug strategy was utilized to improve corneal permeation. Even though permeability across the cornea was improved, aqueous solubility of the compounds diminished. In another previous report from our laboratory, cyclodextrins were used to increase the solubility of these lipophilic acyl ester prodrugs of GCV. This strategy of using prodrugs and cyclodextrins together was effective to a certain degree but inclusion of more than 5% wt/v cyclodextrins in the formulation resulted in corneal toxicity [6, 114]. There are numerous reports suggesting the

use of various prodrugs of GCV as an antiviral agent. In our laboratory, dipeptide prodrugs of GCV were synthesized to treat various HSV ocular infections [35].

Recently, nutrient transporters are being targeted for efficient delivery of drugs across cell membranes. Previously published reports from our laboratory have demonstrated utilization of such strategies. Transporters such as peptide (PEPT1, PEPT2), amino acid ($B^{0,+}$, $b^{0,+}$ and LAT), folate and other vitamin transporters as well as transferrin and insulin receptors can be excellent targets for drug delivery. Peptide transporters (PEPT1 and PEPT2) have so far been the most widely utilized. Several drugs including cephalosporins, L-Val-ACV and L-Val-GCV are substrates of peptide transporters [35, 39-40]. Oral bioavailabilities of L-Valine linked antiviral agents have improved significantly. These L-Valine ester prodrugs, after oral administration, were broken down into their parent drugs by enzymes such as peptidases and esterases present in intestinal mucosa and blood. Our earlier reports have shown that hydrophilic GCV is not a substrate for nucleoside/nucleobase transporters present on the cornea and its permeation across the cornea occurs primarily by passive diffusion [60]. Peptide derivatives of hydrophilic molecules, such as GCV, may enhance both aqueous solubility and PEPT aided permeation across the cornea.

Our earlier work has demonstrated the utilization of peptide transporter for transcorneal delivery of GCV [35]. In these studies, dipeptide monoester prodrugs

of GCV were synthesized and their superior aqueous solubility and stability were shown. Inhibition studies of radio labeled gly-sar and gly-pro with these prodrugs demonstrated their affinity towards the peptide transporter on the cornea. These derivatives also demonstrated higher antiviral efficacies *in vitro* and *in vivo*, against HSV-1, HSV-2, VZV and HCMV relative to parent drug. In this report we describe a strategy to deliver GCV in the form of dipeptide prodrugs to increase its oral bio-availability which in turn would be very effective against systemic and genital herpes infections.

Currently, liquid chromatography–coupled mass spectrometry (LC–MS/MS) has been applied more extensively to measure drug concentrations in various biological matrices such as plasma, serum and urine due to its sensitivity, selectivity and reproducibility. To the best of our knowledge, no method on LC-MS/MS method has been reported in literature for simultaneous measurement of drug concentrations of GCV and GCV peptide prodrugs. The aim of the present study is to develop a selective and reproducible LC-MS/MS method for the quantitative estimation of GCV and GCV peptide prodrugs in rat matrices. This method is successfully applied to determine pharmacokinetic behavior of GCV and GCV peptide prodrugs in jugular vein cannulated Sprague Dawley rats following oral administration.

Methods and materials

GCV and ACV (internal standard) were purchased from Sigma Chemical Co (St. Louis, MO) while L-Val-GCV and L-Tyr-L-Val-GCV were synthesized in our laboratory [35]. HPLC grade methanol, acetonitrile, diethyl ether, dichloromethane, isopropyl alcohol and analytical grade and formic acid procured from Fisher Scientific (New Brunswick, NJ). Ultrapure water from MilliQ-system (Millipore, Molshecin France) was used in all experiments and analysis. All chemicals were of HPLC grade and used as received without further purification.

Preparation of standard stocks and spike solutions:

GCV, L-Val-GCV, L-Tyr-L-Val-GCV and ACV stock solutions were prepared at 1 mg mL^{-1} in methanol. Calibration curves and spike dilutions of 0.50 – 1000 ng mL^{-1} for GCV, 10.0 – 500 ng mL^{-1} for both L-Val-GCV and L-Tyr-L-Val-GCV were prepared in mobile phase and were summarized in Table 15. Stock dilution of internal standard (ACV) at $10 \text{ } \mu\text{g mL}^{-1}$ was prepared in 20% v/v methanol in water. All the solutions were stored at -80°C until further use.

Procedure for sample preparation and extraction:

Rat serum samples were thawed at room temperature and vortexed. Samples of 0.1 mL were transferred into 1.5 mL poly propylene micro centrifuge tubes (PPMCT) using calibrated pipettes, followed by the addition of 25 μL of $10.0 \text{ } \mu\text{g mL}^{-1}$ freshly prepared IS solution to all samples, except for blank. These

Table 15. GCV and its prodrug(s) calibration curve standards calculated value(s) and percentage accuracy(s)

Nominal Conc. (ng mL ⁻¹)	Calculated Conc. (ng mL ⁻¹)			Percentage accuracy		
	GCV	L-Val- GCV	Try-L- Val-GCV	GCV	L-Val- GCV	L-Tyr-L- Val-GCV
0.50	0.53			107.0		
1.00	1.00			99.6		
10.00	10.14	9.90	9.90	101.4	99.6	99.0
50.00	53.19	50.85	50.85	106.4	101.0	101.7
100.00	102.37	112.36	112.36	102.4	105.3	112.4
250.00	238.06	212.94	212.94	95.2	98.5	85.2
500.00	454.23	508.98	508.98	90.8	97.2	101.8
1000.00	948.94			94.9		

GCV: Ganciclovir; L-Val-GCV: L-Valine -ganciclovir prodrug; L-Tyr-L-Val-GCV: L-Tyrosine- L-Valine -ganciclovir prodrug

LOQ for GCV: 0.50 ng mL⁻¹; L-Val-GCV: 10.0 ng mL⁻¹ and L-Tyr-L-Val-GCV: 10.0 ng mL⁻¹

ULOQ for GCV: 1000.00 ng mL⁻¹; L-Val-GCV: 500.0 ng mL⁻¹ and L-Tyr-L-Val-GCV: 500.0 ng mL⁻¹

Percentage of coefficient of variation (% CV): within 7.3 % for GCV; 11.2 for L-Val-GCV and 16.2 for L-Tyr-L-Val-GCV

solutions were vortexed for 30 seconds. The samples were extracted by the addition of 1000 μL of isopropyl alcohol – dichloromethane (40:60 v/v) followed by vortexing for approximately 2 min. After centrifugation at 12000 rpm at 4 $^{\circ}\text{C}$ for 25 min, 850 μL of organic layer was transferred to a pre- labeled fresh 1.5 mL of poly propylene micro centrifuge tube and evaporated in the Speed Vac[®] at 35 $^{\circ}\text{C}$ for 60 min. The residue was reconstituted with 100 μL of mobile phase, vortexed for 30 seconds and transferred into a pre-labeled HPLC autosampler vial with silanized inserts. Fifteen microliters of the resulting solution was injected into LC-MS/MS for analysis.

In vivo Studies with Sprague-Dawley Rats:

Oral absorption studies of GCV and its prodrugs were carried out at an equivalent dose of 10 mg/kg. Animals were fasted overnight (12–18 h) with free access to water. Freshly prepared drug solutions in water were administered by oral gavage (0.8 mL). Blood samples (200 μl) were collected from jugular veins at predetermined time intervals over a period of 8 h. Heparinized saline (200 μl) was injected through both the veins to maintain a fairly constant fluid volume. Plasma was immediately separated by centrifugation and then stored at -80°C until further analysis. Prior to the analysis, plasma samples were thawed at room temperature and extracted as described earlier.

Calculation of Pharmacokinetic Parameters:

All relevant pharmacokinetic parameters were calculated with noncompartmental analyses of plasma concentration vs time curves following oral administration of GCV and the dipeptide prodrug. A pharmacokinetic software package Phoenix WinNonlin v6.1, (Pharsight, Mountain View, CA) was employed to calculate primary and secondary pharmacokinetic parameters. Maximum plasma concentrations (C_{max}) were obtained from the plasma concentration vs time curves and the area under the plasma concentration time curves (AUC_{last} and $AUC_{infinity}$) were determined by the linear-log linear trapezoidal method with extrapolation. Where the absorption phase of curves is estimated by linear regression and disposition phase is modeled by exponential or log-linear extrapolation. The slopes of the terminal phase of plasma profiles were estimated by log-linear regression and the terminal rate constant (λ_z) was derived from the slope. The terminal plasma half-lives were calculated from the equation $t_{1/2} = 0.693/\lambda_z$. Clearance (Cl/F) and mean residence time (MRT) were calculated as ratio of dose and $AUC_{infinity}$, and area under the first moment curve ($AUMC$)/ $AUC_{infinity}$, respectively. The total concentration parameters were calculated by adding the concentrations of the administered drug and the regenerated intermediates in terms of GCV.

Liquid-Chromatographic operating conditions:

Chromatographic analysis was carried out on API 3200 triple quadrupole linear ion Qtrap mass spectrometer. Prominence Series of Shimadzu ultra fast liquid chromatographic (UFLC) system consists of Shimadzu 20 M Vp Binary pump, Shimadzu SIL 20 AM autosampler (Shimadzu Scientific Instruments North America) with a reversed phase Xterra C8 column (50 x 4.6 mm i.d, 5 μ m, Waters, USA). Isocratic mobile phase composed of 85 % v/v of acetonitrile in water containing 0.05 % v/v of formic acid was pumped at a rate of 0.2 mL min⁻¹.

Mass spectrometer operating conditions:

MDS Sciex API 3200 Triple Quadrupole linear QTrap mass spectrometry (Applied Biosystems/MDS Sciex, Foster City, CA) system interfaced by turbo ionspray (TIS) with positive ion source in MRM mode was applied for detection. Ultra high pure nitrogen served as collision activated dissociation (CAD) at 4 psi and curtain gas at 20 psi. Nebulizer and turbo gas were optimized at 40 and 50 psi respectively. TIS source temperature was maintained at 200⁰C, with source voltage and dwell time optimized at 5200V and 200 milliseconds respectively. Mass dependent parameters were tuned and optimized for GCV, L-Val-GCV and L-Tyr-L-Val-GCV. Parent and daughter ions obtained by direct infusion mode (20 μ L min⁻¹) were injected with built-in Harvard infusion syringe pump and were optimized.

Statistical Analysis:

All experiments were conducted at least in triplicate, and results are expressed as mean \pm SD. Student's t-test was applied to detect statistical significance between the parameters of the prodrug and GCV, and $p < 0.05$ was considered to be statistically significant. Statistical comparisons between the parameters of the prodrugs were performed using the analysis of variance (SPSS for Windows, release 10.0.7; SPSS Inc., Chicago, IL).

Results

Mass spectrometer operation condition for GCV, L-Val-GCV and L-Tyr-L-Val-GCV:

In order to optimize electrospray ionization condition for GCV, L-Val-GCV and L-Tyr-L-Val-GCV, full scan mass spectra were acquired in the positive ion mode. During a direct infusion experiment, the mass spectra for GCV, L-Val-GCV and L-Tyr-L-Val-GCV, the internal standard ACV revealed peaks at mass to charge ratio (m/z) 256.20, 355.40, 518.50 and 226.3, respectively, as protonated molecular ions $[M+H]^+$. The most stable abundant fragment ion observed in each product MS/MS spectrum was at m/z 152.3 for GCV, 338.3 for L-Val-GCV, 367.5 for L-Tyr-L-Val-GCV and 152.20 for IS ACV. These spectra were achieved by optimizing the collision energies at 18.0 V, 30.0 V and 18.0 V respectively as shown in Figure 30 - 32). Quantitative determination was

performed in MRM scan positive ion mode with the following mass transitions: 256.20→152.30 for GCV, 355.4→338.3 L-Val-GCV, 518.5→367.5 for L-Tyr-L-Val-GCV, and 226.20→152.20 for ACV (Figure 30 - 32)

Precision and accuracy:

Accuracy was determined by analyzing multiple (n=2) calibration curve samples (0.5 – 1000.0 ng mL⁻¹) using the methods presented in Table 15. Percent of accuracy for GCV (90.8 – 107.0 %), L-Val-GCV (97.2 – 105.3 %) and L-Tyr-L-Val-GCV (85.2 – 112.4 %) was observed for calibration curve standards. Linearity of GCV, L-Val-GCV and L-Tyr-L-Val-GCV was obtained over the concentration range of 0.5 -1000 and 10.0-500.0 ng mL⁻¹ respectively in rat serum at pH=7.2 (Table 15). Linear regression, best fit 1/x² “weighting” factor mean correlation coefficient (r) were calculated to be 0.9995, 0.9981 and 0.9895 for GCV, L-Val-GCV and L-Tyr-L-Val-GCV, respectively. Pharmacokinetic studies in rats: Plasma pharmacokinetics of GCV (Figure 33) and its prodrug L-Tyr-L-Val-GCV (Figure 34) were studied in male sprague-dawley rats. Experiments were conducted for 8 h after drug administration at a dosage of 10 mg/kg of GCV and its molar equivalent amount of L-Tyr-L-Val-GCV. Blood samples were collected, processed and analyzed with a LC-MS/MS spectrometry method developed in our laboratory.

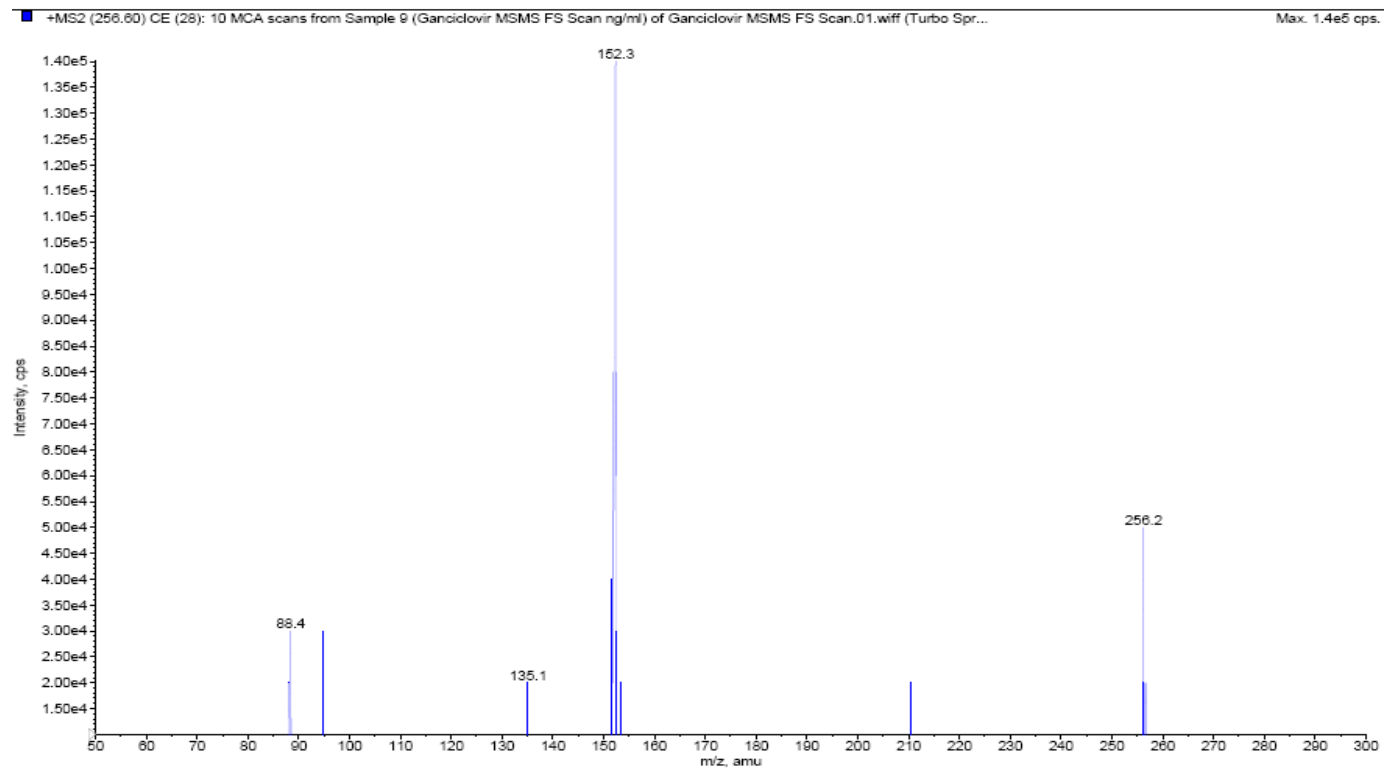


Figure 30. LC-MS/MS spectrum of GCV and its respective ions produced by MRM method. The major ion of GCV was found to be 152.3

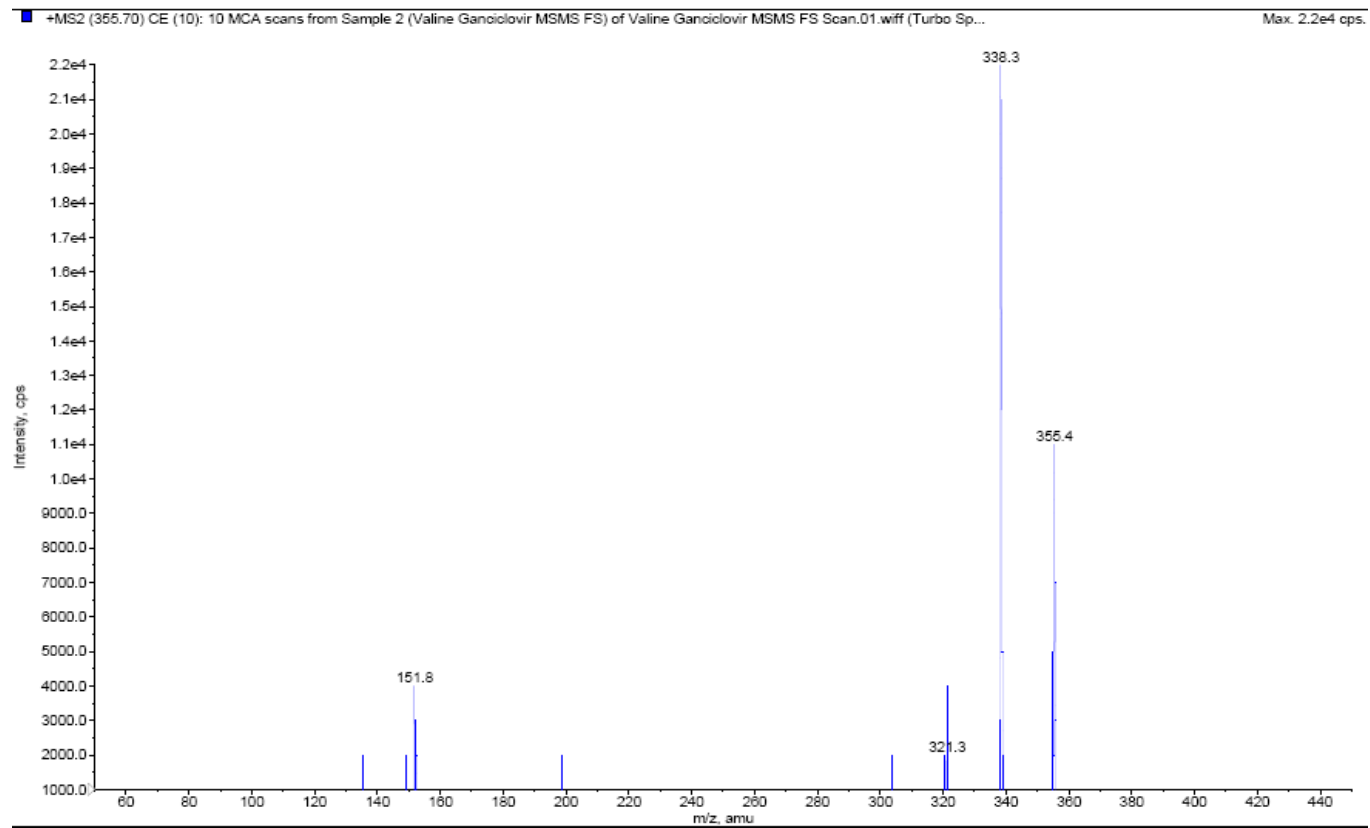


Figure 31. LC-MS/MS spectrum of L-Val-GCV and its respective ions produced by MRM method.

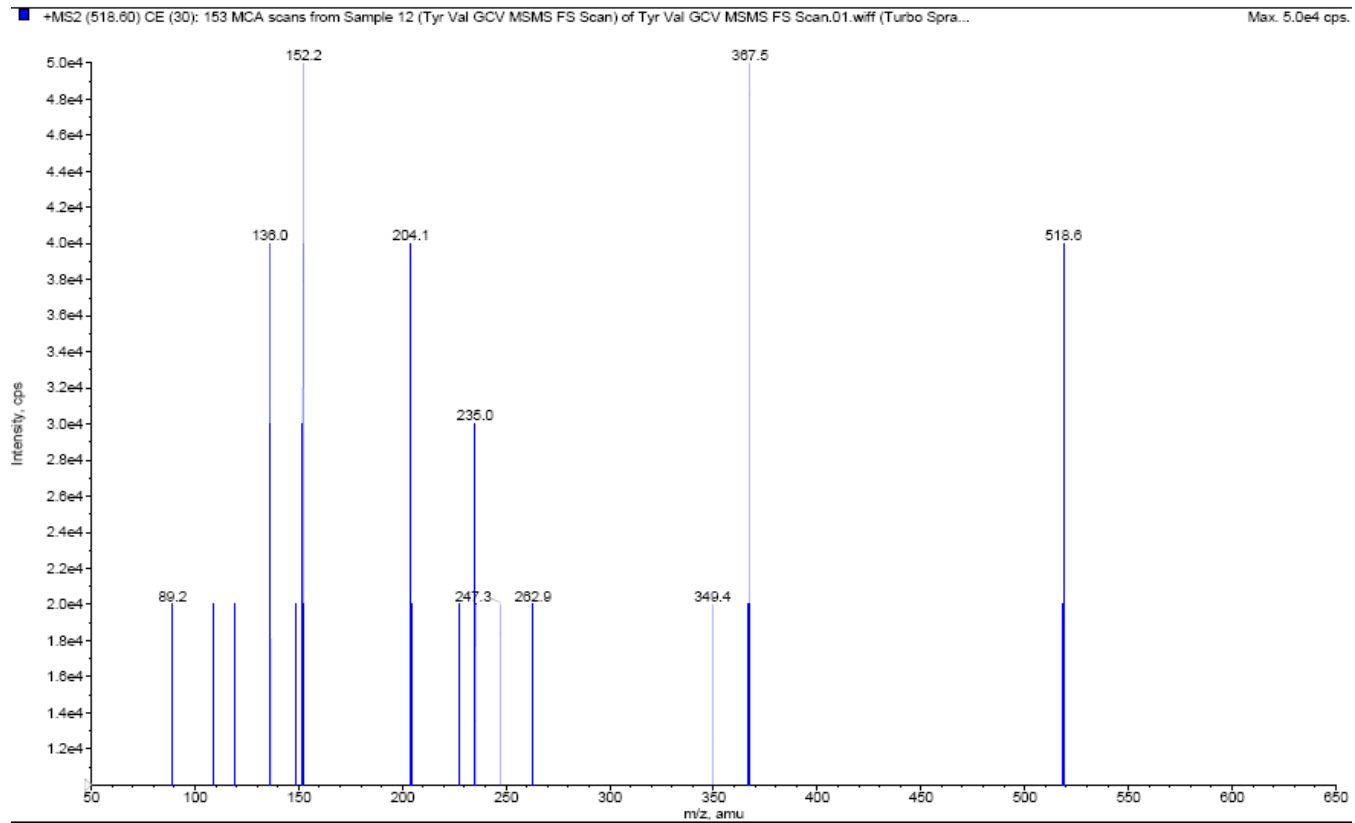


Figure 32. LC-MS/MS spectrum of L-Tyr-L-Val-GCV and its respective ions produced by MRM method.

L-Tyr-L-Val-GCV and its amino acid metabolite L-Val-GCV were not found in the blood at any sampling time point as expected. GCV dipeptide was found to be completely and rapidly metabolized by enzymes present in the Figure 34. Ganciclovir was analyzed in both the control and the test experiments (Figure 34 and Figure 34). AUC_{last} and AUC_{infinity} of GCV in control and regenerated GCV in test groups were found to be $31214 \pm 4951 \text{ min} \cdot \text{ng mL}^{-1}$, $54115 \pm 16747 \text{ min} \cdot \text{ng mL}^{-1}$ and $32988 \pm 4839 \text{ min} \cdot \text{ng mL}^{-1}$, $77177 \pm 2920 \text{ min} \cdot \text{ng mL}^{-1}$ respectively. Values of C_{max} of GCV in control and regenerated GCV in test groups were found to be $220 \pm 110 \text{ ng mL}^{-1}$ and $448 \pm 47 \text{ ng mL}^{-1}$ at T_{max} of 65 ± 35 in control and 30 ± 14 min in test groups, respectively. Elimination rate constants of GCV in both control and tests subjects were found to be similar with values of 0.0065 ± 0.0011 and $0.0054 \pm 0.0014 \text{ min}^{-1}$ respectively. Elimination half time of GCV and regenerated GCV after L-Tyr-L-Val-GCV administration was found to be 108 ± 19 and 148 ± 20 min, respectively. Clearance and volume of distribution of GCV in both control and test animals were calculated to be 77 ± 11 , $79 \pm 3 \text{ mL min}^{-1}$ and 12121 ± 3918 , $12121 \pm 3918 \text{ mL}$ respectively. Mean residence time (MRT) of GCV in test control rats was found to be 137 ± 47 min and of regenerated GCV in test rats was 148 ± 20 min (Table 16 and Table 17).

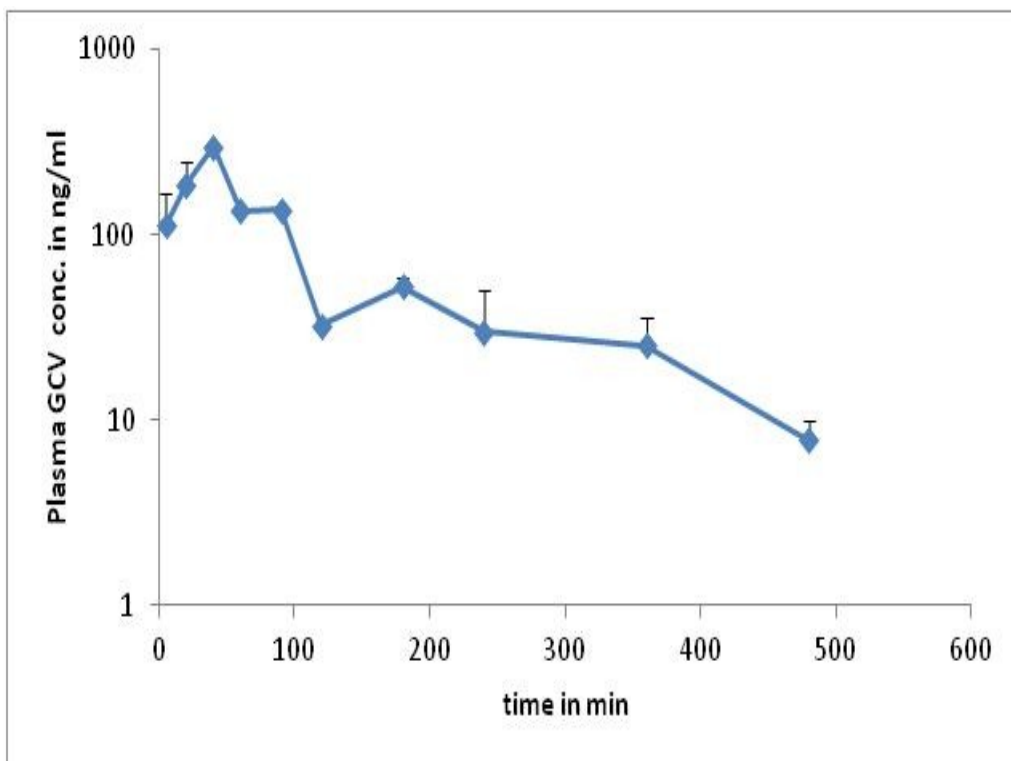


Figure 33. Plasma drug log-concentration vs Time profile of GCV (Blue diamonds) after intravenous administration of 10 mg/kg dose of GCV in rats. Data points presented are in Mean \pm S.D. Number of animals used, n=3.

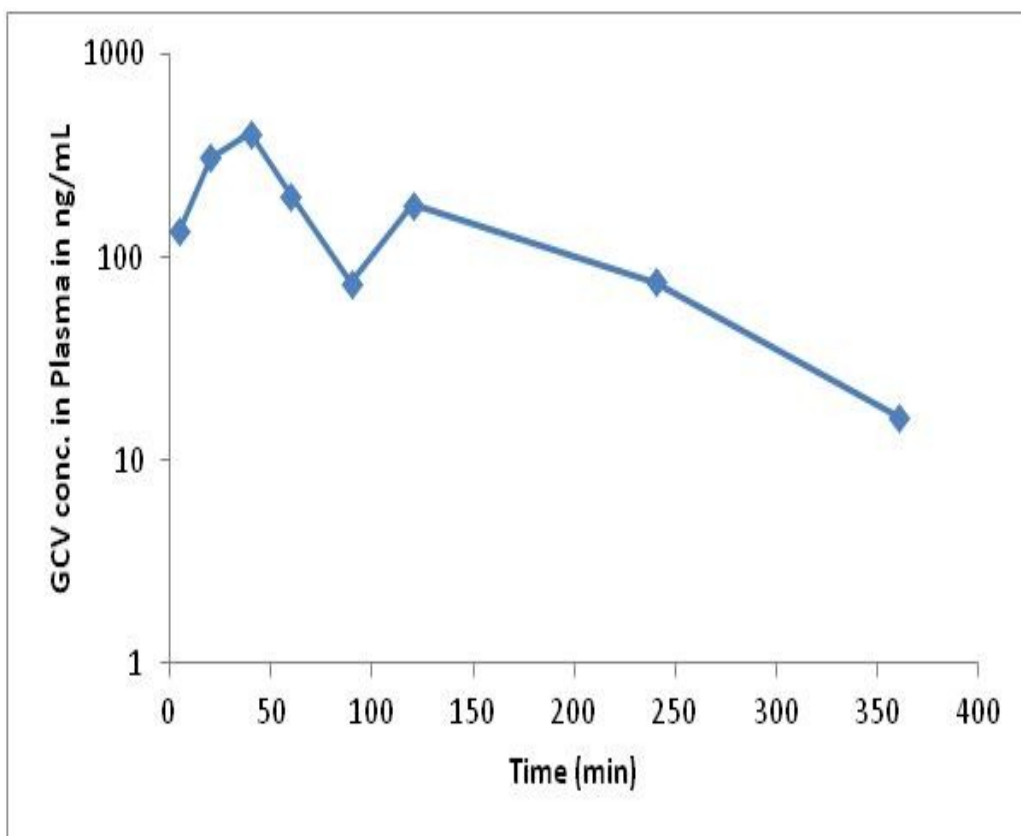


Figure 34. Plasma drug log-concentration vs Time profile of GCV (Blue diamonds) after intravenous administration of 10 mg/kg dose of L-Tyr-L-Val-GCV in rats. Data points presented are in Mean \pm S.D. Number of animals used, n=4.

Discussion and conclusions

Recovery of GCV and its monoester peptide prodrugs from rat serum by simple liquid-liquid extraction procedure resulted in clean samples with consistent and high extraction efficiency. We have investigated various sample extraction methods, including protein precipitation and liquid-liquid extraction with different organic solvents (acetonitrile, methanol, isopropyl alcohol, perchloric acid, trichloro acetic acid, ethyl acetate, methyl (t)-butyl ether, dichloromethane, hexane and diethyl ether and their combinations at various ratios). Isopropyl alcohol-dichloromethane combination efficiently precipitated proteins and extracted analytes from the serum. Though the sample extraction was efficient with acetonitrile and methanol, results were found to be inconsistent. Extraction of analytes with a mixture of isopropyl alcohol- methyl (t)-butyl ether also gave high recovery for L-Val-GCV and L-Tyr-L-Val-GCV but low recovery for GCV. Extraction with the combination of isopropyl alcohol- dichloromethane (40: 60 v/v) further improved accuracy and reproducibility of data but with reduced recovery of analytes. Finally, a solution of Isopropyl alcohol- dichloromethane (40: 60 v/v) was used for extraction of pharmacokinetic samples because of its consistence and ruggedness in the method.

Although it is not yet possible to cure herpes virus infections, the management of genital herpes infections has improved considerably since the

Table 16. Plasma pharmacokinetic parameters of GCV after oral administration at a dose of 10 mg/kg. Values presented as Mean \pm S.D.

pk parameters	Plasma GCV (Mean \pm S.D.)
AUClast (min*ng mL ⁻¹)	31214 \pm 4951
AUCinfinity (min*ng mL ⁻¹)	32988 \pm 4839
Cmax (ng mL ⁻¹)	220 \pm 110
Tmax (min)	65 \pm 35
λ_z (min ⁻¹)	0.0065 \pm 0.0011
t _{1/2} (min)	108 \pm 19
Cl (mL min ⁻¹)	77 \pm 11
Vz (mL)	12121 \pm 3918
AUMC (min*min* ng mL ⁻¹)	26164881 \pm 28635541
MRT (min)	137 \pm 47

Table 17. Plasma pharmacokinetic parameters of GCV after oral administration of L-Tyr-L-Val-GCV equivalent to dose of 10 mg/kg of GCV. Values presented as Mean \pm S.D.

pk parameters	Regenerated GCV in plasma (Mean \pm S.D.)
AUClast (min*ng mL ⁻¹)	54115 \pm 16747
AUCinfinity (min*ng mL ⁻¹)	77177 \pm 2920
Cmax (ng mL ⁻¹)	448 \pm 47
Tmax (min)	30 \pm 14
λ_z (min)	0.0054 \pm 0.0014
t _{1/2} (min)	133 \pm 35
Cl (mL min ⁻¹)	79 \pm 3
V _z (mL)	15017 \pm 3419
AUMC (min*min*ng mL ⁻¹)	21943245 \pm 7636512
MRT (min)	148 \pm 20

introduction of acyclo-guanosine based antiviral drugs in the early 1980s. The incidence of genital herpes infections caused by HSV-1 and 2 has increased significantly in the past 20 years [156]. Although genital herpes is self-limiting in healthy adults, the disease is painful and distressing, with severe psychosocial impact [157-158]. Acyclovir was the first effective antiviral drug approved for widespread use and is still extensively prescribed, particularly in the treatment of immuno-competent patients with genital HSV disease [159]. Although ACV is a well tolerated and effective antiviral drug, its bioavailability after oral administration is very low. As a result, up to 5 times administration per day is often necessary for the management of genital HSV infections. L-Valacyclovir, L-Valyl ester prodrug of ACV, enhances the bioavailability of ACV due to the recognition of VACV by intestinal peptide transporter hPEPT1, which mediates transport across intestinal epithelium to blood. In this study, we have utilized hPEPT1 to increase the oral bioavailability of GCV intended to treat genital herpes infections with Dipeptide prodrugs. In an earlier article we have reported the aqueous solubility, chemical and enzymatic stability of the prodrug. Dipeptide prodrugs have exhibited high aqueous solubility and chemical stability [35]. In a similar trend, GCV prodrugs were converted to parent drug by esterases and peptidases present in the intestine and blood. An intermediate, L-Val-GCV was generated in blood which was observed in few samples (data not shown),

indicating the breakdown of peptide bond between the two amino acids by peptidases present in the blood which in turn was converted into GCV by esterases.

C_{max} of regenerated GCV after oral administration of L-Tyr-L-Val-GCV was found to be approximately two times of GCV. A similar pattern was seen observed with AUC_{last} and AUC_{infinity}, where the mean value of GCV after prodrug administration were approximately 2 times that of control GCV (Table 16 and Table 17). Terminal elimination rate constants and plasma half lives in both test and control rats were found to be very similar as expected, since the regenerated GCV will be eliminated in by the same passive elimination process of the parent drug. The mean value of T_{max} for test rats after oral administration of L-Tyr-L-Val-GCV was found to be approximately half of the mean value of control rats which indicates that the prodrug was rapidly absorbed into the blood compared to GCV. This rapid absorption is probably due to active transport across the intestinal barrier through PEPT. Our earlier studies suggested that peptide prodrugs of GCV were found to be substrates of PEPT on the corneal epithelium [40]. L-Tyr-L-Val-GCV also has higher lipophilicity [35] compared to the relatively hydrophilic GCV, a factor that may be responsible for rapid absorption across the intestinal epithelium. Since the peptide prodrugs also exhibited higher aqueous solubility [35], these can also be given at higher doses

compared to relatively poor soluble GCV. In conclusion, L-Tyr-L-Val-GCV exhibited better absorption and higher plasma concentration compared to GCV. This prodrug can be a substitute for GCV intended to treat both systemic and genital herpes infections, especially in immune compromised patients.

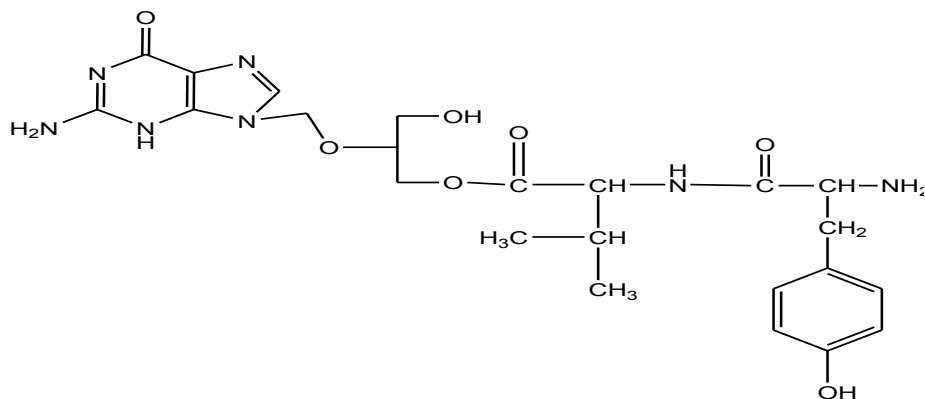
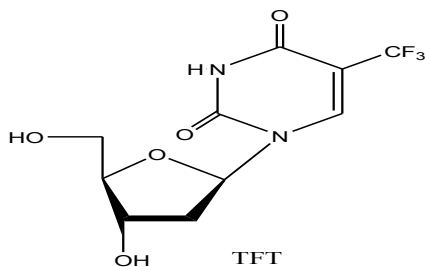
CHAPTER 7

ANTIVIRAL STUDIES OF L-TYR-L-VAL-GCV ON HSV-1 INDUCED RABBIT EPITHELIAL KERATITIS MODEL

Rationale

Herpes simplex virus is one of the leading causes of ocular morbidities in United States. Dendritic structures, opacities and inflammations are the common signs of infection to the cornea [121-122]. Drugs developed initially for the treatment of HSV infections were TFT, IDU, and cytosine arabinoside (Ara-A). All these drugs are non-specific, which is the root cause of systemic toxicities [160]. Even though some of them are prescribed as the first line of therapy, their use in long-term therapy causes corneal surface toxicities. One of the drugs, TFT, causes toxicity when used for a longer time [127]. Acyclovir, a nucleoside analogue was also found to be clinically effective against HSV [161]. Ganciclovir, another nucleoside analogue has also shown good therapeutic efficacy against HSV infections. A 0.15% wt/wt gel of GCV is approved by U.S. FDA for the treatment of superficial herpes corneal keratitis. Both ACV and GCV have low aqueous solubility and low corneal permeability due to their relative hydrophilic nature. An optimum balance between hydrophilicity and lipophilicity is required to obtain good ocular bio-availability. A achieve better ocular absorption, a series of dipeptide prodrugs of GCV were designed. Preliminary studies indicated that L-Tyr-L-Val-GCV, a dipeptide monoester prodrug of GCV,

has shown promising pharmacokinetic profile and better ocular bio-availability. It is found that the high absorption of Try-L-Val-GCV could be due to both transcellular diffusion and active transport by PEPT1 transporter present on the corneal epithelium. In the current study, an anti-viral efficacy experiment of L-Tyr-L-Val-GCV and TFT (Figure 35) was conducted in HSV-1 strain McKrae induced rabbit models. The trial was conducted for 14 days, to study reduction in corneal scarring and lesions as well as the survival of analysis.



L-Tyrosine-Valine-GCV

Figure 35. Structures of TFT (above) and L-Tyr-Val-GCV (below)

Methods and materials

Epithelial Keratitis: A 10 µl stock of HSV-1 strain McKrae (100,000 pfu/eye) suspension was inoculated in 30 New Zealand male albino rabbits. Corneas of rabbits, weighing 1.5-2.5 Kg, were mildly scarred to subsequently infect with virus. Slit-lamp examinations were performed post infection day 3-10, 12, and 14. Rabbits were divided into three groups of 10 animals each, first as a control (BSA), second with 50 µl of 1% wt/v TFT treatment, third with 50 µl of 1% wt/v L-Tyr-L-Val-GCV. Rabbits were masked for days of treatment and SLE scoring. Groups were color coded as red for L-Tyr-L-Val-GCV, Blue for TFT and yellow for BSA. Drugs were administered in aqueous solutions as topical drops, for five days PI 3-7 days. Frequency of administration was five times daily, for every 2h starting at 8 AM and ending at 4PM. After the 2 hr of last administration, SLE scores were taken. The Table 19 describes the detailed information on dosing schedule and treatment. SLE scores were based on the type of lesions found on cornea. The below Table 18 has the detailed scoring system of Slit-lamp examination. Survival of animals was also observed for PI 14 days.

Statistical Analysis:

For slit-lamp scores, nonparametric one-way analysis of variance was performed (Kruskal-Wallis test) was used. Wilcoxon scores were used for

Table 18. SLE Scoring System to measure lesions of epithelial keratitis caused by HSV-1 strain Mckrae on Rabbit cornea

SLE scores	Characteristics
0 – 0.5	Normal to nonspecific, random superficial lesion
0.6 – 0.9	Punctate ulcerations
1.0 - 1.9	One or more dendritic ulcerations
2.0 – 2.9	Geographic ulceration or trophic erosion (less than 50% of cornea involved)
3.0 +	Geographic ulceration or trophic erosion (more than 50% of cornea involved)

Table 19. Treatment and scoring schedule of three groups of HSV-1 infected rabbits. Inoc.- Inoculation of virus; PI – Post inoculation; SLE – Slit-lamp examination; TFT – Trifluorothymidine, BSA – Control group/placebo, L-Tyr-L-Val-GCV – L-Tyrosine-L-Valine-Ganciclovir

Treatment	PI 1 day	PI 3 day	PI 4 day	PI 5 day	PI 6 day	PI 7 day	PI 8 day	PI 9 day	PI 10 day
Control (BSA)	Inoc.	5 times Dosing SLE	5 times Dosing SLE	5 times Dosing SLE	5 times Dosing SLE	5 times Dosing SLE	SLE	SLE	SLE
150 1% wt/v TFT (50 µL drop)	Inoc.	5 times Dosing SLE	5 times Dosing SLE	5 times Dosing SLE	5 times Dosing SLE	5 times Dosing SLE	SLE	SLE	SLE
1% wt/v L-Tyr-L-Val- GCV (50 µL drop)	Inoc.	5 times Dosing SLE	5 times Dosing SLE	5 times Dosing SLE	5 times Dosing SLE	5 times Dosing SLE	SLE	SLE	SLE

comparison among groups in this analysis. The software used was IBM SPSS statistics 20.0. Mean data was also fitted to polynomial equations to explain the non-linear behavior of the data. Microsoft excel was used to perform fitting of the models.

Results

Antiviral efficacy studies conducted rabbit models were analyzed for SLE scores based on the size and characteristics of lesions. Both the TFT and L-Tyr-L-Val-GCV showed comparable profiles (Figure 36). By the end of PI 10 days, no sign of lesions were observed in both the study groups. On the contrary, the control group had still shown observable lesions on the corneal epithelium. The 1% wt/v dose of L-Tyr-L-Val-GCV used was equivalent to 19.4 mM and 1% wt/v TFT equals to 33.3 mM. At approximately 2/3 rd the molar concentration of TFT, L-Tyr-L-Val-GCV exhibited therapeutically equivalent anti viral effect.

Discussion and conclusions

L-Tyr-L-Val-GCV was observed to have higher absorption across rabbit cornea in our earlier pharmacokinetic studies. Its better pharmacokinetic profile enabled it to be the choice of drug for the anti viral studies. A 1% wt/v aqueous solution of the prodrug was compared to 1% wt/v TFT, which is the current drug of choice. Both the eyes of rabbits were treated with 5 doses a day of 50 µl each (Table 19).

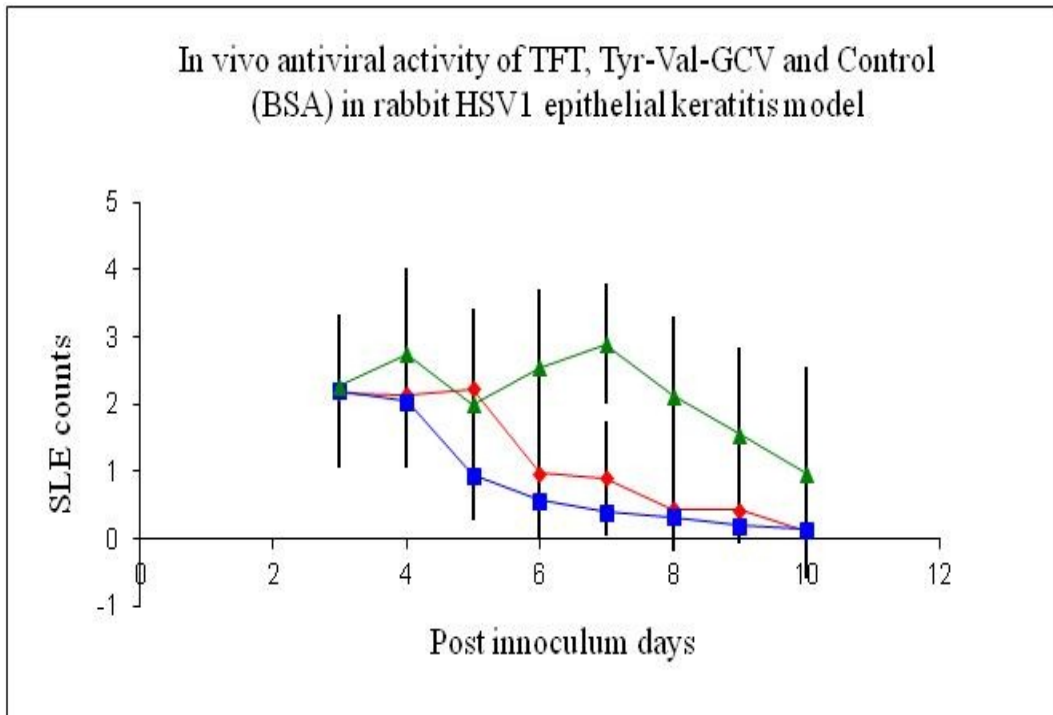


Figure 36. *In vivo* antiviral activity of 1% wt/v TFT (blue), 1% wt/v Try-L-Val-GCV (red) and control/BSA (Green). Five doses of 50 μ l drops were topically administered every day to the HSV-1 infected eyes of New Zealand Albino male rabbits, from PI day 3 to PI day 7. SLE scores were taken from PI day 3 to PI day 10. Total number of animals used for the studies is 30, n=10 for each group.

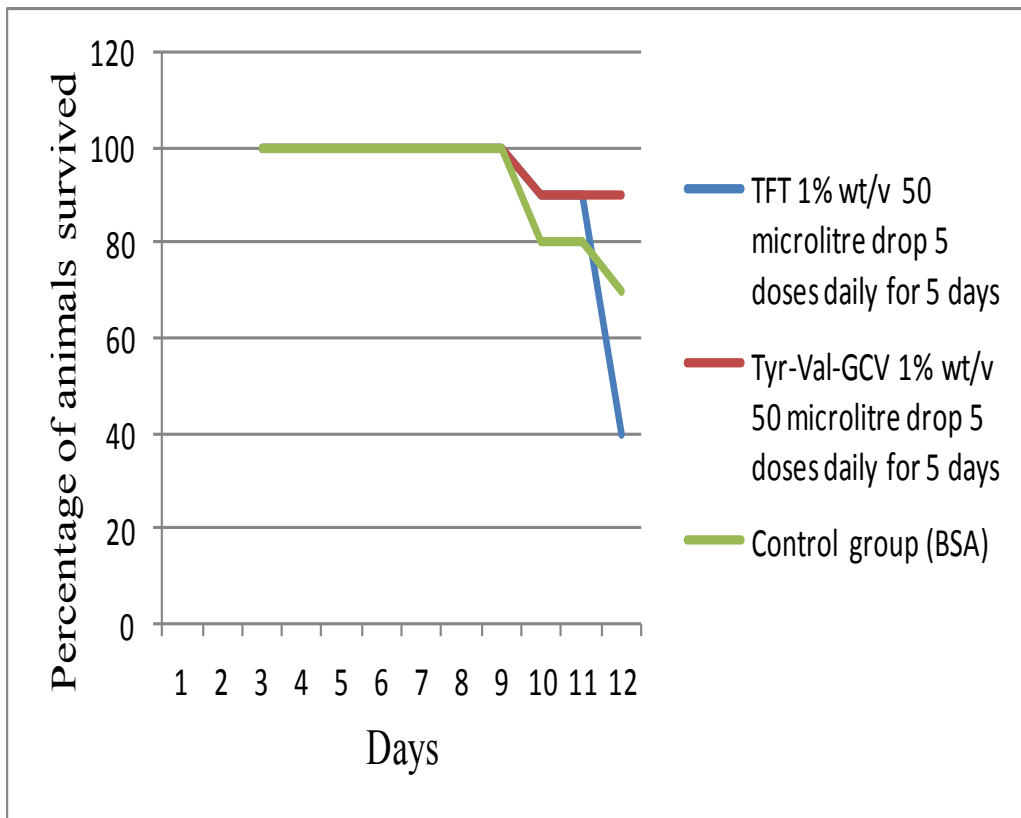


Figure 37. Survival analysis graph of three groups of rabbits, 10 each, treated with 1% wt/v TFT (blue), 1% wt/v L-Tyr-L-Val-GCV (red), and BSA (green). Five doses of 50 μ l drops were administered per day on PI days 3-7. Survival of animals was observed till day 12.

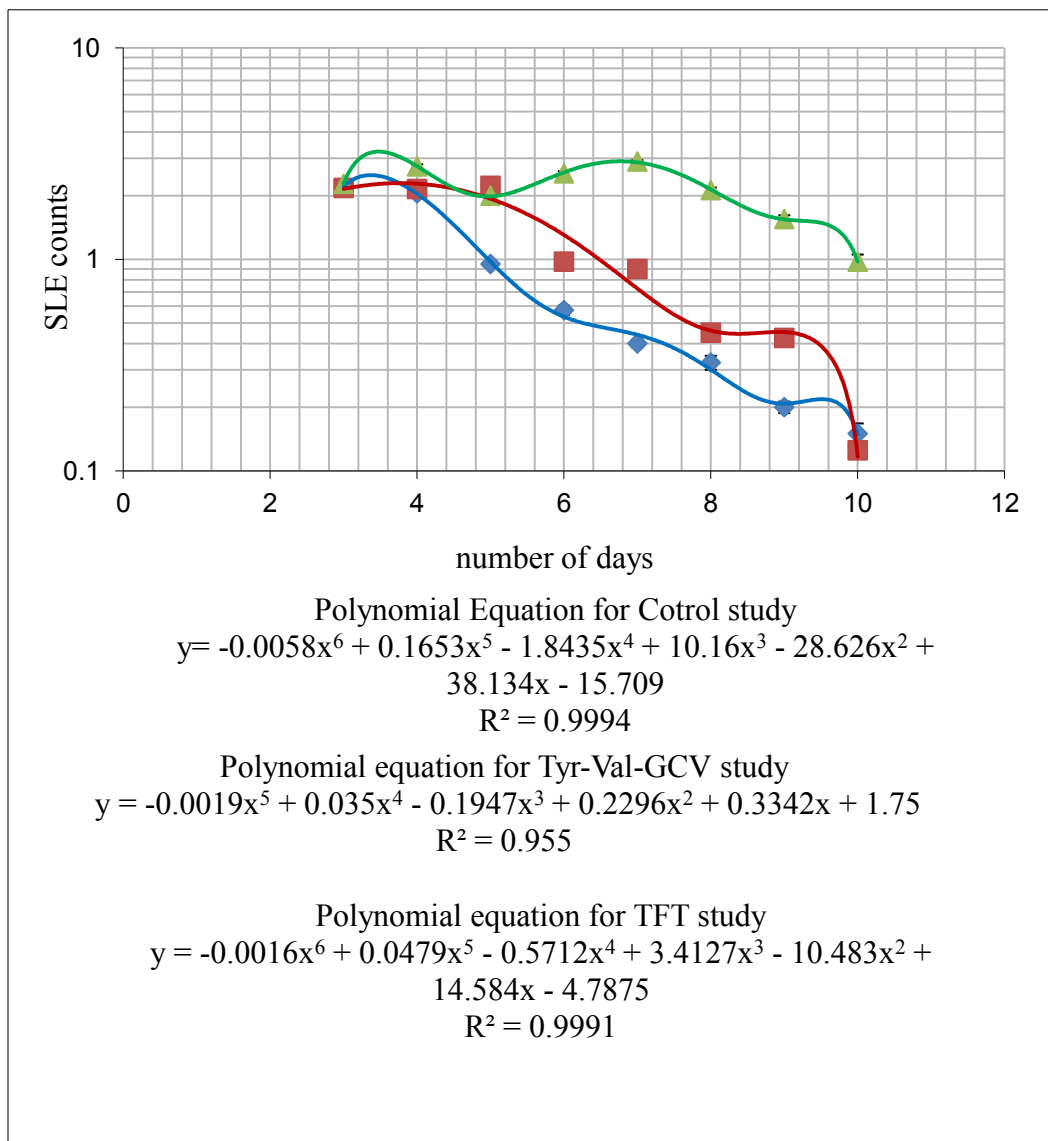


Figure 38. Models of mean SLE scores of three groups after treatment with BSA (Green), 1% wt/v TFT (blue) and 1% wt/v L-Tyr-L-Val-GCV (red). Three polynomial equations represent the three groups of treatment.

An initial lag period in both treatment groups was observed from the data. It can be attributed to both the start of antiviral action and the healing. The lesions are an indirect effect of the viral activity. In essence, the study measures an indirect effect rather than the direct viral counts. Healing of corneas would start after the viral load is reduced in the cornea. Statistical analysis of the data suggests no significant difference in both the treatments groups. The mean data of the three groups behave in a polynomial regression. Disease progression in all the three groups is modeled in five or six level polynomial equations (Figure 38).

All three groups of animals were observed for survival (Figure 37) for 12 days. Animals started dying after at least PI day 10. The control group had lost 3 (30%) animals by the end of the study, TFT treatment group had lost 6 (60%) animals, and L-Tyr-L-Val-GCV group had lost 1 (10%) animal by PI 12 days.

In conclusion L-Tyr-L-Val-GCV monoester exhibited equivalent antiviral activity compared to TFT at $2/3^{\text{rd}}$ the molar dose. Treatment group also exhibited very high survival rate compared to the control and TFT.

CHAPTER 8

SUMMARY AND RECOMMENDATIONS

Summary

Ganciclovir is an acyclo guanosine analogue which possess excellent anti viral efficacies against Cytomegalo viruses (CMV), Herpes simplex virus 1 (HSV-1) and 2 (HSV-2), Epstein-Barr virus (EBV), Varicella-zoster virus (VZV) both *in vitro* and *in vivo*. It is indicated for the treatment of systemic and ocular human CMV infections as a prophylactic as well as for therapy. It is also indicated for ocular herpes infections as gels and ointments, but it has low ocular bio-availability and aqueous solubility.

The broad overall objective of this dissertation was to identify functional activity of sodium dependent large neutral and cationic amino acid transporter *in vivo*, study the absorption mechanisms of L-Arginine across intact rabbit cornea and its disposition in the anterior chamber of the eye. Also, to study the ocular bio-availability of the various amino acid and di-peptide prodrugs of GCV, their metabolism and disposition *in vivo*, utilizing zero-order input well infusion and ocular microdialysis in the rabbit models, and studying their antiviral activity against HSV-1 infections in rabbit models.

In earlier part of this dissertation (Chapter 4), functional activity of the sodium dependent large neutral and cationic amino acid transporter ($B^{0,+}$) was

studied *in vitro* and *in vivo* using rabbit primary corneal epithelial cells (rPCEC) and New Zealand albino male rabbits respectively. The AUC, T_{max} and C_{max} of the natural substrate L-Arginine was estimated and compared with parameters in presence and absence of various inhibitors and ions. Both AUC and C_{max} of radio labeled [³H] L-Arginine were found to be decreased in presence of cold L-Arginine, and BCH, a specific inhibitor of B^{0,+} transporter. Even though absence of sodium ions didn't show significant change in the respective pharmacokinetic parameters, absence of chloride ion did. This proves the functionality of the B^{0,+} transporter. Interaction studies of L-Phenylalanine-GCV, L-Tyrosine-GCV and γ -L-Glutamate-GCV with B^{0,+} transporter *in vitro* showed that these prodrugs have affinity for the transporter. Ocular pharmacokinetics studies of these prodrugs showed significant increase, about 80%, in the AUC and C_{max} over GCV. Utility of targeting B^{0,+} transporter on the corneal epithelium was found to be a useful strategy to improve ocular bio-availability of drugs. Even though amino acid prodrugs were found to be better than GCV, they did not show great improvement as expected.

Therefore the next aim of this dissertation was to utilize the hPEPT1 present on the corneal epithelium for the improvement of GCV delivery (Chapter 5). A series of di-peptide monoester prodrugs of GCV were synthesized and evaluated. Among those prodrugs L-Valine-L-Valine-GCV, L-Tyrosine-L-

Valine-GCV, L-Glycine-L-Valine-GCV were studied for their ocular bio-availability and absorption. These prodrugs were also compared with L-Valine-GCV, which is also recognized by PEPT1, and GCV. Two di-peptide prodrugs, L-Val-L-Val-GCV and L-Tyr-L-Val-GCV, were found to have superior pharmacokinetic characteristics relative to GCV. Both these prodrugs showed about 10-12 times improvement in AUC and Cmax. Both of these prodrugs showed bio-reversion patterns where an amino-acid metabolite, L-Val-GCV, was produced along with parent GCV molecule. In comparison, GCV regenerated from L-Tyr-L-Val-GCV administration was 6 times more than the bio-availability of GCV. Both AUC and Cmax of regenerated GCV from L-Tyr-L-Val-GCV administration were higher compared to the regenerated GCV after L-Val-L-Val-GCV. Terminal elimination rate constants of regenerated GCV from L-Val-L-Val-GCV and L-Tyr-L-Val-GCV were slower than that of parent drug GCV. Ganciclovir is not known for non-linear kinetics. It follows a linear process of elimination from kidneys. In anterior chamber, drugs are eliminated from the aqueous humor through trabecular mesh work into canal of Schlemm (Figure 39). We expect the GCV to eliminate from anterior chamber through this process. Non-linearity in the elimination of the regenerated GCV could be attributed to the depot formation of lipophilic L-Tyr-L-Val-GCV and L-Val-L-Val-GCV in the lipoidal corneal epithelium. These prodrugs are slowly converted to L-Val-GCV

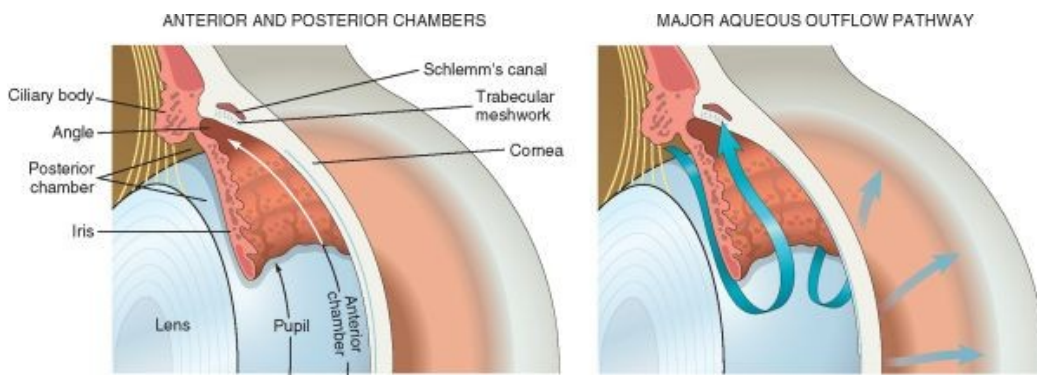


Figure 39. The above picture depicts (i) anterior and posterior chambers (left) of anterior segment and (ii) the aqueous humor generation in ciliary body in the posterior chamber and clearance through trabecular meshwork into canal of schlemm in the anterior chamber. Drugs in the anterior segment are eliminated *via* this route [162].

Table 20. Table of pharmacokinetic parameters comparing the parent GCV and regenerated GCV from prodrugs

Ratios of PK parameters	GCV	Regenerated GCV from YVGCV	Regenerated GCV from VVGCV	Regenerated GCV from GVGCV	Regenerated GCV from VGCV
AUC_{PD}/AUC_D	1	~8.6	~1.5	~0.4	~1.25
C_{maxPD}/C_{maxD}	1	~4.9	~0.6	~0.25	~2
$\lambda_{zPD}/\lambda_{zD}$	1	~0.7	~0.4	~1	~1

and GCV in the cornea by peptidases and esterases present in the epithelium, and then are released into the aqueous humor due their higher hydrophilicity.

Even though the regenerated GCV from L-Val-L-Val-GCV is twice the bio-availability of parent drug GCV, it was lesser compared to regenerated GCV after L-Tyr-L-Val-GCV administration. Eight fold more regenerated GCV (Table 20) from L-Tyr-L-Val- GCV was a compelling evidence to suggest it for further *in vivo* anti viral studies.

In the subsequent study, L-Tyr-L-Val-GCV, TFT and control groups of 10 rabbits each were inoculated with HSV-1 strain McKrae (Chapter 7). Corneal epithelium of all animals were infected and studied for lesions on the surface by SLE (slit-lamp examination) scoring method. Five doses of 50 μ L drops of 1% wt/v drug solutions were given every day. SLE scores were estimated after 2 hours of last dose every day. After 5 days of therapy, drug dosing was stopped but the SLE scores were taken till post-inoculum 10 days. This was an indirect effect model, where the scoring was performed by classifying size of lesions on the cornea. Since the lesions are the inflammatory response against the virus, they were used as response estimators. Even though the reduction in the inflammation is considered, actual viral loads may have subjugated before the observed response. Therapeutic response of L-Tyr-L-Val-GCV was found to be equivalent to TFT response. It is also observed that the dose of L-Tyr-L-Val-GCV was

approximately 19 mM compared to the 33 mM of TFT used. Therapeutic equivalency was observed at 2/3rd the molar concentrations of GCV. By the end of 12 day study, 6 animals in the TFT treatment group were found to be dead, compared to 3 animals in the control and 1 animal in the study group, which is L-Tyr-L-Val-GCV. Polynomial models were fitted to data from three groups. The data fitted well with 5 level and 6 level polynomial behaviors.

In conclusion, the objective of the study to develop a good prodrug of GCV comparable to efficacy of TFT with less toxicity was achieved with success by utilizing oligopeptide transporter on the cornea. L-Tyrosine-L-Valine-GCV, a novel di-peptide monoester prodrug of GCV targeted to PEPT1 on the cornea exhibited excellent characteristics for the HSV-1 ocular infections.

Recommendation

Based on the above studies it is proven that designing of anti-viral prodrugs of GCV would be beneficial to improve ocular and oral bio-availabilities of GCV. There are two ways of improving ocular bio-availability by topical administration, (i) by increasing the drug stay in the pre-corneal cul-de-sac, (ii) by increasing the rate of absorption across cornea. A few recommendations that could be made for the second type of improvement, from the above dissertation project are

- 1). All the amino acids used are L type isomers. A combination of L and D isomers could be used to make amino acid monoesters and di-peptide prodrugs to control drug bio-reversion.
- 2). Two hydroxyl groups of GCV could be used to attach two different pro-moieties, to target two different transporters expressed on either side of the cell. A sequential targeting, bio-reversion and then targeting might improve targeting as well as drug disposition.
- 3). A methodology can be developed to combine rate constants obtained from tear pharmacokinetics and aqueous humor pharmacokinetics, and simulate pharmacokinetics data for drops. It could accurately predict bio-availability and drug concentrations, and drug dosing schedule.
- 4). There is a potential to explore more transporters, such as MCTs, on the cornea for drug targeting.
- 5). Peptide prodrugs of GCV can also be utilized in combination with tk enzymes as anticancer therapy.

COPYRIGHT PERMISSIONS

Copy right Permission 1:



RightsLink®



Title: Corneal Absorption and Anterior Chamber Pharmacokinetics of Dipeptide Monoester Prodrugs of Ganciclovir (GCV): In Vivo Comparative Evaluation of These Prodrugs with Val-GCV and GCV in Rabbits

Author: Sriram Gunda, Sudharshan Hariharan, Ashim K. Mitra

Publication: Journal of Ocular Pharmacology and Therapeutics

Publisher: Mary Ann Liebert, Inc.

Date: Dec 1, 2006

Copyright © 2006, Mary Ann Liebert, Inc.

Logged in as:
Sriram Gunda
Account #:
3000549792

LOGOUT

Permissions Request

Mary Ann Liebert, Inc. publishers does not require authors of the content being used to obtain a license for their personal reuse of full article, charts/graphs/tables or text excerpt.

Copyright © 2012 [Copyright Clearance Center, Inc.](#) All Rights Reserved.
[Privacy statement](#).

Comments? We would like to hear from you. E-mail us at
customer care@copyright.com

Copy right Permission 2



RightsLink®



ACS Publications
High quality. High impact.

Title: In Vivo Ocular
Pharmacokinetics of
Acyclovir Dipeptide
Ester Prodrugs by
Microdialysis in
Rabbits

Author: Banmeet S.
Anand, Suresh
Katragadda, Sriram
Gunda, and, and Ashim
K. Mitra*

Publication: Molecular
Pharmaceutics

Publisher: American Chemical
Society

Date: Aug 1, 2006

Copyright © 2006, American
Chemical Society

Logged in as:
Sriram Gunda
Account #:
3000549792

LOGOUT

PERMISSION/LICENSE IS GRANTED FOR YOUR ORDER AT NO CHARGE

This type of permission/license, instead of the standard Terms & Conditions, is sent to you because no fee is being charged for your order. Please note the following:

- Permission is granted for your request in both print and electronic formats, and translations.
- If figures and/or tables were requested, they may be adapted or used in part.
- Please print this page for your records and send a copy of it to your publisher/graduate school.
- Appropriate credit for the requested material should be given as follows: "Reprinted (adapted) with permission from (COMPLETE REFERENCE

CITATION). Copyright (YEAR) American Chemical Society." Insert appropriate information in place of the capitalized words.

- One-time permission is granted only for the use specified in your request. No additional uses are granted (such as derivative works or other editions). For any other uses, please submit a new request.

Copyright © 2012 Copyright Clearance Center, Inc. All Rights Reserved. Privacy statement.

Comments? We would like to hear from you. E-mail us at customer-care@copyright.com

Copy right Permission 3



RightsLink®



ACS Publications
High quality. High impact.

Title: Identification of a Na⁺-Dependent Cationic and Neutral Amino Acid Transporter, B₀,⁺, in Human and Rabbit Cornea
Author: Blisse Jain-Vakkalagadda et al.
Publication: Molecular Pharmaceutics
Publisher: American Chemical Society
Date: Sep 1, 2004
Copyright © 2004, American Chemical Society

Logged in as:
Sriram Gunda
Account #:
3000549792

LOGOUT

PERMISSION/LICENSE IS GRANTED FOR YOUR ORDER AT NO CHARGE

This type of permission/license, instead of the standard Terms & Conditions, is sent to you because no fee is being charged for your order. Please note the following:

- Permission is granted for your request in both print and electronic formats, and translations.
- If figures and/or tables were requested, they may be adapted or used in part.
- Please print this page for your records and send a copy of it to your publisher/graduate school.
- Appropriate credit for the requested material should be given as follows: "Reprinted (adapted) with permission from (COMPLETE REFERENCE CITATION). Copyright (YEAR) American Chemical Society." Insert

- appropriate information in place of the capitalized words.
- One-time permission is granted only for the use specified in your request. No additional uses are granted (such as derivative works or other editions). For any other uses, please submit a new request.

Copyright © 2012 Copyright Clearance Center, Inc. All Rights Reserved.

[Privacy statement](#).

Comments? We would like to hear from you. E-mail us at customer care@copyright.com

Copy right Permission 4



RightsLink®



ACS Publications
High quality. High impact.

Title: Functional Activity
of a
Monocarboxylate
Transporter, MCT1,
in the Human
Retinal Pigmented
Epithelium Cell
Line, ARPE-19

Logged in as:
Sriram Gunda
Account #:
3000549792

LOGOUT

Author: Soumyajit
Majumdar, Sriram
Gunda, Dhananjay
Pal, and, and Ashim
K. Mitra*

Publication: Molecular
Pharmaceutics

Publisher: American Chemical
Society

Date: Apr 1, 2005

Copyright © 2005, American
Chemical Society

PERMISSION/LICENSE IS GRANTED FOR YOUR ORDER AT NO
CHARGE

This type of permission/license, instead of the standard Terms & Conditions, is sent to you because no fee is being charged for your order. Please note the following:

- Permission is granted for your request in both print and electronic formats, and translations.
- If figures and/or tables were requested, they may be adapted or used in part.
- Please print this page for your records and send a copy of it to your

publisher/graduate school.

- Appropriate credit for the requested material should be given as follows: "Reprinted (adapted) with permission from (COMPLETE REFERENCE CITATION). Copyright (YEAR) American Chemical Society." Insert appropriate information in place of the capitalized words.
- One-time permission is granted only for the use specified in your request. No additional uses are granted (such as derivative works or other editions). For any other uses, please submit a new request.

Copyright © 2012 Copyright Clearance Center, Inc. All Rights Reserved.

Privacy statement.

Comments? We would like to hear from you. E-mail us at customercare@copyright.com

Copy right Permission 5

ELSEVIER LICENSE
TERMS AND CONDITIONS

Jul 06, 2012

This is a License Agreement between Sriram Gunda ("You") and Elsevier ("Elsevier") provided by Copyright Clearance Center ("CCC"). The license consists of your order details, the terms and conditions provided by Elsevier, and the payment terms and conditions.

All payments must be made in full to CCC. For payment instructions, please see information listed at the bottom of this form.

Supplier	Elsevier Limited The Boulevard,Langford Lane Kidlington,Oxford,OX5 1GB,UK
Registered Company Number	1982084
Customer name	Sriram Gunda
Customer address	4922 grand ave apt#9 Kansas City, MO 64112
License number	2942881439146

License date	Jul 06, 2012
Licensed content publisher	Elsevier
Licensed content publication	International Journal of Pharmaceutics
Licensed content title	Ocular pharmacokinetics of acyclovir amino acid ester prodrugs in the anterior chamber: Evaluation of their utility in treating ocular HSV infections
Licensed content author	Suresh Katragadda, Sriram Gunda, Sudharshan Hariharan, Ashim K. Mitra
Licensed content date	9 July 2008
Licensed content volume number	359
Licensed content issue number	1-2
Number of pages	10
Start Page	15
End Page	24
Type of Use	reuse in a thesis/dissertation
Intended publisher of new work	other
Portion	excerpt
Number of excerpts	2

Format	both print and electronic
Are you the author of this Elsevier article?	Yes
Will you be translating?	No
Order reference number	
Title of your thesis/dissertation	ocular pharmacokinetics and efficacy of various prodrugs of ganciclovir
Expected completion date	Aug 2012
Estimated size (number of pages)	170
Elsevier VAT number	GB 494 6272 12
Permissions price	0.00 USD
VAT/Local Sales Tax	0.0 USD / 0.0 GBP
Total	0.00 USD
Terms and Conditions	

INTRODUCTION

1. The publisher for this copyrighted material is Elsevier. By clicking "accept" in connection with completing this licensing transaction, you agree that the following terms and conditions apply to this transaction (along with the Billing and Payment terms and conditions established by Copyright Clearance Center, Inc. ("CCC"), at the time that you opened your Rightslink account and that are available at any time at <http://myaccount.copyright.com>).

GENERAL TERMS

2. Elsevier hereby grants you permission to reproduce the aforementioned material subject to the terms and conditions indicated.

3. Acknowledgement: If any part of the material to be used (for example, figures) has appeared in our publication with credit or acknowledgement to another source, permission must also be sought from that source. If such permission is not obtained then that material may not be included in your publication/copies. Suitable acknowledgement to the source must be made, either as a footnote or in a reference list at the end of your publication, as follows:

“Reprinted from Publication title, Vol /edition number, Author(s), Title of article / title of chapter, Pages No., Copyright (Year), with permission from Elsevier [OR APPLICABLE SOCIETY COPYRIGHT OWNER].” Also Lancet special credit - “Reprinted from The Lancet, Vol. number, Author(s), Title of article, Pages No., Copyright (Year), with permission from Elsevier.”

4. Reproduction of this material is confined to the purpose and/or media for which permission is hereby given.

5. Altering/Modifying Material: Not Permitted. However figures and illustrations may be altered/adapted minimally to serve your work. Any other abbreviations, additions, deletions and/or any other alterations shall be made only with prior written authorization of Elsevier Ltd. (Please contact Elsevier at permissions@elsevier.com)

6. If the permission fee for the requested use of our material is waived in this instance, please be advised that your future requests for Elsevier materials may attract a fee.

7. Reservation of Rights: Publisher reserves all rights not specifically granted in the combination of (i) the license details provided by you and accepted in the course of this licensing transaction, (ii) these terms and conditions and (iii) CCC's Billing and Payment terms and conditions.

8. License Contingent Upon Payment: While you may exercise the rights licensed immediately upon issuance of the license at the end of the licensing process for the transaction, provided that you have disclosed complete and accurate details of your proposed use, no license is finally effective unless and until full payment is received from you (either by publisher or by CCC) as provided in CCC's Billing and Payment terms and conditions. If full payment is not received on a timely basis, then any license preliminarily granted shall be deemed automatically revoked and shall be void as if never granted. Further, in the event that you breach any of these terms and conditions or any of CCC's Billing and Payment terms and conditions, the license is automatically revoked and shall be void as if never granted. Use of materials as described in a revoked license, as well as any use of the materials beyond the scope of an unrevoked license, may constitute copyright infringement and publisher reserves the right to take any and all action to protect its copyright in the materials.

9. Warranties: Publisher makes no representations or warranties with respect to the licensed material.

10. Indemnity: You hereby indemnify and agree to hold harmless publisher and CCC, and their respective officers, directors, employees and agents, from and against any and all claims arising out of your use of the licensed material other than as specifically authorized pursuant to this license.

11. No Transfer of License: This license is personal to you and may not be sublicensed, assigned, or transferred by you to any other person without publisher's written permission.

12. No Amendment Except in Writing: This license may not be amended except in a writing signed by both parties (or, in the case of publisher, by

CCC on publisher's behalf).

13. **Objection to Contrary Terms:** Publisher hereby objects to any terms contained in any purchase order, acknowledgment, check endorsement or other writing prepared by you, which terms are inconsistent with these terms and conditions or CCC's Billing and Payment terms and conditions. These terms and conditions, together with CCC's Billing and Payment terms and conditions (which are incorporated herein), comprise the entire agreement between you and publisher (and CCC) concerning this licensing transaction. In the event of any conflict between your obligations established by these terms and conditions and those established by CCC's Billing and Payment terms and conditions, these terms and conditions shall control.

14. **Revocation:** Elsevier or Copyright Clearance Center may deny the permissions described in this License at their sole discretion, for any reason or no reason, with a full refund payable to you. Notice of such denial will be made using the contact information provided by you. Failure to receive such notice will not alter or invalidate the denial. In no event will Elsevier or Copyright Clearance Center be responsible or liable for any costs, expenses or damage incurred by you as a result of a denial of your permission request, other than a refund of the amount(s) paid by you to Elsevier and/or Copyright Clearance Center for denied permissions.

LIMITED LICENSE

The following terms and conditions apply only to specific license types:

15. **Translation:** This permission is granted for non-exclusive world **English** rights only unless your license was granted for translation rights. If you licensed translation rights you may only translate this content into the languages you requested. A professional translator must perform all translations and reproduce the content word for word preserving the integrity of the article. If this license is to re-use 1 or 2 figures then permission is granted for non-exclusive world rights in all languages.

16. **Website:** The following terms and conditions apply to electronic reserve and author websites:

Electronic reserve: If licensed material is to be posted to website, the web

site is to be password-protected and made available only to bona fide students registered on a relevant course if:

This license was made in connection with a course,

This permission is granted for 1 year only. You may obtain a license for future website posting,

All content posted to the web site must maintain the copyright information line on the bottom of each image,

A hyper-text must be included to the Homepage of the journal from which you are licensing at <http://www.sciencedirect.com/science/journal/xxxxx> or the Elsevier homepage for books at <http://www.elsevier.com> , and

Central Storage: This license does not include permission for a scanned version of the material to be stored in a central repository such as that provided by Heron/XanEdu.

17. **Author website** for journals with the following additional clauses:

All content posted to the web site must maintain the copyright information line on the bottom of each image, and the permission granted is limited to the personal version of your paper. You are not allowed to download and post the published electronic version of your article (whether PDF or HTML, proof or final version), nor may you scan the printed edition to create an electronic version. A hyper-text must be included to the Homepage of the journal from which you are licensing at <http://www.sciencedirect.com/science/journal/xxxxx> . As part of our normal production process, you will receive an e-mail notice when your article appears on Elsevier's online service ScienceDirect (www.sciencedirect.com). That e-mail will include the article's Digital Object Identifier (DOI). This number provides the electronic link to the published article and should be included in the posting of your personal version. We ask that you wait until you receive this e-mail and have the DOI to do any posting.

Central Storage: This license does not include permission for a scanned version of the material to be stored in a central repository such as that provided by Heron/XanEdu.

18. **Author website** for books with the following additional clauses:

Authors are permitted to place a brief summary of their work online only.

A hyper-text must be included to the Elsevier homepage at

<http://www.elsevier.com> . All content posted to the web site must maintain the copyright information line on the bottom of each image. You are not allowed to download and post the published electronic version of your chapter, nor may you scan the printed edition to create an electronic version.

Central Storage: This license does not include permission for a scanned version of the material to be stored in a central repository such as that provided by Heron/XanEdu.

19. **Website** (regular and for author): A hyper-text must be included to the Homepage of the journal from which you are licensing at <http://www.sciencedirect.com/science/journal/xxxxx>. or for books to the Elsevier homepage at <http://www.elsevier.com>

20. **Thesis/Dissertation**: If your license is for use in a thesis/dissertation your thesis may be submitted to your institution in either print or electronic form. Should your thesis be published commercially, please reapply for permission. These requirements include permission for the Library and Archives of Canada to supply single copies, on demand, of the complete thesis and include permission for UMI to supply single copies, on demand, of the complete thesis. Should your thesis be published commercially, please reapply for permission.

21. **Other Conditions**:

v1.6

If you would like to pay for this license now, please remit this license along with your payment made payable to "COPYRIGHT CLEARANCE CENTER" otherwise you will be invoiced within 48 hours of the license date. Payment should be in the form of a check or money order referencing your account number and this invoice number RLNK500813250.

Once you receive your invoice for this order, you may pay your invoice by credit card. Please follow instructions provided at that time.

**Make Payment To:
Copyright Clearance Center
Dept 001**

**P.O. Box 843006
Boston, MA 02284-3006**

**For suggestions or comments regarding this order, contact RightsLink
Customer Support: customercare@copyright.com or +1-877-622-5543
(toll free in the US) or +1-978-646-2777.**

**Gratis licenses (referencing \$0 in the Total field) are free. Please retain
this printable license for your reference. No payment is required.**

Copy right Permission 6

SPRINGER LICENSE
TERMS AND CONDITIONS

Jul 06, 2012

This is a License Agreement between Sriram Gunda ("You") and Springer ("Springer") provided by Copyright Clearance Center ("CCC"). The license consists of your order details, the terms and conditions provided by Springer, and the payment terms and conditions.

All payments must be made in full to CCC. For payment instructions, please see information listed at the bottom of this form.

License Number 2942880907870

License date Jul 06, 2012

Licensed content publisher Springer

Licensed content publication Pharmaceutical Research

Licensed content title Enhanced Corneal Absorption of Erythromycin by Modulating P-Glycoprotein and MRP Mediated Efflux with Corticosteroids

Licensed content author Sudharshan Hariharan

Licensed content date Jan 1, 2008

Volume number 26

Issue number 5

Type of Use Thesis/Dissertation

Portion Excerpts

Author of this Springer article Yes and you are the sole author of the new work

Order reference number

Title of your thesis / dissertation ocular pharmacokinetics and efficacy of various prodrugs of ganciclovir

Expected completion date Aug 2012

Estimated size(pages) 170

Total 0.00 USD

Terms and Conditions

Introduction

The publisher for this copyrighted material is Springer Science + Business Media. By clicking "accept" in connection with completing this licensing transaction, you agree that the following terms and conditions apply to this transaction (along with the Billing and Payment terms and conditions established by Copyright Clearance Center, Inc. ("CCC"), at the time that you opened your Rightslink account and that are available at any time at <http://myaccount.copyright.com>).

Limited License

With reference to your request to reprint in your thesis material on which Springer Science and Business Media control the copyright, permission is granted, free of charge, for the use indicated in your enquiry.

Licenses are for one-time use only with a maximum distribution equal to the number that you identified in the licensing process.

This License includes use in an electronic form, provided its password protected or on the university's intranet or repository, including UMI (according to the definition at the Sherpa website: <http://www.sherpa.ac.uk/romeo/>). For any other electronic use, please contact Springer at (permissions.dordrecht@springer.com or permissions.heidelberg@springer.com).

The material can only be used for the purpose of defending your thesis, and with a maximum of 100 extra copies in paper.

Although Springer holds copyright to the material and is entitled to negotiate on rights, this license is only valid, provided permission is also obtained from the (co) author (address is given with the article/chapter) and provided it concerns original material which does not carry references to other sources (if material in question appears with credit to another source, authorization from that source is required as well).

Permission free of charge on this occasion does not prejudice any rights we

might have to charge for reproduction of our copyrighted material in the future.

Altering/Modifying Material: Not Permitted

You may not alter or modify the material in any manner. Abbreviations, additions, deletions and/or any other alterations shall be made only with prior written authorization of the author(s) and/or Springer Science + Business Media. (Please contact Springer at (permissions.dordrecht@springer.com or permissions.heidelberg@springer.com)

Reservation of Rights

Springer Science + Business Media reserves all rights not specifically granted in the combination of (i) the license details provided by you and accepted in the course of this licensing transaction, (ii) these terms and conditions and (iii) CCC's Billing and Payment terms and conditions.

Copyright Notice:Disclaimer

You must include the following copyright and permission notice in connection with any reproduction of the licensed material: "Springer and the original publisher /journal title, volume, year of publication, page, chapter/article title, name(s) of author(s), figure number(s), original copyright notice) is given to the publication in which the material was originally published, by adding; with kind permission from Springer Science and Business Media"

Warranties: None

Example 1: Springer Science + Business Media makes no representations or warranties with respect to the licensed material.

Example 2: Springer Science + Business Media makes no representations or warranties with respect to the licensed material and adopts on its own behalf the limitations and disclaimers established by CCC on its behalf in its Billing and Payment terms and conditions for this licensing transaction.

Indemnity

You hereby indemnify and agree to hold harmless Springer Science + Business Media and CCC, and their respective officers, directors, employees and agents, from and against any and all claims arising out of your use of the licensed material other than as specifically authorized pursuant to this license.

No Transfer of License

This license is personal to you and may not be sublicensed, assigned, or transferred by you to any other person without Springer Science + Business Media's written permission.

No Amendment Except in Writing

This license may not be amended except in a writing signed by both parties (or, in the case of Springer Science + Business Media, by CCC on Springer Science + Business Media's behalf).

Objection to Contrary Terms

Springer Science + Business Media hereby objects to any terms contained in any purchase order, acknowledgment, check endorsement or other writing prepared by you, which terms are inconsistent with these terms and conditions or CCC's Billing and Payment terms and conditions. These terms and conditions, together with CCC's Billing and Payment terms and conditions (which are incorporated herein), comprise the entire agreement between you and Springer Science + Business Media (and CCC) concerning this licensing transaction. In the event of any conflict between your obligations established by these terms and conditions and those established by CCC's Billing and Payment terms and conditions, these terms and conditions shall control.

Jurisdiction

All disputes that may arise in connection with this present License, or the breach thereof, shall be settled exclusively by arbitration, to be held in The Netherlands, in accordance with Dutch law, and to be conducted under the Rules of the 'Netherlands Arbitrage Instituut' (Netherlands Institute of Arbitration). **OR:**

All disputes that may arise in connection with this present License, or the breach thereof, shall be settled exclusively by arbitration, to be held in the Federal Republic of Germany, in accordance with German law.

Other terms and conditions:

v1.3

If you would like to pay for this license now, please remit this license along with your payment made payable to "COPYRIGHT CLEARANCE CENTER" otherwise you will be invoiced within 48 hours of the license

date. Payment should be in the form of a check or money order referencing your account number and this invoice number RLNK500813245.

Once you receive your invoice for this order, you may pay your invoice by credit card. Please follow instructions provided at that time.

Make Payment To:

Copyright Clearance Center

Dept 001

P.O. Box 843006

Boston, MA 02284-3006

For suggestions or comments regarding this order, contact RightsLink

Customer Support: customercare@copyright.com or +1-877-622-5543 (toll free in the US) or +1-978-646-2777.

Gratis licenses (referencing \$0 in the Total field) are free. Please retain this printable license for your reference. No payment is required.

Copyright Permission 7

Permission to use Future Science Ltd copyright material

Request from:

- Contact name: Sriram Gunda
- Publisher/company name:
- Address:
- Telephone/e-mail: sghc5@mail.umkc.edu

Request details:

- Request to use the following content: Author - Full Article - Bioanalysis, March 2010, Vol. 2, No. 3, Pages 487-507
- In the following publication: Doctoral Dissertation
- In what media (print/electronic/print & electronic): Print and Electronic
- In the following languages: All

We, Future Science Ltd, grant permission to reuse the material specified above within the publication specified above.

Notes and conditions:

1. This permission is granted free of charge, for one-time use only.
2. Future Science Ltd grant the publisher non-exclusive world rights to publish the content in the publication/website specified above.
3. Future Science Ltd retains copyright ownership of the content.
4. Permission is granted on a one-time basis only. Separate permission is required for any further use or edition.
5. The publisher will make due acknowledgement of the original publication wherever they republish the content: citing the author, content title, publication name and Future Science Ltd as the original publisher.
6. The publisher will not amend, abridge, or otherwise change the content without authorization from Future Science Ltd.
7. Permission does not include any copyrighted material from other sources that may be incorporated within the content.
8. Failure to comply with the conditions above will result in immediate revocation of the permission here granted.

Date: 06/07/2012.....

Future Science Ltd, Unitec House, 2 Albert Place, London, N3 1QB, UK
T: +44 (0)20 8371 6080 F: +44 (0) 20 8371 6099 E: info@future-science.com
www.future-science.com

Copy right permission # 8

berti:Users:berti:Desktop:ssbm_stationery_02.png

August 15, 2012

fritzi:Users:oskar:Desktop:versendet_zusatz:s_letter_heidelberg_e:s_letter_heidelberg_e_unten.png

Springer title and material

Ocular Transporters in Ophthalmic Diseases and Drug Delivery

Series: Ophthalmology Research

Tombran-Tink, Joyce; Barnstable, Colin J. (Eds.) 2008, XVIII, 472 p. 98 illus.

A product of Humana Press

ISBN 978-1-58829-958-1

pp. 399-414

Your Thesis: University: University of Missouri - Kansas City, at Kansas City, Missouri, USA

Title: "Ocular pharmacokinetics and antiviral efficacy of various prodrugs of Ganciclovir"

Territory: Worldwide

With reference to your request to reuse material in which Springer

Science+Business Media controls the copyright, our permission is granted free of charge under the following conditions:

Springer material

1. represents original material which does not carry references to other sources (if material in question
2. refers with a credit to another source, authorization from that source is required as well);
3. full credit (book title, volume, year of publication, page, chapter title, name(s) of author(s), original copyright notice) is given to the publication in which the material was originally published by adding: "With kind permission of Springer Science+Business Media";
4. figures and illustrations may be altered minimally to serve your work. Any other abbreviations, additions, deletions and/or any other alterations shall be made only with prior written authorization of the author and/or Springer.
5. can only be used for the purpose of defending your thesis, and with a maximum of 100 extra copies in paper.

This permission

1. is non-exclusive;
2. is valid for one-time use only with a maximum distribution equal to the number that you identified in your request;
3. includes use in an electronic form, provided it is password protected, on intranet or or university's repository, including UMI (according to the definition at the Sherpa website: <http://www.sherpa.ac.uk/romeo/>), or CD-Rom/DVD, or E-book/E-journal;
4. is only valid provided consent is also obtained from the co-author (address is given in the chapter);
5. may not be sublicensed, assigned, or transferred to any other person without Springer's written permission;
6. is valid only when the conditions noted above are met.

Best regards,
Rights and Permissions
Springer-Verlag GmbH
Tiergartenstr. 17
69121 Heidelberg
Germany
E-mail: permissions.heidelberg@springer.com

REFERENCES

1. Liesegang, T.J., *Herpes simplex virus epidemiology and ocular importance*. Cornea, 2001. **20**(1): p. 1-13.
2. Whitley, R., *Herpes simplex viruses*. 3 ed. Fields Virology, ed. K.D. Fields BN and Howley PM. Vol. 2. 1996, Philadelphia: Lippincott-Raven. 2297-2342.
3. Marquardt, H., J. Westendorf, and E. De Clercq, *Potent anti-viral 5-(2-bromovinyl) uracil nucleosides are inactive at inducing gene mutations in Salmonella typhimurium and V79 Chinese hamster cells and unscheduled DNA synthesis in primary rat hepatocytes*. Carcinogenesis, 1985. **6**(8): p. 1207-9.
4. De Clercq, E., *Guanosine analogues as anti-herpesvirus agents*. Nucleosides Nucleotides Nucleic Acids, 2000. **19**(10-12): p. 1531-41.
5. Castela, N., et al., *Ganciclovir ophthalmic gel in herpes simplex virus rabbit keratitis: intraocular penetration and efficacy*. J Ocul Pharmacol, 1994. **10**(2): p. 439-51.
6. Tirucherai, G.S., C. Dias, and A.K. Mitra, *Corneal permeation of ganciclovir: mechanism of ganciclovir permeation enhancement by acyl ester prodrug design*. J Ocul Pharmacol Ther, 2002. **18**(6): p. 535-48.
7. Gunda, S., et al., *Barriers in Ocular Drug Delivery Ocular Transporters In Ophthalmic Diseases And Drug Delivery*, J. Tombran-Tink and C.J. Barnstable, Editors. 2008, Humana Press. p. 399-413.
8. Majumdar, S., et al., *Functional differences in nucleoside and nucleobase transporters expressed on the rabbit corneal epithelial cell line (SIRC) and isolated rabbit cornea*. AAPS PharmSci, 2003. **5**(2): p. E15.
9. Dey, S. and A.K. Mitra, *Transporters and receptors in ocular drug delivery: opportunities and challenges*. Expert Opin Drug Deliv, 2005. **2**(2): p. 201-4.
10. Pinto, V., et al., *Age-related changes in the renal dopaminergic system and expression of renal amino acid transporters in WKY and SHR rats*. Mech Ageing Dev, 2011. **132**(6-7): p. 298-304.
11. DelMonte, D.W. and T. Kim, *Anatomy and physiology of the cornea*. J Cataract Refract Surg, 2011. **37**(3): p. 588-98.
12. Sampat, K.M. and S.J. Garg, *Complications of intravitreal injections*. Curr Opin Ophthalmol, 2010. **21**(3): p. 178-83.
13. Madara, J.L. and J.S. Trier, *Structure and permeability of goblet cell tight junctions in rat small intestine*. J Membr Biol, 1982. **66**(2): p. 145-57.
14. Tornquist, P., A. Alm, and A. Bill, *Permeability of ocular vessels and transport across the blood-retinal-barrier*. Eye, 1990. **4** (Pt 2): p. 303-9.

15. Zhang, W., M.R. Prausnitz, and A. Edwards, *Model of transient drug diffusion across cornea*. J Control Release, 2004. **99**(2): p. 241-58.
16. Kawazu, K., et al., *Characterization of cyclosporin A transport in cultured rabbit corneal epithelial cells: P-glycoprotein transport activity and binding to cyclophilin*. Invest Ophthalmol Vis Sci, 1999. **40**(8): p. 1738-44.
17. Dey, S., et al., *Molecular evidence and functional expression of P-glycoprotein (MDR1) in human and rabbit cornea and corneal epithelial cell lines*. Invest Ophthalmol Vis Sci, 2003. **44**(7): p. 2909-18.
18. Dey, S., S. Gunda, and A.K. Mitra, *Pharmacokinetics of erythromycin in rabbit corneas after single-dose infusion: role of P-glycoprotein as a barrier to in vivo ocular drug absorption*. J Pharmacol Exp Ther, 2004. **311**(1): p. 246-55.
19. Jack, K.J., P.E. Carlos, and T.J. Stephen, *Keratitis*, in *Ocular Inflammatory Disease*, J.J. Kanski, C.E. Pavesio, and S.J. Tuft, Editors. 2006, Elsevier Mosby. p. pp. 69-126.
20. Holash, J.A. and P.A. Stewart, *The relationship of astrocyte-like cells to the vessels that contribute to the blood-ocular barriers*. Brain Res, 1993. **629**(2): p. 218-24.
21. Schlingemann, R.O., et al., *Ciliary muscle capillaries have blood-tissue barrier characteristics*. Exp Eye Res, 1998. **66**(6): p. 747-54.
22. Saha, P., J.J. Yang, and V.H. Lee, *Existence of a p-glycoprotein drug efflux pump in cultured rabbit conjunctival epithelial cells*. Invest Ophthalmol Vis Sci, 1998. **39**(7): p. 1221-6.
23. Duvvuri, S., M.D. Gandhi, and A.K. Mitra, *Effect of P-glycoprotein on the ocular disposition of a model substrate, quinidine*. Curr Eye Res, 2003. **27**(6): p. 345-53.
24. Aukunuru, J.V., et al., *Expression of multidrug resistance-associated protein (MRP) in human retinal pigment epithelial cells and its interaction with BAPSG, a novel aldose reductase inhibitor*. Pharm Res, 2001. **18**(5): p. 565-72.
25. Esser, J., et al., *Multidrug resistance-associated proteins in glaucoma surgery*. Graefes Arch Clin Exp Ophthalmol, 2000. **238**(9): p. 727-32.
26. Ambati, J., et al., *Diffusion of high molecular weight compounds through sclera*. Invest Ophthalmol Vis Sci, 2000. **41**(5): p. 1181-5.
27. Sasaki, H., et al., *Ocular membrane permeability of hydrophilic drugs for ocular peptide delivery*. J Pharm Pharmacol, 1997. **49**(2): p. 135-9.
28. Mitra, A.K. and T.J. Mikkelsen, *Mechanism of transcorneal permeation of pilocarpine*. J Pharm Sci, 1988. **77**(9): p. 771-5.

29. Pitkanen, L., et al., *Permeability of retinal pigment epithelium: effects of permeant molecular weight and lipophilicity*. Invest Ophthalmol Vis Sci, 2005. **46**(2): p. 641-6.
30. Luckner, P. and M. Brandsch, *Interaction of 31 beta-lactam antibiotics with the H⁺/peptide symporter PEPT2: analysis of affinity constants and comparison with PEPT1*. Eur J Pharm Biopharm, 2005. **59**(1): p. 17-24.
31. Terada, T., et al., *Recognition of beta-lactam antibiotics by rat peptide transporters, PEPT1 and PEPT2, in LLC-PK1 cells*. Am J Physiol, 1997. **273**(5 Pt 2): p. F706-11.
32. Yamaguchi, H., et al., *Secretory mechanisms of grepafloxacin and levofloxacin in the human intestinal cell line caco-2*. J Pharmacol Exp Ther, 2000. **295**(1): p. 360-6.
33. MacDougall, C. and B.J. Guglielmo, *Pharmacokinetics of valaciclovir*. J Antimicrob Chemother, 2004. **53**(6): p. 899-901.
34. Bras, A.P., D.S. Sitar, and F.Y. Aoki, *Comparative bioavailability of acyclovir from oral valacyclovir and acyclovir in patients treated for recurrent genital herpes simplex virus infection*. Can J Clin Pharmacol, 2001. **8**(4): p. 207-11.
35. Majumdar, S., et al., *Dipeptide monoester ganciclovir prodrugs for treating HSV-1-induced corneal epithelial and stromal keratitis: in vitro and in vivo evaluations*. J Ocul Pharmacol Ther, 2005. **21**(6): p. 463-74.
36. Anand, B., Y. Nashed, and A. Mitra, *Novel dipeptide prodrugs of acyclovir for ocular herpes infections: Bioreversion, antiviral activity and transport across rabbit cornea*. Curr Eye Res, 2003. **26**(3-4): p. 151-63.
37. Anand, B.S., et al., *In vivo antiviral efficacy of a dipeptide acyclovir prodrug, val-val-acyclovir, against HSV-1 epithelial and stromal keratitis in the rabbit eye model*. Invest Ophthalmol Vis Sci, 2003. **44**(6): p. 2529-34.
38. Katragadda, S., R.S. Talluri, and A.K. Mitra, *Modulation of P-glycoprotein-mediated efflux by prodrug derivatization: an approach involving peptide transporter-mediated influx across rabbit cornea*. J Ocul Pharmacol Ther, 2006. **22**(2): p. 110-20.
39. Atluri, H., et al., *Mechanism of a model dipeptide transport across blood-ocular barriers following systemic administration*. Exp Eye Res, 2004. **78**(4): p. 815-22.
40. Anand, B.S. and A.K. Mitra, *Mechanism of corneal permeation of L-valyl ester of acyclovir: targeting the oligopeptide transporter on the rabbit cornea*. Pharm Res, 2002. **19**(8): p. 1194-202.
41. Macha, S. and A.K. Mitra, *Ocular pharmacokinetics of cephalosporins using microdialysis*. J Ocul Pharmacol Ther, 2001. **17**(5): p. 485-98.

42. Bagshawe, K.D., et al., *A cytotoxic agent can be generated selectively at cancer sites*. Br J Cancer, 1988. **58**(6): p. 700-3.
43. Jain-Vakkalagadda, B., et al., *Identification and functional characterization of a Na⁺-independent large neutral amino acid transporter, LAT1, in human and rabbit cornea*. Invest Ophthalmol Vis Sci, 2003. **44**(7): p. 2919-27.
44. Jain-Vakkalagadda, B., et al., *Identification of a Na⁺-dependent cationic and neutral amino acid transporter, B(0,+), in human and rabbit cornea*. Mol Pharm, 2004. **1**(5): p. 338-46.
45. Anand, B.S., et al., *Amino acid prodrugs of acyclovir as possible antiviral agents against ocular HSV-1 infections: interactions with the neutral and cationic amino acid transporter on the corneal epithelium*. Curr Eye Res, 2004. **29**(2-3): p. 153-66.
46. Katragadda, S., et al., *Identification and characterization of a Na⁺-dependent neutral amino acid transporter, ASCT1, in rabbit corneal epithelial cell culture and rabbit cornea*. Curr Eye Res, 2005. **30**(11): p. 989-1002.
47. Lee, S.C., Y.M. Zhong, and X.L. Yang, *Expression of glycine receptor and transporter on bullfrog retinal Muller cells*. Neurosci Lett, 2005. **387**(2): p. 75-9.
48. Tomi, M., et al., *L-type amino acid transporter 1-mediated L-leucine transport at the inner blood-retinal barrier*. Invest Ophthalmol Vis Sci, 2005. **46**(7): p. 2522-30.
49. Maenpaa, H., G. Gegelashvili, and H. Tahti, *Expression of glutamate transporter subtypes in cultured retinal pigment epithelial and retinoblastoma cells*. Curr Eye Res, 2004. **28**(3): p. 159-65.
50. Halestrap, A.P. and N.T. Price, *The proton-linked monocarboxylate transporter (MCT) family: structure, function and regulation*. Biochem J, 1999. **343 Pt 2**: p. 281-99.
51. Chidlow, G., et al., *Expression of monocarboxylate transporters in rat ocular tissues*. Am J Physiol Cell Physiol, 2005. **288**(2): p. C416-28.
52. Hosoya, K., et al., *MCT1-mediated transport of L-lactic acid at the inner blood-retinal barrier: a possible route for delivery of monocarboxylic acid drugs to the retina*. Pharm Res, 2001. **18**(12): p. 1669-76.
53. Philp, N.J., et al., *Polarized expression of monocarboxylate transporters in human retinal pigment epithelium and ARPE-19 cells*. Invest Ophthalmol Vis Sci, 2003. **44**(4): p. 1716-21.
54. Majumdar, S., et al., *Functional activity of a monocarboxylate transporter, MCT1, in the human retinal pigmented epithelium cell line, ARPE-19*. Mol Pharm, 2005. **2**(2): p. 109-17.

55. Kannan, R., et al., *Vitamin C transport in human lens epithelial cells: evidence for the presence of SVCT2*. Exp Eye Res, 2001. **73**(2): p. 159-65.
56. Lam, K.W., et al., *Sodium-dependent ascorbic and dehydroascorbic acid uptake by SV-40-transformed retinal pigment epithelial cells*. Ophthalmic Res, 1993. **25**(2): p. 100-7.
57. Chancy, C.D., et al., *Expression and differential polarization of the reduced-folate transporter-1 and the folate receptor alpha in mammalian retinal pigment epithelium*. J Biol Chem, 2000. **275**(27): p. 20676-84.
58. Smith, S.B., et al., *Expression of folate receptor alpha in the mammalian retinol pigmented epithelium and retina*. Invest Ophthalmol Vis Sci, 1999. **40**(5): p. 840-8.
59. Kansara, V., et al., *Identification and functional characterization of riboflavin transporter in human-derived retinoblastoma cell line (Y-79): mechanisms of cellular uptake and translocation*. J Ocul Pharmacol Ther, 2005. **21**(4): p. 275-87.
60. Majumdar, S., S. Gunda, and A. Mitra, *Functional expression of a sodium dependent nucleoside transporter on rabbit cornea: Role in corneal permeation of acyclovir and idoxuridine*. Curr Eye Res, 2003. **26**(3-4): p. 175-83.
61. Majumdar, S., et al., *Mechanism of ganciclovir uptake by rabbit retina and human retinal pigmented epithelium cell line ARPE-19*. Curr Eye Res, 2004. **29**(2-3): p. 127-36.
62. Wilhelmus, K.R., *The treatment of herpes simplex virus epithelial keratitis*. Trans Am Ophthalmol Soc, 2000. **98**: p. 505-32.
63. Hyndiuk R, G.D., *Herpes Simplex Keratitis*. 2 ed. Infections of the Eye, ed. H.R. Tabbara KF. 1996, Boston, MA: Little Brown & Co.,.
64. Brien, W.O., *Antiviral Agents*. 2 ed. Infections of the Eye, ed. H.R. Tabbara KF. 1996, Boston, MA: Little Brown & Co.,.
65. Elftman, M.D., et al., *Stress-induced glucocorticoids at the earliest stages of herpes simplex virus-1 infection suppress subsequent antiviral immunity, implicating impaired dendritic cell function*. J Immunol, 2010. **184**(4): p. 1867-75.
66. El Hayderi, L., et al., *Severe herpes simplex virus type-1 infections after dental procedures*. Med Oral Patol Oral Cir Bucal, 2011. **16**(1): p. e15-8.
67. Matthews, T. and R. Boehme, *Antiviral activity and mechanism of action of ganciclovir*. Rev Infect Dis, 1988. **10 Suppl 3**: p. S490-4.
68. Davies, M.E., et al., *2'-Nor-2'-deoxyguanosine is an effective therapeutic agent for treatment of experimental herpes keratitis*. Antiviral Res, 1987. **7**(2): p. 119-25.

69. Gordon, Y.J., et al., *2'-nor-cGMP, a new cyclic derivative of 2'NDG, inhibits HSV-1 replication in vitro and in the mouse keratitis model.* Curr Eye Res, 1987. **6**(1): p. 247-53.
70. Shiota, H., T. Naito, and Y. Mimura, *Anti-herpes simplex virus (HSV) effect of 9-(1,3-dihydroxy-2-propoxymethyl)guanine (DHPG) in rabbit cornea.* Curr Eye Res, 1987. **6**(1): p. 241-5.
71. Mishima, S., et al., *Determination of tear volume and tear flow.* Invest Ophthalmol, 1966. **5**(3): p. 264-76.
72. Mishima, A., *Some physiologic aspects of the precorneal tear film.* Archives of Ophthalmology 1965. **73**: p. 233.
73. Maurice, D.M., *The dynamics and drainage of tears.* Int Ophthalmol Clin, 1973. **13**(1): p. 103-16.
74. Brown, R.H. and M.G. Lynch, *Drop size of commercial glaucoma medications.* Am J Ophthalmol, 1986. **102**(5): p. 673-4.
75. Adler, F., *Physiology of the Eye.* Vol. 38. 1965, St. Louis: CV Mosby.
76. Patton, T.F. and J.R. Robinson, *Influence of topical anesthesia on tear dynamics and ocular drug bioavailability in albino rabbits.* J Pharm Sci, 1975. **64**(2): p. 267-71.
77. Brown, R.H. and M.G. Lynch, *Design of eyedropper tips for topical beta-blocking agents.* Am J Ophthalmol, 1986. **102**(1): p. 123-4.
78. Lederer, C.M., Jr. and R.E. Harold, *Drop size of commercial glaucoma medications.* Am J Ophthalmol, 1986. **101**(6): p. 691-4.
79. Zimmerman, T.J., et al., *Improving the therapeutic index of topically applied ocular drugs.* Arch Ophthalmol, 1984. **102**(4): p. 551-3.
80. Huang, T.C. and D.A. Lee, *Punctal occlusion and topical medications for glaucoma.* Am J Ophthalmol, 1989. **107**(2): p. 151-5.
81. White, W.L., A.T. Glover, and A.B. Buckner, *Effect of blinking on tear elimination as evaluated by dacryoscintigraphy.* Ophthalmology, 1991. **98**(3): p. 367-9.
82. Zimmerman, T.J., et al., *Therapeutic index of pilocarpine, carbachol, and timolol with nasolacrimal occlusion.* Am J Ophthalmol, 1992. **114**(1): p. 1-7.
83. Ellis, P.P., et al., *Effect of nasolacrimal occlusion on timolol concentrations in the aqueous humor of the human eye.* J Pharm Sci, 1992. **81**(3): p. 219-20.
84. Sorensen, T. and F.T. Jensen, *Methodological aspects of tear flow determination by means of a radioactive tracer.* Acta Ophthalmol (Copenh), 1977. **55**(5): p. 726-38.
85. Zimmerman, T.J., et al., *Therapeutic index of epinephrine and dipivefrin with nasolacrimal occlusion.* Am J Ophthalmol, 1992. **114**(1): p. 8-13.

86. Chrai, S.S., et al., *Lacrimal and instilled fluid dynamics in rabbit eyes*. J Pharm Sci, 1973. **62**(7): p. 1112-21.
87. Lee, V.H., K.A. Takemoto, and D.S. Iimoto, *Precorneal factors influencing the ocular distribution of topically applied liposomal inulin*. Curr Eye Res, 1984. **3**(4): p. 585-91.
88. Ludwig, A. and M. Van Ooteghem, *The influence of the drop size on the elimination of an ophthalmic solution from the precorneal area of human eyes*. Pharm Acta Helv, 1987. **62**(2): p. 56-60.
89. Brown, R.H., et al., *Improving the therapeutic index of topical phenylephrine by reducing drop volume*. Ophthalmology, 1987. **94**(7): p. 847-50.
90. Chrai, S.S., et al., *Drop size and initial dosing frequency problems of topically applied ophthalmic drugs*. J Pharm Sci, 1974. **63**(3): p. 333-8.
91. Miller, D. and P. O'Connor, *The influence of the nictitating membrane on steroid inhibition of limbal wound healing*. Acta Ophthalmol (Copenh), 1977. **55**(4): p. 586-90.
92. Mikkelsen, T.J., S.S. Chrai, and J.R. Robinson, *Altered bioavailability of drugs in the eye due to drug-protein interaction*. J Pharm Sci, 1973. **62**(10): p. 1648-53.
93. Mikkelsen, T.J., S.S. Chrai, and J.R. Robinson, *Competitive inhibition of drug-protein interaction in eye fluids and tissues*. J Pharm Sci, 1973. **62**(12): p. 1942-5.
94. Carney, L.G., T.F. Mauger, and R.M. Hill, *Buffering in human tears: pH responses to acid and base challenge*. Invest Ophthalmol Vis Sci, 1989. **30**(4): p. 747-54.
95. Perrin, J.H. and D.A. Nelson, *Displacement of sulfaethidole from bovine serum albumin by some alkyldimethylbenzylammonium chlorides*. Biochem Pharmacol, 1974. **23**(22): p. 3139-45.
96. Green, K. and S.J. Downs, *Prednisolone phosphate penetration into and through the cornea*. Invest Ophthalmol, 1974. **13**(4): p. 316-9.
97. Doane, M.G., A.D. Jensen, and C.H. Dohlman, *Penetration routes of topically applied eye medications*. Am J Ophthalmol, 1978. **85**(3): p. 383-6.
98. Miller, M.H., et al., *Fleroxacin pharmacokinetics in aqueous and vitreous humors determined by using complete concentration-time data from individual rabbits*. Antimicrob Agents Chemother, 1992. **36**(1): p. 32-8.
99. Lee, V.H. and J.R. Robinson, *Mechanistic and quantitative evaluation of precorneal pilocarpine disposition in albino rabbits*. J Pharm Sci, 1979. **68**(6): p. 673-84.

100. Patton, T.F. and J.R. Robinson, *Quantitative precorneal disposition of topically applied pilocarpine nitrate in rabbit eyes*. J Pharm Sci, 1976. **65**(9): p. 1295-301.
101. Makoid, M.C. and J.R. Robinson, *Pharmacokinetics of topically applied pilocarpine in the albino rabbit eye*. J Pharm Sci, 1979. **68**(4): p. 435-43.
102. Oh, C., et al., *A compartmental model for the ocular pharmacokinetics of cyclosporine in rabbits*. Pharm Res, 1995. **12**(3): p. 433-7.
103. Chiang, C.H. and R.D. Schoenwald, *Ocular pharmacokinetic models of clonidine-3H hydrochloride*. J Pharmacokinetic Biopharm, 1986. **14**(2): p. 175-211.
104. Burstein, N.L. and J.A. Anderson, *Corneal penetration and ocular bioavailability of drugs*. J Ocul Pharmacol, 1985. **1**(3): p. 309-26.
105. Schoenwald, R.D., *Ocular drug delivery. Pharmacokinetic considerations*. Clin Pharmacokinetic, 1990. **18**(4): p. 255-69.
106. Eller, M.G., et al., *Topical carbonic anhydrase inhibitors IV: Relationship between excised corneal permeability and pharmacokinetic factors*. J Pharm Sci, 1985. **74**(5): p. 525-9.
107. Hariharan, S., et al., *Enhanced corneal absorption of erythromycin by modulating P-glycoprotein and MRP mediated efflux with corticosteroids*. Pharm Res, 2009. **26**(5): p. 1270-82.
108. Katragadda, S., et al., *Ocular pharmacokinetics of acyclovir amino acid ester prodrugs in the anterior chamber: evaluation of their utility in treating ocular HSV infections*. Int J Pharm, 2008. **359**(1-2): p. 15-24.
109. Anand, B.S., et al., *In vivo ocular pharmacokinetics of acyclovir dipeptide ester prodrugs by microdialysis in rabbits*. Mol Pharm, 2006. **3**(4): p. 431-40.
110. Gunda, S., S. Hariharan, and A.K. Mitra, *Corneal absorption and anterior chamber pharmacokinetics of dipeptide monoester prodrugs of ganciclovir (GCV): in vivo comparative evaluation of these prodrugs with Val-GCV and GCV in rabbits*. J Ocul Pharmacol Ther, 2006. **22**(6): p. 465-76.
111. Gandhi, M.D., D. Pal, and A.K. Mitra, *Identification and functional characterization of a Na(+)-independent large neutral amino acid transporter (LAT2) on ARPE-19 cells*. Int J Pharm, 2004. **275**(1-2): p. 189-200.
112. Majumdar, S., *Ocular drug delivery: Evaluation of dipeptide monoester ganciclovir prodrugs in School of Pharmacy*. 2005, University of Missouri Kansas City: Kansas City. p. 195.

113. Martin, J.C., et al., *9-[(1,3-Dihydroxy-2-propoxy)methyl]guanine: a new potent and selective antiherpes agent*. J Med Chem, 1983. **26**(5): p. 759-61.
114. Tirucherai, G.S. and A.K. Mitra, *Effect of hydroxypropyl beta cyclodextrin complexation on aqueous solubility, stability, and corneal permeation of acyl ester prodrugs of ganciclovir*. AAPS PharmSciTech, 2003. **4**(3): p. E45.
115. Jwala, J., et al., *Functional characterization of folate transport proteins in Staten's Seruminstitut rabbit corneal epithelial cell line*. Curr Eye Res, 2011. **36**(5): p. 404-16.
116. Tirucherai, G.S., *Corneal Permeation of Ganciclovir and Its Acyl Ester Prodrugs and Modulation by Hydroxypropyl Beta Cyclodextrin Complexation*, in *School of Pharmacy*. 2002, University of Missouri Kansas City: Kansas City.
117. Gandhi, M.D., *An Amino Acid Transporter Targeted Approach for the Treatment of Cytomegalovirus Infections*, in *School of Pharmacy*. 2005, University of Missouri Kansas City: Kansas City
118. Atluri, H., "*Part I: Vitreous Disposition of Alcohols as A Function of Lipophilicity; Part II: Transporter Mediated Delivery of Acycloguanosine Antivirals To Retina*", in *School of Pharmacy*, University of Missouri Kansas City: Kansas City.
119. Hatanaka, T., et al., *Transport of amino acid-based prodrugs by the Na⁺- and Cl⁻-coupled amino acid transporter ATB0,+ and expression of the transporter in tissues amenable for drug delivery*. J Pharmacol Exp Ther, 2004. **308**(3): p. 1138-47.
120. Colin, J., et al., [*Superficial herpes simplex keratitis. Double-blind comparative trial of acyclovir and idoxuridine (author's transl)*]. Nouv Presse Med, 1981. **10**(36): p. 2969-70, 2975.
121. E., D.L., *Clinical Aspects of Ocular Herpes Simplex Virus Infection*. 1985, Chicago: Yearbook Medical Publishers.
122. Green, M., Dunkel, E. , *Herpes Simplex Virus Infections* ed. L.a. Febiger. 1985, Philadelphia.
123. Kaufman, H.E., *Clinical cure of herpes simplex keratitis by 5-iodo-2-deoxyuridine*. Proc Soc Exp Biol Med, 1962. **109**: p. 251-2.
124. Lass, J.H., et al., *Antiviral medications and corneal wound healing*. Antiviral Res, 1984. **4**(3): p. 143-57.
125. la Lau, C., et al., *Aciclovir and trifluorothymidine in herpetic keratitis. Preliminary report of a multicentered trial*. Doc Ophthalmol, 1981. **50**(2): p. 287-90.

126. Hovding, G., *A comparison between acyclovir and trifluorothymidine ophthalmic ointment in the treatment of epithelial dendritic keratitis. A double blind, randomized parallel group trial.* Acta Ophthalmol (Copenh), 1989. **67**(1): p. 51-4.
127. Pavan-Langston, D., *Clinical Disease Herpetic Infections.* Smolin G, Throft RA eds. ed, ed. B. Little. 1994, Boston. 83-215.
128. Andrei, G., et al., *Comparative activity of selected antiviral compounds against clinical isolates of human cytomegalovirus.* Eur J Clin Microbiol Infect Dis, 1991. **10**(12): p. 1026-33.
129. Shigeta, S., et al., *Comparative inhibitory effects of nucleoside analogues on different clinical isolates of human cytomegalovirus in vitro.* J Infect Dis, 1991. **163**(2): p. 270-5.
130. Balzarini, J., et al., *Superior cytostatic activity of the ganciclovir elaidic acid ester due to the prolonged intracellular retention of ganciclovir anabolites in herpes simplex virus type 1 thymidine kinase gene-transfected tumor cells.* Gene Ther, 1998. **5**(3): p. 419-26.
131. Smee, D.F., et al., *Anti-herpesvirus activity of the acyclic nucleoside 9-(1,3-dihydroxy-2-propoxymethyl)guanine.* Antimicrob Agents Chemother, 1983. **23**(5): p. 676-82.
132. Hoh, H.B., et al., *Randomised trial of ganciclovir and acyclovir in the treatment of herpes simplex dendritic keratitis: a multicentre study.* Br J Ophthalmol, 1996. **80**(2): p. 140-3.
133. Colin, J., et al., *Ganciclovir ophthalmic gel (Virgan; 0.15%) in the treatment of herpes simplex keratitis.* Cornea, 1997. **16**(4): p. 393-9.
134. Dias, C.S., B.S. Anand, and A.K. Mitra, *Effect of mono- and di-acylation on the ocular disposition of ganciclovir: physicochemical properties, ocular bioreversion, and antiviral activity of short chain ester prodrugs.* J Pharm Sci, 2002. **91**(3): p. 660-8.
135. Duvvuri, S., S. Majumdar, and A.K. Mitra, *Drug delivery to the retina: challenges and opportunities.* Expert Opin Biol Ther, 2003. **3**(1): p. 45-56.
136. Majumdar, S., S. Duvvuri, and A.K. Mitra, *Membrane transporter/receptor-targeted prodrug design: strategies for human and veterinary drug development.* Adv Drug Deliv Rev, 2004. **56**(10): p. 1437-52.
137. Amasheh, S., et al., *Transport of charged dipeptides by the intestinal H⁺/peptide symporter PepT1 expressed in Xenopus laevis oocytes.* J Membr Biol, 1997. **155**(3): p. 247-56.
138. Balimane, P.V., et al., *Direct evidence for peptide transporter (PepT1)-mediated uptake of a nonpeptide prodrug, valacyclovir.* Biochem Biophys Res Commun, 1998. **250**(2): p. 246-51.

139. Okamura, M., et al., *Inhibitory effect of zinc on PEPT1-mediated transport of glycylsarcosine and beta-lactam antibiotics in human intestinal cell line Caco-2*. *Pharm Res*, 2003. **20**(9): p. 1389-93.
140. Hoglund, M., P. Ljungman, and S. Weller, *Comparable aciclovir exposures produced by oral valaciclovir and intravenous aciclovir in immunocompromised cancer patients*. *J Antimicrob Chemother*, 2001. **47**(6): p. 855-61.
141. Reusser, P., *Oral valganciclovir: a new option for treatment of cytomegalovirus infection and disease in immunocompromised hosts*. *Expert Opin Investig Drugs*, 2001. **10**(9): p. 1745-53.
142. Miller, S.C., K.J. Himmelstein, and T.F. Patton, *A physiologically based pharmacokinetic model for the intraocular distribution of pilocarpine in rabbits*. *J Pharmacokinetic Biopharm*, 1981. **9**(6): p. 653-77.
143. Macha, S. and A.K. Mitra, *Ocular pharmacokinetics in rabbits using a novel dual probe microdialysis technique*. *Exp Eye Res*, 2001. **72**(3): p. 289-99.
144. Zetterstrom, T., et al., *Purine levels in the intact rat brain. Studies with an implanted perfused hollow fibre*. *Neurosci Lett*, 1982. **29**(2): p. 111-5.
145. Benveniste, H. and P.C. Huttemeier, *Microdialysis--theory and application*. *Prog Neurobiol*, 1990. **35**(3): p. 195-215.
146. Cheng, Y.C., et al., *Metabolism of 9-(1,3-dihydroxy-2-propoxymethyl)guanine, a new anti-herpes virus compound, in herpes simplex virus-infected cells*. *J Biol Chem*, 1983. **258**(20): p. 12460-4.
147. Cheng, Y.C., et al., *Effects of 9-(1,3-dihydroxy-2-propoxymethyl)guanine, a new antiherpesvirus compound, on synthesis of macromolecules in herpes simplex virus-infected cells*. *Antimicrob Agents Chemother*, 1984. **26**(3): p. 283-8.
148. Hamzeh, F.M., et al., *Identification of the lytic origin of DNA replication in human cytomegalovirus by a novel approach utilizing ganciclovir-induced chain termination*. *J Virol*, 1990. **64**(12): p. 6184-95.
149. Hamzeh, F.M. and P.S. Lietman, *Intranuclear accumulation of subgenomic noninfectious human cytomegalovirus DNA in infected cells in the presence of ganciclovir*. *Antimicrob Agents Chemother*, 1991. **35**(9): p. 1818-23.
150. Crumpacker, C.S., *Ganciclovir*. *N Engl J Med*, 1996. **335**(10): p. 721-9.
151. Freeman, S. and J.M. Gardiner, *Acyclic nucleosides as antiviral compounds*. *Mol Biotechnol*, 1996. **5**(2): p. 125-37.
152. Black, M.E., et al., *Creation of drug-specific herpes simplex virus type 1 thymidine kinase mutants for gene therapy*. *Proc Natl Acad Sci U S A*, 1996. **93**(8): p. 3525-9.

153. Moolten, F.L. and J.M. Wells, *Curability of tumors bearing herpes thymidine kinase genes transferred by retroviral vectors*. J Natl Cancer Inst, 1990. **82**(4): p. 297-300.
154. Smythe, W.R., et al., *Treatment of experimental human mesothelioma using adenovirus transfer of the herpes simplex thymidine kinase gene*. Ann Surg, 1995. **222**(1): p. 78-86.
155. Vile, R.G. and I.R. Hart, *Use of tissue-specific expression of the herpes simplex virus thymidine kinase gene to inhibit growth of established murine melanomas following direct intratumoral injection of DNA*. Cancer Res, 1993. **53**(17): p. 3860-4.
156. Fleming, D.T., et al., *Herpes simplex virus type 2 in the United States, 1976 to 1994*. N Engl J Med, 1997. **337**(16): p. 1105-11.
157. Manne, S. and I. Sandler, *Coping and adjustment to genital herpes*. J Behav Med, 1984. **7**(4): p. 391-410.
158. Goldmeier, D., et al., *Psychosocial implications of recurrent genital herpes simplex virus infection*. Genitourin Med, 1988. **64**(5): p. 327-30.
159. Perry, C.M. and D. Faulds, *Valaciclovir. A review of its antiviral activity, pharmacokinetic properties and therapeutic efficacy in herpesvirus infections*. Drugs, 1996. **52**(5): p. 754-72.
160. *Infectious diseases: antiviral drugs*. Beers MH, Berkow R, eds ed. The Merck Manual of Diagnosis and Therapy INDEX. 1999., 17th ed. Rahway, NJ: Merck, Inc.
161. Richards, D.M., et al., *Acyclovir. A review of its pharmacodynamic properties and therapeutic efficacy*. Drugs, 1983. **26**(5): p. 378-438.
162. Available from:
<http://akramania.byethost11.com/Robbins/393.html@printing=true.htm>.

VITA

Sriram Gunda was born in Mahabubnagar, India. He was educated in Hyderabad, India and obtained a high school degree from Shantiniketan High School. Thereafter, he pursued a Bachelor's degree in Pharmacy from Kakatiya University, Warangal in 2000. He joined the Master's program in Pharmaceutical Sciences Division in the School of Pharmacy, University of Missouri-Kansas City in 2001. He later joined doctoral program in 2002 in the same division in Dr. Mitra's lab. He served as a Chair-elect from 2004 – 2005 and chair from 2005-2006 for American Association of Pharmaceutical Scientists (AAPS), UMKC student chapter. He is also a member of Pharmaceutical Sciences Graduate Student Association (PSGSA), American Conference on Pharmacometrics (ACoP), AAPS and Association for Research in Vision, and Ophthalmology (ARVO). He received student travelship award from Interdisciplinary Student Council (IDSC, UMKC). He was selected for podia presentation at Pharmaceutical Graduate Student Research Meeting (PGSRM). He has many peer reviewed publications in various scientific journals and peer reviewed abstracts in various national and international conferences. He has accepted a position of Pharmacokineticists in the Clinical Pharmacology Division of PPD Inc., and plans to pursue a career in Pharmacokinetics and Pharmacodynamics upon graduation from the Pharmaceutical Sciences program.